



University of
Stavanger

FACULTY OF SCIENCE AND TECHNOLOGY

MASTER'S THESIS

Study programme/specialisation: Petroleum Geoscience Engineering	Spring semester, 2018 Open
Author: Signe Kristoffersen (signature of author)
Supervisor: Rodmar Ravnås	
Title of master's thesis: An Integrated Study of the Transition of the Ula Formation from the Cod Terrace to the Sørvestlandet High; Implications for Reservoir Types, Distribution, and Carrier Beds for Hydrocarbon Migration	
Credits: 30	
Keywords: Ula Formation Ula Field Oda Field Interpod deposit Supra salt reservoir Upper Jurassic reservoir Sørvestlandet High	Number of pages: + supplemental material/other: Stavanger, 16th of July 2018

**An Integrated Study of the
Transition of the Ula Formation from
the Cod Terrace to the Sørvestlandet
High; Implications for Reservoir
Types, Distribution, and Carrier
Beds for Hydrocarbon Migration**

by

Signe Kristoffersen

Msc. Thesis

Presented to the Faculty of Science and Technology
The University of Stavanger

The University of Stavanger
2018

Acknowledgments

Firstly, I thank my supervisor Rodmar for enabling me to write about this very interesting topic I also want to thank him for his guidance throughout this last year. Secondly, I thank Norske Shell for allowing me access to the data and their help with sculpting it is greatly appreciated. Then I thank the other companies which have kindly offered me their thoughts on this topic, thank you Suncore and Spirit Energy for opening your doors to me. I also thank Dmitry Shogin for teaching me how to use LaTeX and Paul Nadeau for some interesting discussions.

To my classmates you're the best, thank you for the tea breaks, procrastination, thesis discussions, lunches, technical support, moral support, good company, and laughs. I would list you all by name but my thesis is getting really long at this point and I don't want to make it worse, you know who you are and I couldn't have done it without you.

To my family, thank you for supporting me throughout everything. And to my mom, thank you for the occasional late-night pick-ups at the university and making sure I ate a proper dinner every now and then.

Abstract

The Upper Jurassic deposits of the Eastern Margin in the Central Graben were influenced by syn-depositional halokinesis, which in turn affected the partitioning of environments and the resulting stratigraphic architecture. The focus of this thesis is on the sandstones deposited along and on top of collapsing salt diapirs and salt walls, the so-called interpod deposits, in a transect from the Cod Terrace and onto the Sørvestlandet High. A refined understanding of the detailed stratigraphic architecture and facies partitioning in the reservoir is a prerequisite for risk mitigation of the Upper Jurassic play within this play segment. The main risks for the successful extension of the exploration model onto the Sørvestlandet High is the presence of reservoir and migration. The prime objective of the thesis is to gain insight into the distribution and connectivity of reservoir beds in a transect from the Ula Field to the Oda Field.

This has been accomplished using the following data: New 3D seismic data and older merged seismic data; all wells in the study area for seismic interpretation, with focus on three wells for correlation; and core data from three focus wells. Seismic interpretation was focused on defining seismic stratigraphic units within the Ula Formation which can be characterized via seismic facies and amplitude/frequency analysis to infer the stratigraphic architecture and architectural elements. Core interpretation was done by identifying variations in grain size, trace fossils, fossil content, sedimentary structures, and bed stacking pattern(s) with emphasis on identifying architectural elements and depositional sub-environments.

The current preferred model of a storm influenced shoreface cannot account for the results found in this study. The older part of the Ula Formation show tidal dominance, and the younger part seem to be more affected by unidirectional currents. This indicates that the shoreface morphology has had great influence on the dominant process through abating the waves. Attribute maps indicate compound dunes deposited in a strait setting. Correlation and core interpretation suggest that there are fluvial systems bringing sediments out into the Cod Terrace, which could function as migration pathways from the Cod Terrace onto the Sørvestlandet High. Integration of wells and seismic has proved vital in this study as including the shoreface morphology has been a key part in understanding the system.

Table of Contents

Acknowledgments	II
Abstract	III
1. Introduction	1
1.1. Objectives	2
2. Theoretical Background	4
2.1. Basin Type	4
2.2. Salt Structuring in Rift-Basins	4
2.3. Facies Models for Coastal Depositional Environments	9
2.3.1. Basin Physiographies Along Open-Coast Settings	9
2.3.2. Conceptual Basin Physiographies in a Pod-Interpod Basin	9
2.3.3. Storm Influenced Shorefaces	9
2.3.4. Tide-Dominated Shorelines Including Deltas and Estuaries	11
2.3.5. Shelfal Settings	11
2.3.6. Strait Settings	12
2.4. Syn-Rift Basin-Fills – Sequence Stratigraphy of Salt- Structured Rift-Basins	17
3. Geological Setting	18
3.1. Tectonic Evolution of the Central Graben (Central North Sea)	18
3.2. Structural Elements in the Study Area	18
3.3. Triassic-Jurassic-Early Cretaceous Lithostratigraphy	19
4. Data and Methodology	22
4.1. Data	22
4.1.1. Cores and Wells	22
4.1.2. Seismic	22
4.2. Methodology	24
4.2.1. Cores and Wells	24
4.2.2. Seismic	27
4.2.2.1. Accounting for Evaporite Effect on Seismic Imaging	27
4.2.2.2. Seismic Vertical Resolution	27
4.2.2.3. Seismic Well-Tie	27
4.2.2.4. Seismic Interpretation	33
4.2.2.5. Attributes	34
5. Results	40
5.1. Lithofacies Descriptions	40
5.1.1. Facies with Sedimentary Structures	40

5.1.2.	Facies Lacking Sedimentary Structures	42
5.1.3.	Mudstone Facies	44
5.2.	Facies Associations	45
5.3.	Seismic	53
5.3.1.	Well-Tie	53
5.3.2.	Vertical Resolution	54
5.3.3.	Seismic Interpretation	55
5.3.3.1.	Confidence Map	55
5.3.3.2.	Surfaces	55
5.3.4.	Ula Formation Isochore Map	64
5.3.5.	Ula Formation Thickness Estimation Map	64
5.3.6.	Seismic Attributes	67
5.3.6.1.	Sculpting	67
5.3.6.2.	RMS	68
5.4.	Correlation	76
6.	Discussion	79
6.1.	Data	79
6.2.	Salt Effect on Depositional Environment	79
6.3.	Depositional Environment in the Interpod Setting	80
6.4.	Ula Formation Distribution and Architectural Elements	80
6.5.	Correlation From the Cod Terrace to the Sørvestlandet High	81
7.	Conclusions	82
	References	83

List of Figures

1.	Map of the study area	3
2.	Salt structures	6
3.	Structural evolution according to Penge, Munns, Taylor, and Windle (1999), Penge, Taylor, Huckerby, and Munns (1993), Hodgson, Farnsworth, and Fraser (1992), and Clark, Cartwright, and Stewart (1999)	7
4.	Structural evolution according to Mannie, Jackson, and Hampson (2014)	8
5.	The interpod depositional environment	10
6.	Storm influenced shoreface	13
7.	Tidal depositional environments	14
8.	Shelfal Depositional Environments	15
9.	Strait	16
10.	Sequence stratigraphic framework	21
11.	Map containing extent of seismic cubes and well log positions	23
12.	A visualisation of the bioturbation index	26
13.	Synthetic seismogram and well-tie for well 7/12-6	29
14.	Synthetic seismogram and well-tie for well 7/12-10, 7/12-4, and 7/12-11	31
15.	Synthetic seismogram and well-tie for well 1/3-3, 7/12-7, and 7/12-8	32
16.	Attribute maps using sculpting for MEGA cube	37
17.	Attribute maps using sculpting for PGS cube	38
18.	Seismic cross-section showing issues with artifacts influencing the attributes	39
19.	Core photos from Facies 1 to 6	49
20.	Core photos for Facies 7 to 10	50
21.	Legend for core description	51
22.	Core description of well 8/10-6S	51
23.	Core description of well 7/12-6	52
24.	Core description of well 8/10-5S	53
25.	Confidence map for seismic interpretation	58
26.	Seismic cross-section	59
27.	Top Ekofisk Formation surface	60
28.	Farsund Formation internal reflector surface	61
29.	Top Ula Formation surface	62
30.	Base Ula Formation surface	63
31.	Internal Ula reflection surface	65
32.	Ula Formation isochore	65
33.	Thickness variation map	66
34.	Seismic line illustrating window of examination for RMS and Sculpting	70
35.	Sculpt attribute	71
36.	RMS attribute	72
37.	Interpretation of geometries in Sculpt attribute	73

38.	Interpretation of geometries in RMS attribute	74
39.	Well 7/12-9 and 7/12-8	75
40.	Well log correlation	78

List of Tables

1.	Information about seismic cubes	24
2.	Information about cored intervals	25
3.	Wells containing sonic and density	30
4.	Windows of investigation for attribute generation	36
5.	Lithofacies description	48
7.	Wells tied to seismic with amount of bulk shift	54
8.	Measurements of seismic vertical resolution	55
9.	Horizon characteristics	57

1 Introduction

The Upper Jurassic shallow marine sandstones of the Ula Formation have long been a target for hydrocarbon exploration and production within and on terraces along the Central Graben in the Central North Sea. On the Cod Terrace (Figure 1), situated at the transition between the deep Central Graben and the bordering Sørvestlandet High, three hydrocarbon fields are currently producing from the Ula Formation. The Ula Field (discovered in 1976), the Gyda Field (discovered in 1980), and the Tambar Field (discovered in 1983) (Norwegian Petroleum Directorate, 2017), are all situated in what is informally referred to as the Ula Trend, which is defined in its broadest sense by the extent of Ula sandstones along the eastern margin of the Central Graben (Baniak, Gingras, Burns, & Pemberton, 2014). A more restricted definition of the term applies to the part of the trend where the Ula sandstones historically have been considered prospective. This area is normally delineated by, but not restricted to the Cod Terrace (Figure 1). The restricted definition of the term Ula Trend thus applies to the proven part of the ‘Ula segment’ of the Upper Jurassic play fairway in the Central North Sea. Outside the proven part of the Ula segment, exploration within the Ula reservoir fairway has been disappointing. This statement also applies to the large Sørvestlandet High where exploration for additional Upper Jurassic opportunities has resulted in a series of dry wells, in turn cementing a general belief that the Upper Jurassic play in this vast area is non-prospective due to the lack of charge. As a consequence, the Upper Jurassic play has traditionally been considered exhausted within the Norwegian areas of the mature Central North Sea hydrocarbon province.

This general ‘consensus’ was initially challenged by Lundin’s re-appraisal of the Brynhild Field (discovered in 1992, production start-up in 2014; Norwegian Petroleum Directorate (2017)) and more recently by Centrica’s (now Spirit Energy) discovery and subsequent appraisal of the Oda Field (discovered in 2011; Norwegian Petroleum Directorate (2017)). The Oda appraisal campaign (Norwegian Petroleum Directorate, 2017) demonstrates that this structure has had a complex hydrocarbon filling and spilling and/or leakage history, leaving trapped hydrocarbons only in part of the structure. These two discoveries, albeit small, are important as they 1) prove that hydrocarbon migration very likely has occurred onto the western flank of the Sørvestlandet High thereby extending the prospective Ula Trend onto the high, and 2) that migration likely has had a complex and tortuous route into and spill (or leak) out of the structures, in turn suggesting that migration at further distance onto the high is not unrealistic. Most basin modelling efforts demonstrate that hydrocarbon yield within and from the Central Graben and local kitchen areas on the bordering terraces by far outnumbers the yet encountered hydrocarbons within the area (Kubala, Bastow, Thompson, Scotchman, & Oygard, 2003). In consort, this provides additional encouragement to the argument that the prospective Ula Trend can be further

extended north-eastward onto the Sørvestlandet High, if one can demonstrate that the current wells in the area have been drilled on targets within migration shadows or on breached traps.

Further risk mitigation efforts of charge and migration onto the Sørvestlandet High therefore rely on 1) proper assessment of all exploration wells in the area, i.e. a so called drilled-hole analysis, 2) detailed evaluation of structural trapping style including the degree of compartmentalization and potential for post-charge structural reactivation and seal breaching, and 3) detailed evaluation of the distribution, stratigraphic architecture, and property characteristics of carrier beds that can be utilized for migration.

The present thesis addresses the Ula sandstones in fields and discoveries/accumulations along proven migration routes in an attempt to further detail the Upper Jurassic reservoir architecture based on state-of-the-art 3D seismic data integrated with well studies. The study area covers a transect from the Tambar and Ula fields to the Oda discovery, i.e. an area with an extensive high quality broadband seismic and well dataset, and where migration is proven out of the Central Graben area onto the bordering Sørvestlandet High. The main objective of the study is to delineate stratal architectures based on the high-resolution broadband data in an integrated well and seismic study, supplemented with new and previously unpublished core data from the Ula Formation.

1.1 Objectives

The prime objective of the study is accordingly to gain insight into the depositional evolution and stratigraphic architecture of the Ula Formation to further detail possible migration routes from Ula to Oda. In order to achieve this objective the following tasks have been identified:

1. define how salt movement affected the depositional environment;
2. identify the depositional environments of the interpod setting by focusing on a selected area which has the potential to serve as an analogue for other interpod basins;
3. create a conceptual model for the reservoir distribution/partitioning pattern and architecture in the interpod setting; and
4. attempt to link and correlate this area with the more well defined and studied shallow marine system within the Central Graben proper with a source-to-sink approach.

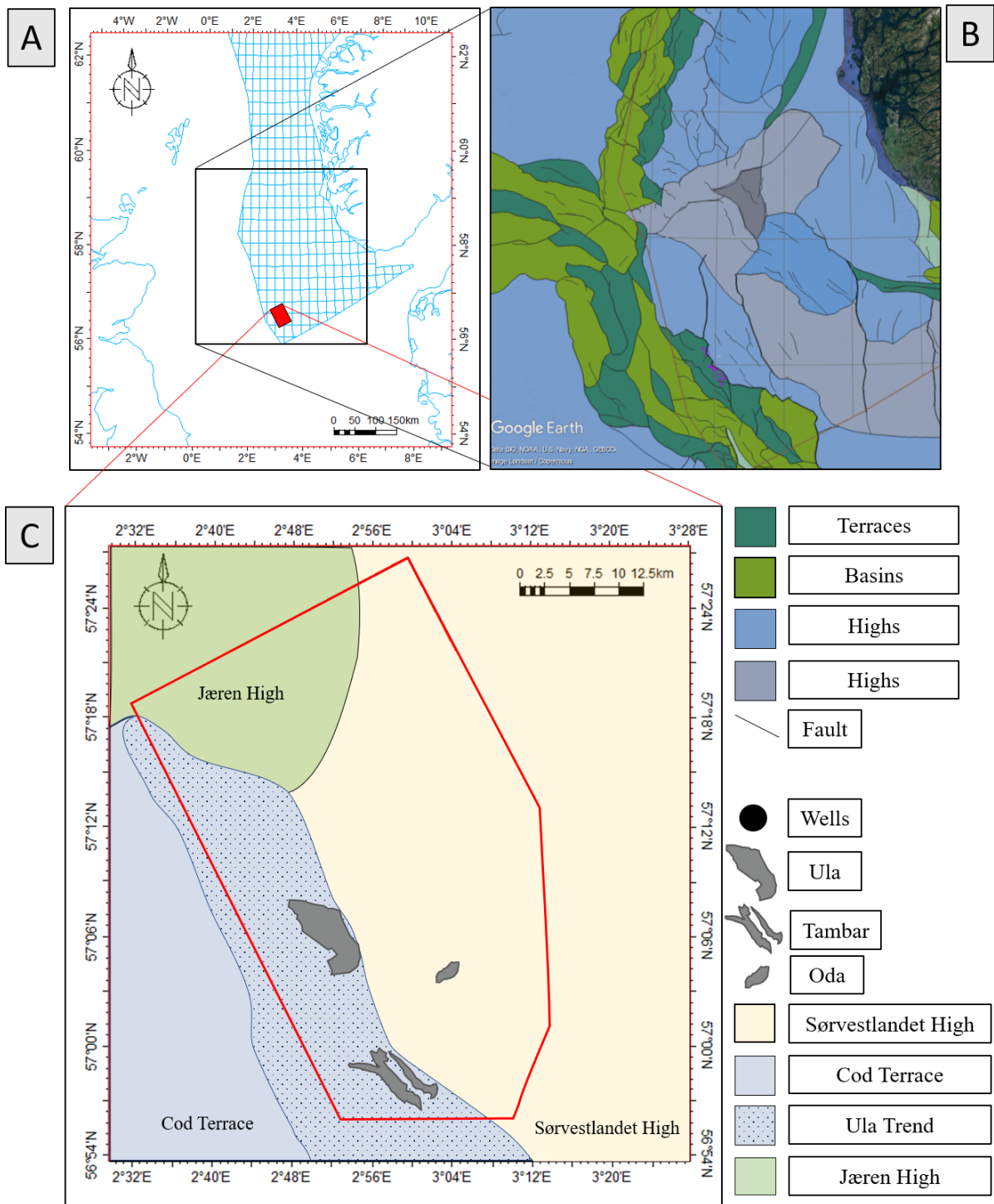


Figure 1: A: Map showing the general location of the study area. B: The geological structures in the area showing faults basins highs and terraces, location of map can be seen in A. C: Location of figure can be seen in A. The study area and its geological basins, Jæren High in green, Sørvestlandet High in yellow, and Cod Terrace in blue. Hydrocarbon fields have been shaded gray. The Ula Trend as it is known in its strictest sense has been illustrated as the dotted area in the Cod Terrace. The red polygon shows the maximum extent of the seismic data. Outlines are provided by Norske Shell, and other data from the map is from Norwegian Petroleum Directorate (2017).

2 Theoretical Background

2.1 Basin Type

The Ula Formation has been deposited along the margins of the Central Graben rift-basin, but due to salt influence the morphology of the basin(s) containing the Ula Formation is very different from a typical rift basin. It has been deposited on top of salt walls in basins which have been called interpod basins. In contrast to typical salt generated minibasins which are thickest where the salt is thinnest, interpod deposits are deposited directly above the thicker parts of the salt structures. The name interpod basins comes from the initial observation of Triassic pods, the typical minibasins in the area, which stand out in the seismic as thick sedimentary packages between the salt diapirs and walls. Between these Triassic pods the Ula Formation can be found, and thus, the formation became known as an interpod deposit.

2.2 Salt Structuring in Rift-Basins

Salt tectonism is very common in the southern to central North Sea due to the presence of the Permian Zechstein Group (Glennie, Higham, & Stemmerik, 2003), in the case of the Ula Formation salt has played a vital role both syn- and post-deposition (Mannie, Jackson, & Hampson, 2014). Salt differs from typical rocks in that it is mechanically very weak and can flow like mud (Hudec & Jackson, 2007), this opens for a whole new range of tectonics which cannot be imagined in most other rock formations. Through differential loading, extension, and compression salt can be triggered to move, rise upwards resulting in several different morphologies as described by (Hudec & Jackson, 2007). In the study area the most common configurations are salt-walls and salt-diapirs (Figure 2).

In the Central Graben the salt diapirs are generally situated above subsalt faults, and in the Cod Terrace they strike northwest-southeast. This indicates that there might be a link between the substrate structures and the salt structures. On the Sørvestlandet High they have a polygonal pattern. Locally the salt is welded or has developed into a salt-diapir, reaching reliefs of 4.5 kilometres and a width of 3.5 kilometres (Mannie et al., 2014).

Currently four different theories (Hodgson, Farnsworth, & Fraser, 1992; Clark, Cartwright, & Stewart, 1999; Penge, Taylor, Huckerby, & Munns, 1993; Penge, Munns, Taylor, & Windle, 1999; Mannie et al., 2014) have been proposed to explain the interplay of halokinetic movements and deposition in these interpod deposits. The first theory, the pod-interpod model, proposed by Hodgson et al. (1992) explains the morphology of the Ula Formation

as being formed mainly by halokinetism. During the Triassic, differential loading led to passive diapirism and dissolution until the salt was depleted below the minibasins. Thereafter, in the Jurassic extension resulted in the diapirs widening which caused the salt to withdraw. This provided the accommodation-space for the Jurassic interpod deposits (Figure 3B).

The second theory, the rift-raft model, Penge et al. (1999), Penge et al. (1993) suggests that the accommodation was generally caused by gravity gliding of Triassic rafts using the salt as a detachment (Figure 3C). The salt would then move into the rifted zone in a reactive-active-passive movement (Penge et al., 1999; Penge et al., 1993).

And the third theory, the salt-dissolution model, proposed by Clark et al. (1999) argues that the local thickness variations of the Jurassic deposits are controlled by salt dissolution as well as pre-existing topography (Figure 3D). The transgression caused increased dissolution of salt. Prior to the Jurassic the dissolution was restricted to the Triassic fluvial systems and rainfall (Clark et al., 1999).

Mannie et al. (2014) proposes in a fourth model (Figure 4), a modification of the model initially proposed by Hodgson et al. (1992), that the main mechanism for the interpod basin creation was Late Jurassic extensional diapir-collapse. Mannie adds a last stage of compression which led to the anticlines seen in the Ula Field. They argue that the dissolution of salt post Triassic is unlikely due to the thick Triassic sediment present on top of many of the salt walls, and that the geometries of the interpod basins do not fit into the models of Hodgson et al. (1992) and Penge et al. (1999), Penge et al. (1993).

The factor which matters the most to the reservoirs in the Upper Jurassic Ula Formation is whether the halokinetism occurred prior to or after the deposition. Meaning whether the Ula Formation was deposited all over, then differentially eroded by the structural deformation, or if it was only deposited above the salt walls because this was the only accommodation space. The theory put forward by Clark et al. (1999) and Hodgson et al. (1992) is dependent on the latter case, that the accommodation space was generated prior to or during the deposition of the Ula Formation. Mannie et al. (2014) and Penge et al. (1993) are not dependent on either scenario. However, Mannie et al. (2014) describes a scenario where the Ula Formation was deposited post accommodation creation, and Penge et al. (1993) concludes that the accommodation was created mainly during the Triassic. Therefore, no matter which model is believed to be true it is generally agreed upon that the accommodation space was generated either during or prior to deposition. Meaning that the Ula Formation was mainly deposited in these interpod basins which would likely have formed interconnecting valleys during deposition following the salt structures.

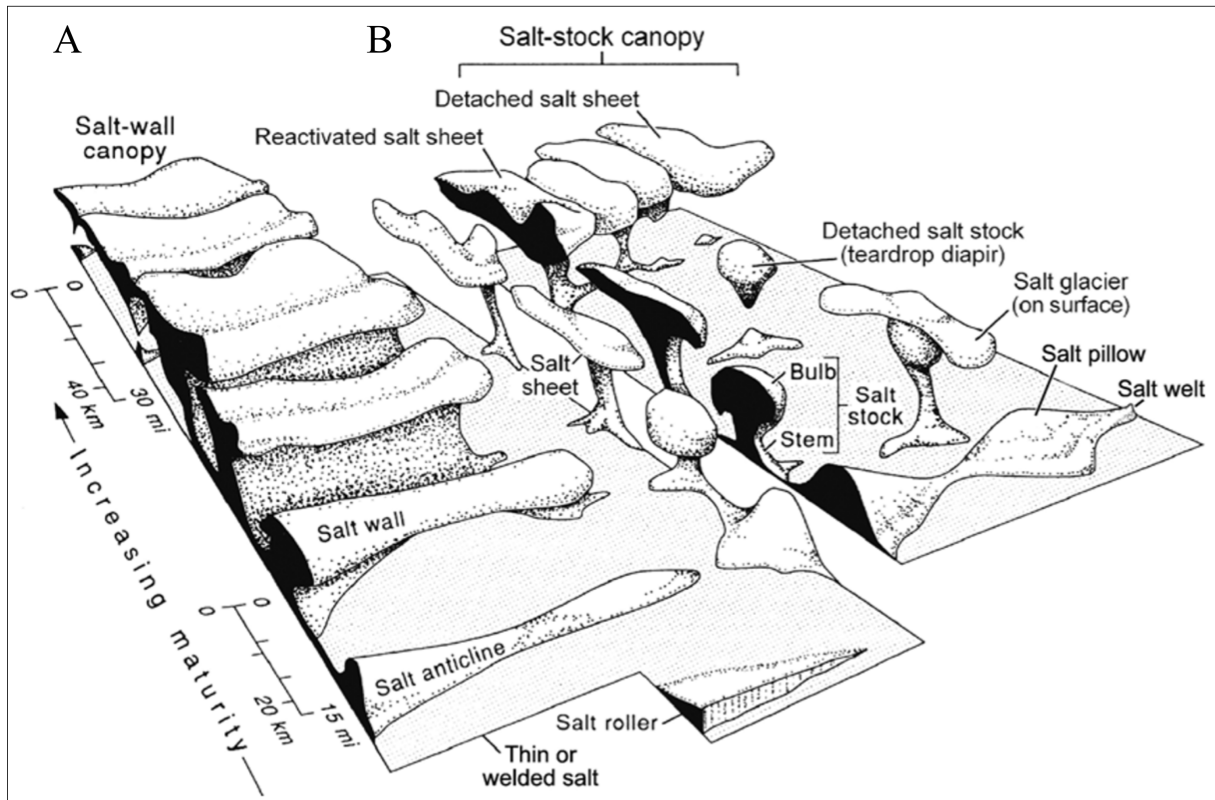
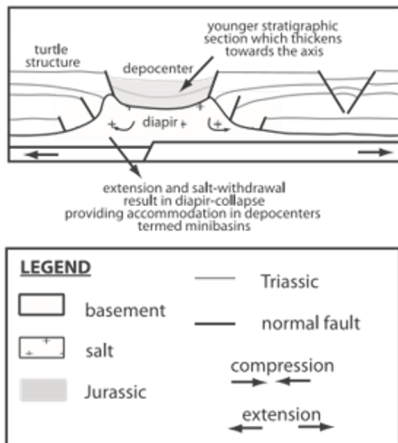
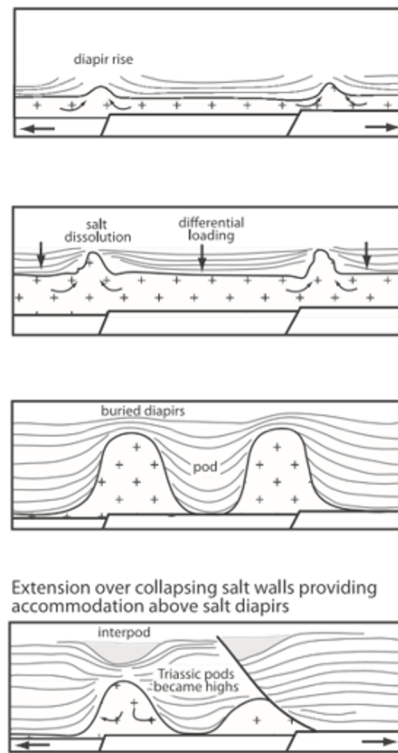


Figure 2: Salt structures as described by Hudec and Jackson (2007) A: Salt structures generated from a line source. B: Salt structures generated from a point source.

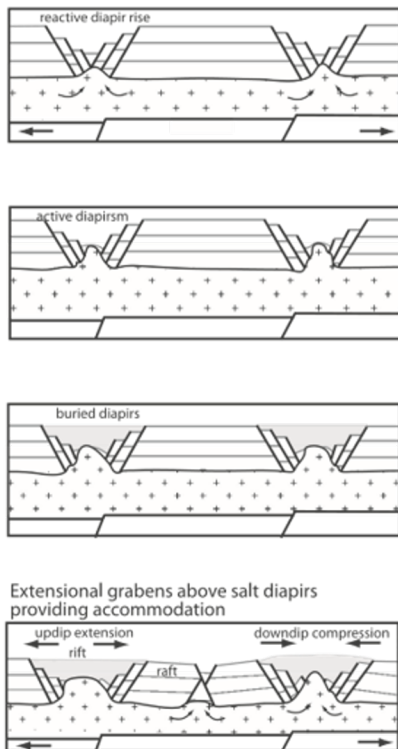
(A) Initial stage diapir-collapse



(B) 'pod-interpod' model (Hodgson et al. 1992)



(C) 'rift-raft' model (Penge et al. 1993, 1999)



(D) 'salt-dissolution' model (Clark et al. 1999)

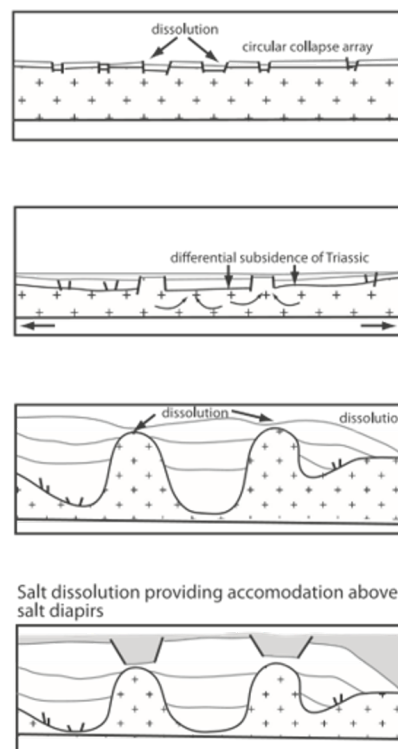


Figure 3: Structural evolution according to Hodgson, Farnsworth, and Fraser (1992). (B) Penge, Munns, Taylor, and Windle (1999), Penge, Taylor, Huckerby, and Munns (1993) (C), and Clark, Cartwright, and Stewart (1999) (D) (Mannie, Jackson, & Hampson, 2014)

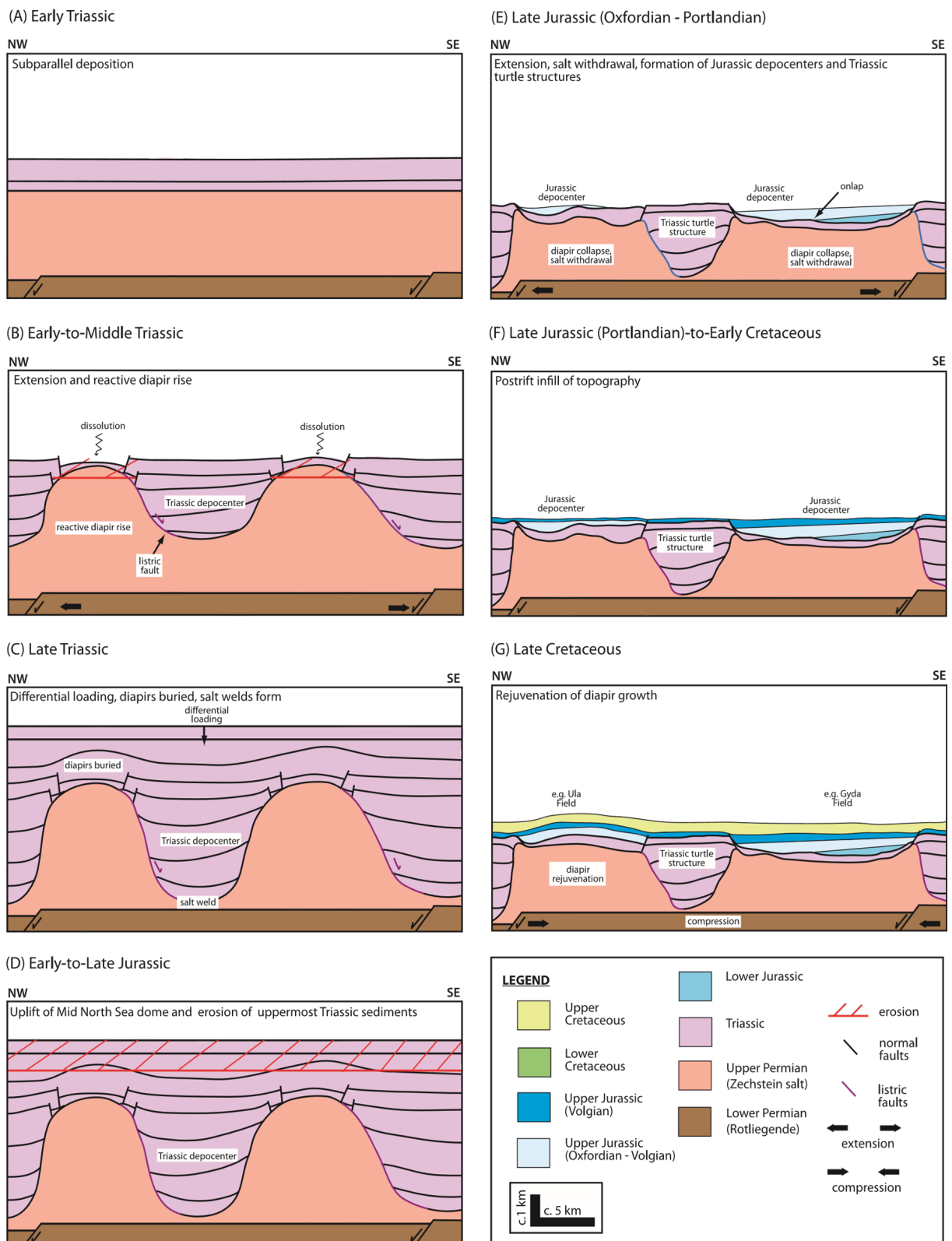


Figure 4: Structural evolution according to Mannie, Jackson, and Hampson (2014).

2.3 Facies Models for Coastal Depositional Environments

2.3.1 Basin Physiographies Along Open-Coast Settings

An open shoreface typically has a linear to lobate physiography, much like typical beaches in present time e.g. the Jæren beaches in Norway. A typical shoreface morphology may vary very little along strike but along dip there is a transition from upper to lower shoreface deposits. Additionally, a coastline with this geometry will be unprotected leaving it exposed to wave processes.

2.3.2 Conceptual Basin Physiographies in a Pod-Interpod Basin

Wonham, Rodwell, Lein-Mathisen, and Thomas (2014) suggests for the time equivalent Fulmar Formation an interpod basin coastline where the basins formed a network of valleys. Thus, they are elongated connected basins for which no analogue today can be presented. However, they might have similarities to drowned valleys or straits e.g. the Messina strait in Italy or the straits separating the North Sea and the Baltic Sea in Denmark. Fraser et al. (2003) created a conceptual model of how this would look like and which processes might influence deposition (Figure 5). The interpod basin physiography, in contrast to the open shoreface, can vary greatly along both dip and strike and can be described as a highly irregular and locally very protected coastline.

2.3.3 Storm Influenced Shorefaces

The Ula Formation has been described as a storm influenced shoreface deposit by several authors (Hodgson et al., 1992; Bjørnseth & Gluyas, 1995; Gowland, 1996; Baniak et al., 2014; Mannie et al., 2014; Baniak, Gingras, Burns, & Pemberton, 2015; Mannie, Jackson, Hampson, & Fraser, 2016). Typical depositional geometries for shoreface deposits are parallel to the shoreface, up to 20 metres thick sandbodies, elongated along strike (can reach lengths of hundreds of kilometres) and along the dip direction they can prograde for tens of kilometres (Walker & Plint, 2006). A typical log motif for a shoreface deposit is coarsening upwards from a bioturbated shelfal silty facies to a lower shoreface with hummocky cross stratification. Following this is the upper shoreface characterized by swaley cross stratification and followed by a breaker zone and beach. The overall profile is about 10 to 20 metres thick and overall coarsening upward from the more distal deposits until the beach facies. Sediments in storm dominated shorefaces are derived either from erosion and reworking of inner shelf or fluvial input or both (Walker & Plint, 2006).

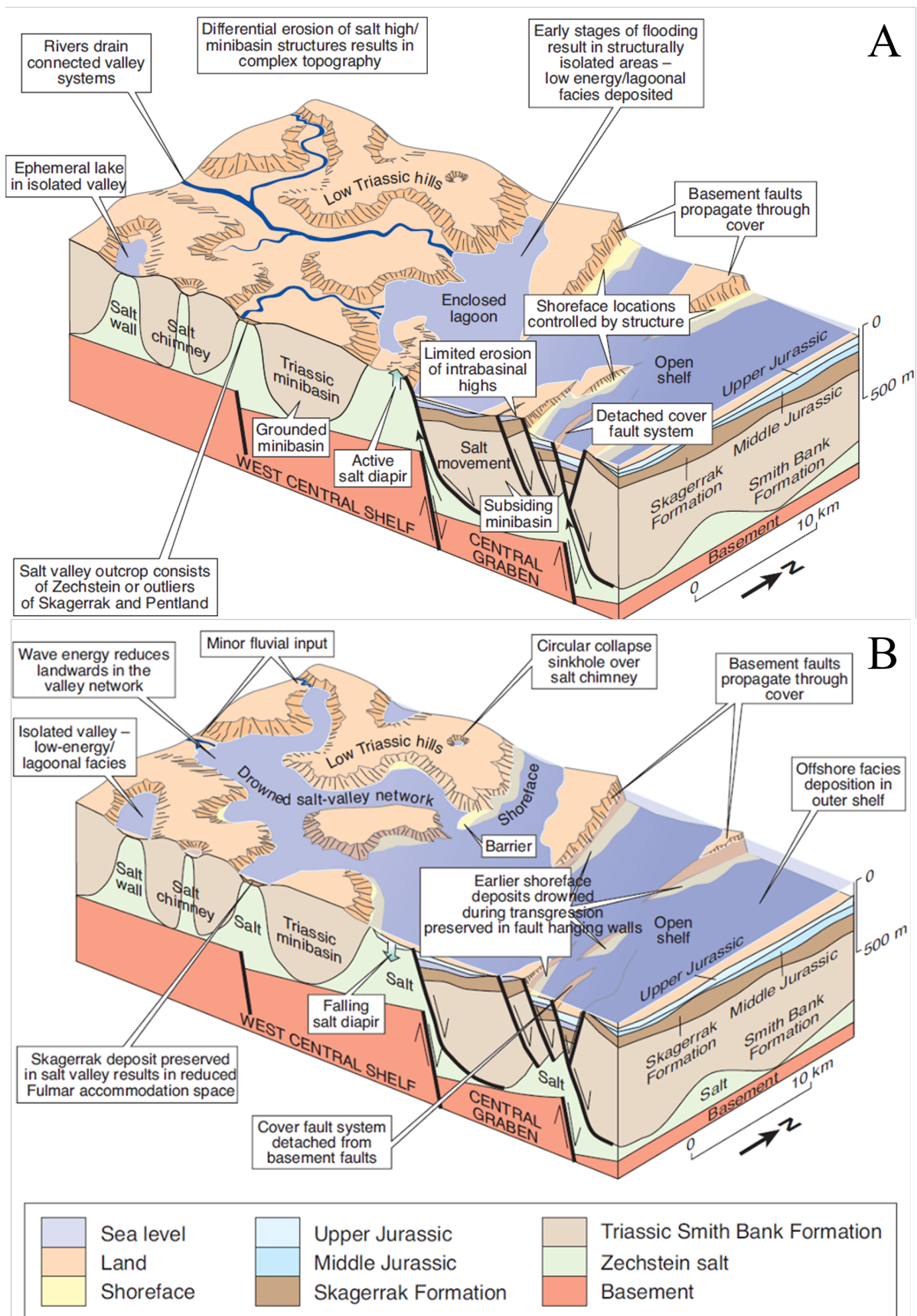


Figure 5: Paleogeographic reconstructions of the West Central Graben Margin, A: Oxfordian and B: Kimmeridgian (Fraser et al., 2003). They illustrate the salt valley network and some of the variability in deposition which can be imagined in such a system.

2.3.4 Tide-Dominated Shorelines Including Deltas and Estuaries

The initial description of the Ula Formation concluded that the depositional environment was tidally dominated with tidal sandwaves (now compound dunes) (Bailey, Price, & Spencer, 1981), later Home (1987) and Bowman (1981) also suggested a tidal environment for the Ula Formation. Typical depositional elements in tidal environments are tidal compound dunes (formerly sandwaves) (Dalrymple & Choi, 2007) and elongated tidal bars (Figure 7). In a 2D outcrop they can easily be confused due to their similarities. The main difference is that bars have their axis nearly parallel to tidal current while compound dunes have their axis orthogonal to the current. The thickness of compound dunes ranges from 1 to 20 metres, and their wavelengths range from 10 to hundreds of metres (McCave, 1971; Dalrymple, 2006). In shallower waters the bedforms are smaller (Dalrymple & Choi, 2007). The sand bars can have thicknesses of around 5 to 10 metres, and lengths of individual bars vary from metres to kilometres (Dalrymple, 2006).

Based on the observations made about the shoreface morphology during the deposition of the Ula Formation in a tidal environment one might expect a drowned valley setting or an estuary when the water transgressed across the valley network. Tidal estuaries are caused by a tidally dominated embayed setting with some fluvial input (after the definition of Dalrymple, Zaitlin, and Boyd (1992)). Since tidal deposition is periodic varying in energy throughout the day and also on larger time scales, tidal deposits are typically heterogenic on every scale and show cyclic variations in thickness and grainsizes (Dalrymple, 2006). Tidal estuaries, and estuaries in general, are typically divided into three parts based on which process is dominant, where the length of each zone will be dependent on the relative intensity of tidal and fluvial processes. Since there is a general agreement on that the Ula Formation is a shallow marine sandstone, the two outermost zones of the estuary will be the most relevant.

The main differences between tidal estuaries and deltas are that deltas might have stable tidal bars, and more fluvial dominance, as well as a sandier prodelta/proestuary area (Dalrymple & Choi, 2007). Tidal deltas can even have inactive zones which undergo subsidence due to compaction and would technically be characterized as an estuary (Dalrymple, 2006). Therefore, for the purpose of this thesis there has not been made any distinction between the two as the resulting sand body geometries are similar.

2.3.5 Shelfal Settings

Shelfal sands typically consist of compound dunes and tidal sand ridges, which are similar structures to the tidal estuary/delta systems and straits, the main difference being scale. Since shelfal areas are less constricted shelfal sand ridges and compound dunes can get

laterally very extensive. They have been recorded at lengths of 30 kilometres, widths of 0.7 to 8 km, and thickness ranges from 5 to 40 metres (Snedden, Dalrymple, & Bergman, 1998). Sand dunes are typically thinner but can be laterally more extensive and particularly wider than the elongated profile of tidal ridges. An analogue which can be used for shelfal sands is the area surrounding the British Isles where tidal currents result in long tidal sand ridges and vast sand compound dunes (Figure 8).

2.3.6 Strait Settings

Alternatively, the drowned valley system could have resulted locally in a strait morphology. This is dependent on the shoreface morphology during deposition. No analogues or models for straits have been previously presented for the Ula Formation. Longhitano (2013) presents a model for tectonically-confined straits wherein the depositional elements are similar to those of a tidally dominated estuary or delta, suggesting tidal dunes as can be seen in the San Francisco Strait. Longhitano and Steel (2017) further presents a model where the strait is deflecting deltas, fandeltas, and rivers which are inputting sediment into the strait. The resulting depositional elements being tidal dune fields, isolated dune fields, and detached sandbanks. The narrowest part of a strait in Longhitano (2013), Longhitano and Steel (2017) models are typically dominated by bypass due to the increase in current velocity (Figure 9).

As a non-tectonic modern analogue, the Danish islands create several straits leading from the North Sea to the Baltic Sea. Studies done in the Fehmarn Belt show the same depositional elements as described by Longhitano and Steel (2017) and the Fehmarn Belt study (Feldens, Diesing, Schwarzer, Heinrich, & Schlenz, 2015), sand ribbons, sand patches, and dune fields. The thicknesses of these sand bodies are very thin at less than 1 to 2 metres (Feldens et al., 2015), additionally it is noted that the dunes appear only directly above the drowned nearshore deposits (Feldens et al., 2015) indicating that the dunes are mainly recycling older sediments. Laterally the sandbodies vary from hundreds of metres to kilometres. Water depths in the area are around 13 to 20 metres (Feldens et al., 2015).

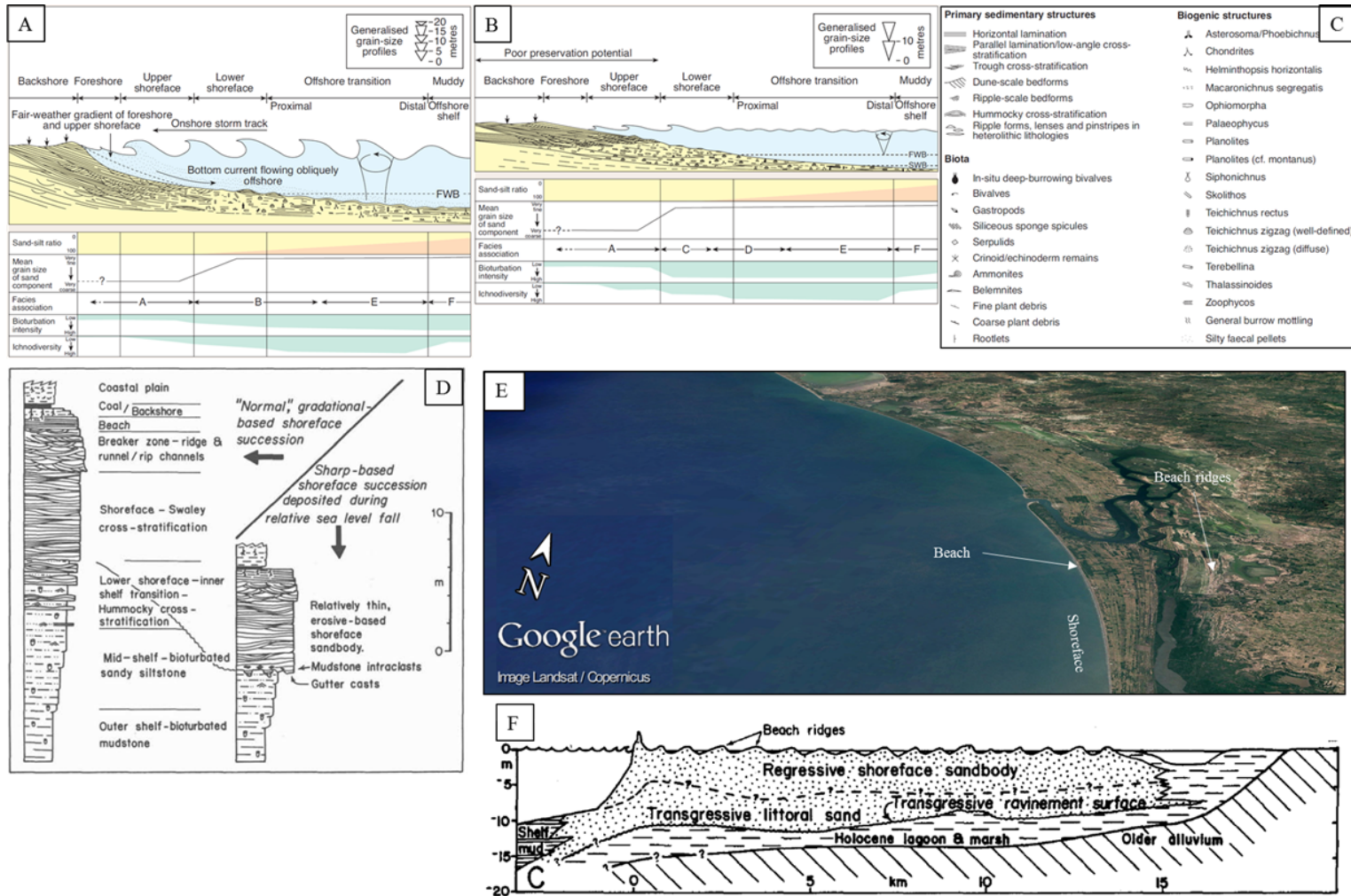


Figure 6: A: High energy shoreface model modified by Fraser et al. (2003) after Gowland (1996). B: Low energy shoreface modified by Fraser et al. (2003) after Gowland (1996). C: Legend for A and B modified by Fraser et al. (2003) after Gowland (1996). D: Facies log showing typical motifs for a storm dominated shoreface deposit (Walker & Plint, 2006) E: Satellite image showing the depositional element geometries in a storm influenced shoreface from the Coast of Nayarit in Mexico. F: A cross-section from the Coast of Nayarit in Mexico (Walker & Plint, 2006))

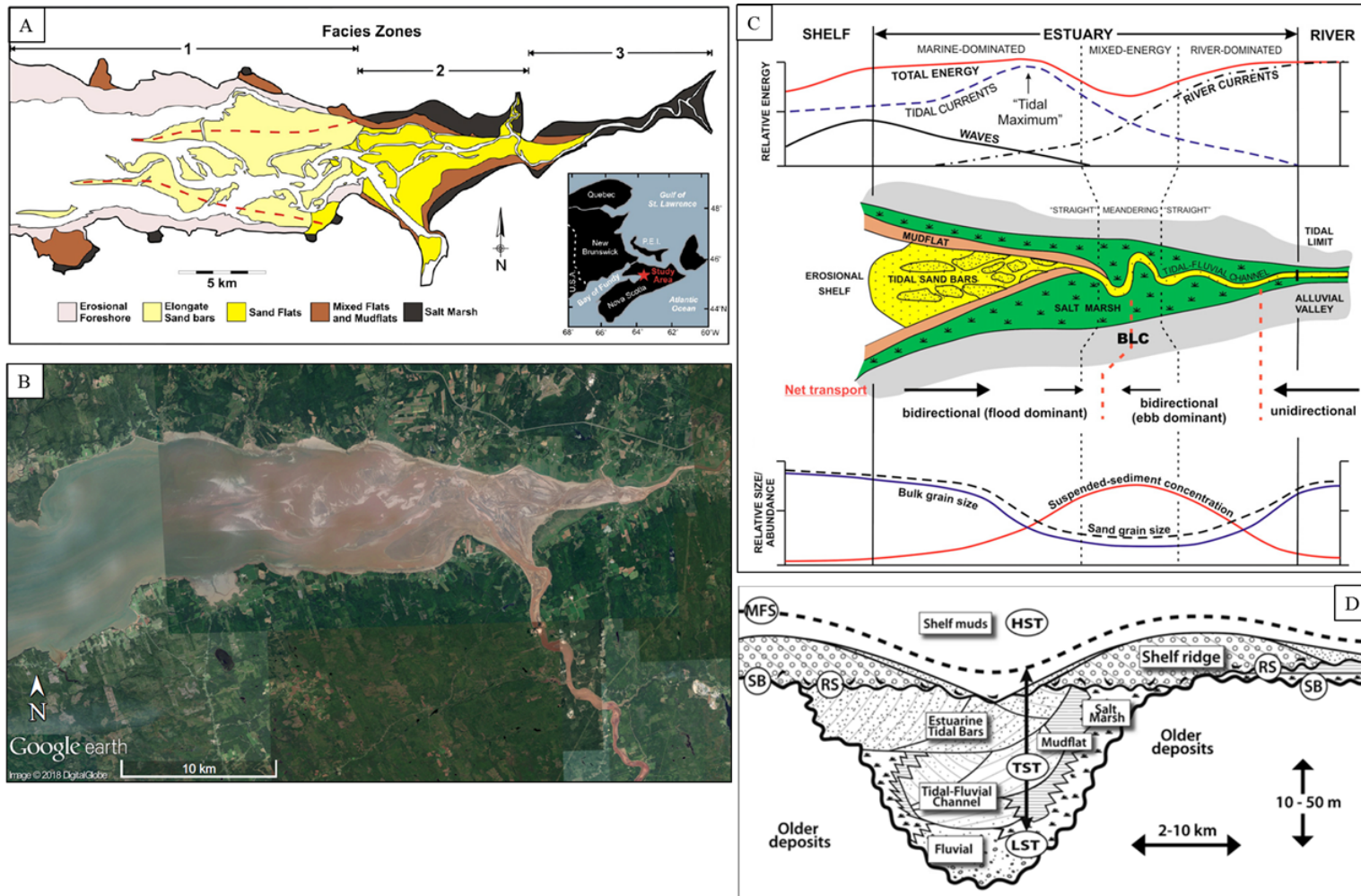


Figure 7: Estuarine depositional environments. A: The facies distribution within the Bay of Fundy See B for satellite photo, the maximal tidal range is 16.3 metres (Dalrymple & Choi, 2007). B: Satellite image of the Bay of Fundy, the sandbodies can be seen. C: A schematic map view figure and graphs showing how the energy and sedimentation varies in the different zones of a typical estuary (Dalrymple & Choi, 2007) D: An ideal cross-section of a transgressive deposit on a tidal shelf, showing possible vertical and lateral relations between different depositional elements (Reynaud & Dalrymple, 2012).

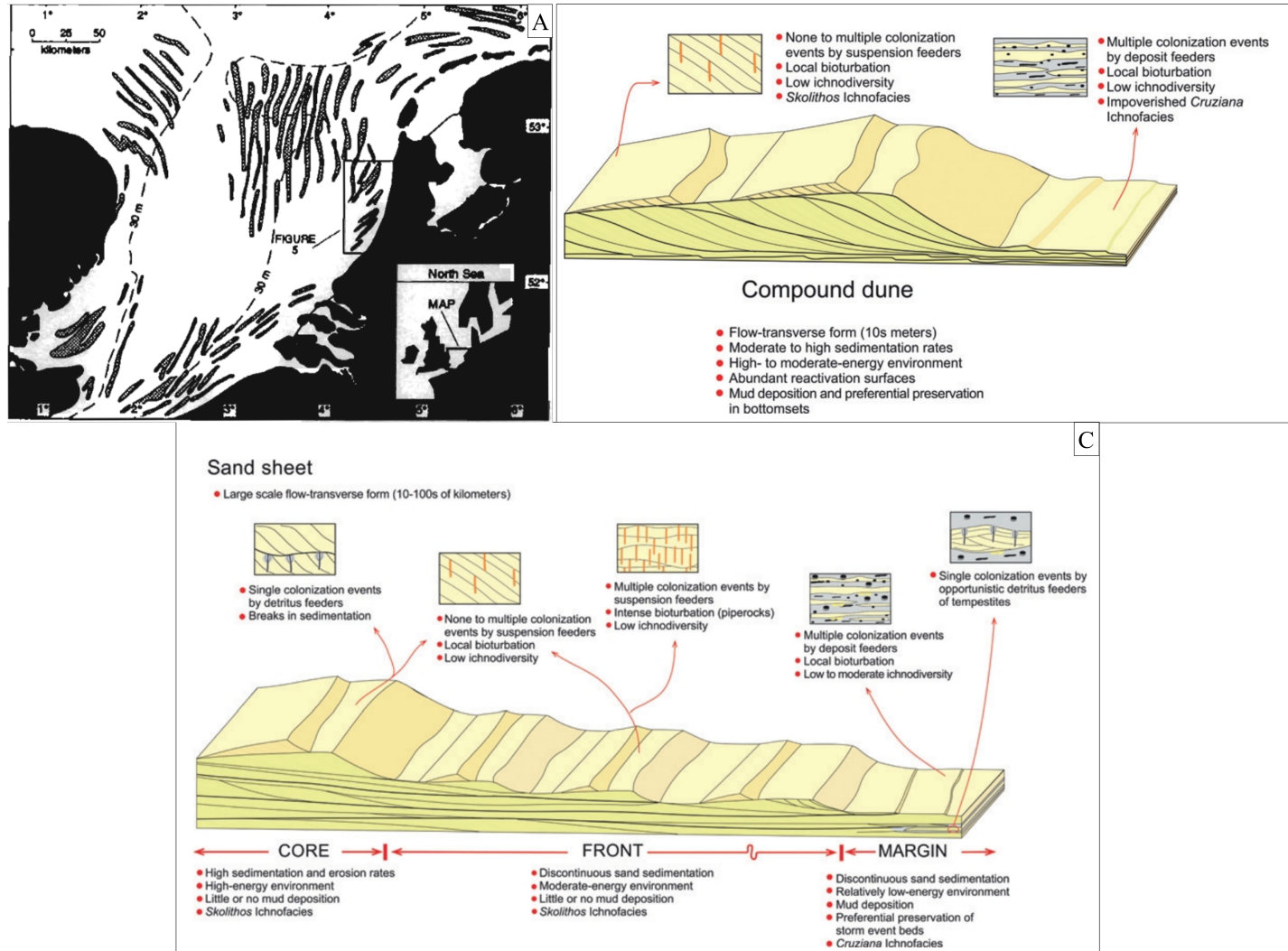


Figure 8: A: Shelfal deposits on the shelf south west of Britain (Snedden & Dalrymple, 1999). B: Expected bioturbation variation and morphology of a compound dune (Reynaud & Dalrymple, 2012). C: Expected bioturbation variation and morphology in a sand sheet (Reynaud & Dalrymple, 2012).

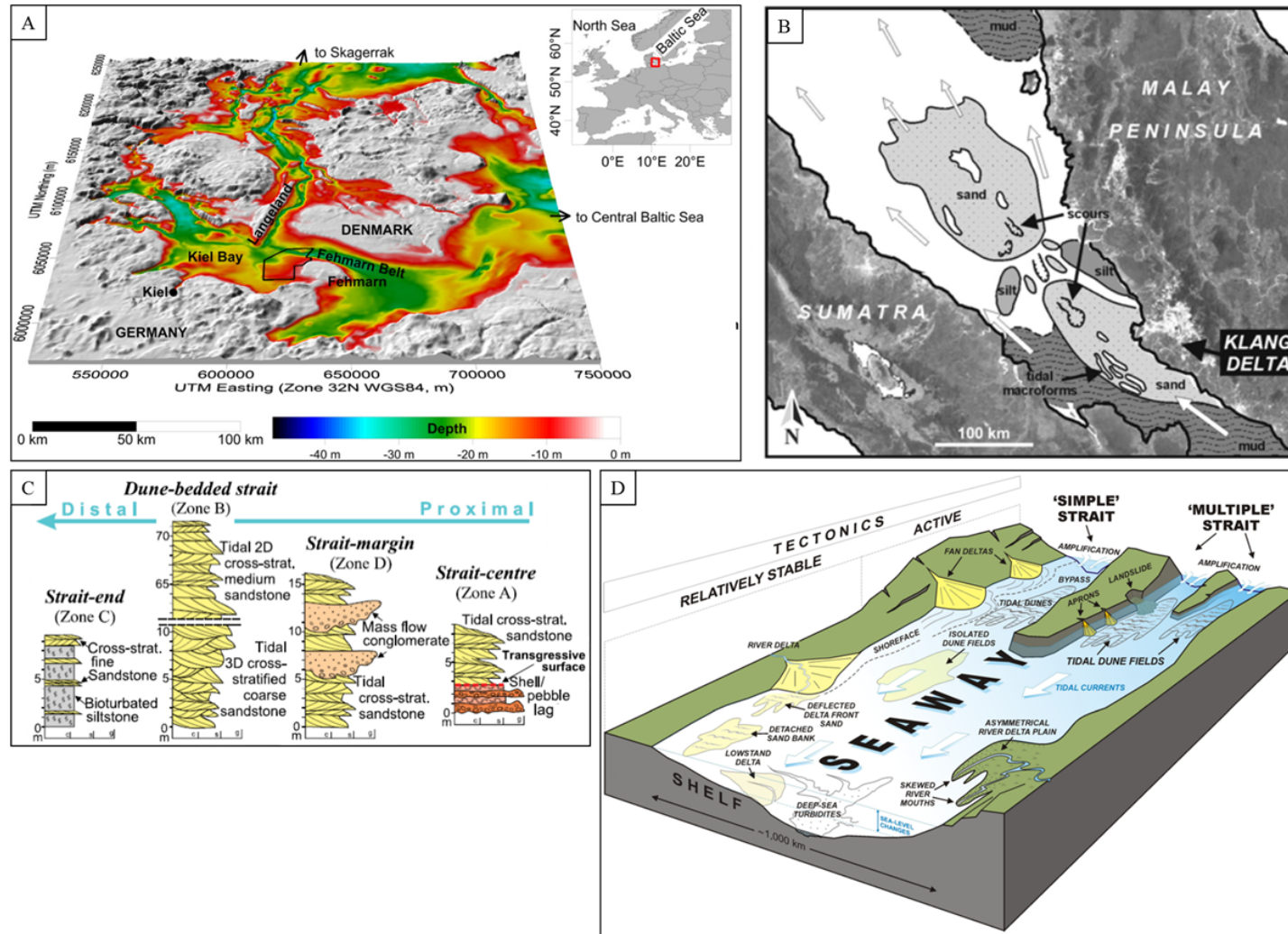


Figure 9: Strait depositional system. A: A topographic map showing the morphology of the Fehmarn Belt, a strait leading to the Baltic Sea (Feldens, Diesing, Schwarzer, Heinrich, & Schlenz, 2015). B: A map showing the deposition in the Malacca strait (Longhitano & Steel, 2017). C: Facies logs showing thicknesses, structures, and grain sizes of sand bodies deposited in straits (Modified after Longhitano (2013)). D: A visualization of depositional elements and architectures in a strait setting (Longhitano & Steel, 2017).

2.4 Syn-Rift Basin-Fills – Sequence Stratigraphy of Salt- Structured Rift-Basins

In syn-rift deposits the local variations in uplift caused by rotating faultblocks complicate the use of typical sequence stratigraphic methods which are meant to be used for passive margin deposits. Steel and Ravnås (1998) describe a syn-rift deposit as being mainly controlled by local fault movements and overall basinwide background subsidence only to a lesser degree by regional eustatic changes. Adding halokinetic movements on top of this makes it easy to understand how the tectonic activity might have overprinted the overall eustatic changes in turn rendering general sequence stratigraphic methods lacking for this kind of basin. There is also uncertainty regarding the salt movement, did it happen everywhere at once or were the salt walls moving independently of each other. This has the potential to affect each individual basin differently. According to Steel and Ravnås (1998) the controlling factor regarding depositional environments in rift-basins is the accommodation creation versus sediment supply. Defining if the basin is overfilled, balanced, underfilled, or starved can help in understanding the types of deposits which are generated. Importantly this might change through time.

3 Geological Setting

3.1 Tectonic Evolution of the Central Graben (Central North Sea)

The Central Graben in the North Sea is a part of an intracratonic basin which has a structural history containing several rift-events and is also shaped by halokinetism and lastly inversion. The basin started taking shape already in the Devonian, with a period of rifting, which continued into the Carboniferous and also formed the “proto” Viking Graben (Coward, Dewey, Hempton, & Holroyd, 2003). The Permian did also have some reactivation of faults, but more importantly it was during the Permian in which the Zechstein salt was deposited (Glennie et al., 2003). During the Triassic there was renewed rifting, combined with halokinetism, and the Triassic “pods” were deposited. The Triassic “pods” are typical minibasin deposits, which were deposited in the areas where salt withdrew. North-westernly trending grabens were formed due to the Triassic rifting event (Coward et al., 2003).

At the beginning of the Jurassic the grabens were fully formed, and the terrain was strongly affected by the diapirs and salt walls (Coward et al., 2003). Initially in the Jurassic there was little rifting, the period was instead characterized by uplift and erosion. During the Late Jurassic the rifting event, which formed the northwest to southeast trending Central Graben as it is known today, took place (Coward et al., 2003). The salt was also moving creating accommodation space for the Ula Formation which was deposited on top of the salt walls (Fraser et al., 2003).

Following the extensional regime which shaped the structural evolution until the Cretaceous was a period of inversion, most probably associated with the early Alpine collision (Coward et al., 2003). This inversion was more prominent in the Central Graben of the Danish sector, but also the Cod Terrace and Sørvestlandet High has been affected (Coward et al., 2003). The effect of this can be seen in the Ula Field where an anticline has been formed due to post Jurassic inversion (Mannie et al., 2014).

3.2 Structural Elements in the Study Area

The Permo-Triassic rifting divided the basin into horsts, terraces, and grabens trending north-west to south-east, in the study area it is the Sørvestlandet High which is the local horst. The Cod Terrace, is a terrace in the transition zone from the deep Central Graben to the Sørvestlandet High horst (Figure 1).

3.3 Triassic-Jurassic-Early Cretaceous Lithostratigraphy

The Ula Formation has been categorized as a shallow marine sandstone with an age of Oxfordian to Volgian (Fraser et al., 2003). It is followed by the Mandal Formation, a marine shale with an age from Portlandian to Ryzanian (Figure 10). The Ula Formation rests on an unconformity which is referred to as the Mid-Cimmerian Unconformity, below this are formations of Late Triassic (The Skagerrak Formation) and Middle Jurassic (The Bryne Formation) ages. They are both fluvial deposits.

It has been ascertained that erosional surfaces cannot be used to correlate across minibasins in the area because it was likely local uplift which caused the erosion as opposed to regional events (Wonham et al., 2014). The sequence-stratigraphic framework was originally defined by maximum flooding surfaces restricted by biostratigraphy (Partington, Mitchener, Milton, & Fraser, 1993). Eleven genetic sequence boundaries were proposed by Partington et al. (1993) to create correlative surfaces across the North Sea (commonly known as the J-sequences; Figure 10). Three cycles have been proposed, separated by tectonically enhanced maximum flooding surfaces and represent times of major basin floor reorganization (Partington et al., 1993). Other authors have since based their sequence-stratigraphic framework on these J-sequences (Wonham et al., 2014; Mannie et al., 2014), however, according to Wonham et al. (2014) some revision is required.

Since the Ula Formation has been heavily influenced by syn-depositional tectonism and halokinesis, local tectonic events might overprint the regional eustatic changes which can complicate correlations across basins as mentioned in Chapter 2.4. For example, Mannie et al. (2014) argues that the deposition of the Ula Formation is highly diachronous, implying that the basins are separated. In general, correlation on a reservoir scale is good, but between interpod-basins it is highly variable. Mannie et al. (2014) also showed the importance of combining seismic and well-data in the correlation of the Ula Formation due to the poor cross interpod-basinal correlation.

The Mid-Cimmerian Unconformity represents a highly erosive regional unconformity caused by a domal uplift (Andsbjerg, Nielsen, Johannessen, & Dybkjær, 2001). The greatest amount of erosion occurred towards the centre of the dome, therefore the transgressive Upper Jurassic sandstones are progressively overlying older formations (Wonham et al., 2014).

The age of the Ula Formation is highly variable, it has been dated younger in the Ula Field compared to the Tambar and Gyda fields (Mannie et al., 2014). Due to the formation being deeply buried in some areas and highly diachronous, there are uncertainties regarding the dating of the rocks (Mannie et al., 2014). Therefore, it is possible that the fluvial Bryne Formation deposited in the Ula Field might be of the same age as the oldest Ula Formation in the Gyda and Tambar fields.

If the sediments for the Ula Formation was not derived locally but transported from the basin margins as proposed by Weibel, Johannessen, Dybkjaer, Rosenberg, and Knudsen (2010) and Mannie et al. (2014) one would expect to have had larger fluvial systems at that time. The only remnants of fluvial deposits in this area which could have a similar age is the Bryne Formation, which is why it is suggested that these deposits might be time equivalent to the older parts of the Ula Formation.

Period	Epoch	Age	Genetic Units	Flooding Surfaces	Lithostratigraphy			
			Partington et al. (1993)		Cod Terrace	Sørvestlandet High		
Neogene	Pliocene							
	Miocene							
Palaeogene	Oligocene				Hordaland Gp.			
	Eocene				Rogaland Gp.			
	Paleocene				Shetland Gp.			
Cretaceous	Late				Cromer Knoll Gp.			
	Early	Ryazanian	L	J76	K10 <i>Stenomphalus</i>			
Jurassic	Late	Portlandian	L	J70	J74	J74 <i>Preplicomphalus</i>	Mandal Fm.	
			E	J73	J73 <i>Anguiformis</i>			
		Kimmeridgian	L	J72	J72 <i>Okusensis</i>			
			E	J71	J71 <i>Fittoni</i>			
			M	J66B	J66B <i>Pectinatus</i>			
			M	J66A	J66A <i>Hudlestoni</i>	Farsund Fm.		
	Oxfordian	L	J64	J64 <i>Autissiodorensis</i>				
		E	J63	J63 <i>Eudoxus</i>				
	Middle	Bathonian	L	J62	J62 <i>Bavlei</i>			
			M	J56	J56 <i>Rosenkrantzi</i>	Ula Fm.		
		E	J54	J54A <i>Glosense</i>				
	Early	Aalenian	L	J52	J52 <i>Densiplicatum</i>			
			E	J46	J46 <i>Lamberti</i>			
		Bajocian	L	J44	J44 <i>Coronatum</i>			
			M	J42	J42 <i>Calloviense</i>			
		Sinemurian	L	J36	J36 ? <i>Discus</i>			
			E	J34	J34 ? <i>Subcontractus</i>			
	Hettangian	L	J33	J33 ? <i>Progracilis</i>				
E		J32	J32 <i>Parkinsoni</i>					
Triassic	Late	Toarcian	L	J26	J26 ? <i>Garantiana</i>	Bryne Fm. ?		
			E	J24	J24 ? <i>Discites</i>			
	Middle	Pliensbachian	L	J22	J22 <i>Levesquei</i>			
			E	J18	J18 <i>Falciferum</i>			
	Early	Sinemurian	L	J16	J16A <i>Maraaritatus</i>			
			E	J14	J14 base <i>Margaritatus</i>			
		Bajocian	L	J12	J12 <i>Raricostatum</i>			
			E	J06	J06 <i>Oxynotum</i>			
		Hettangian	L	J04	J04 <i>Angulata</i>			
			E	J02	<i>Tr Planorbis</i>			
Permian	Early	Hettangian			Mid-Cimmerian Unconformity			
					Skagerrak Fm.			
Permian	Middle	Hettangian			Smith Bank Fm.			
					Zechstein Gp.			
Permian	Late	Hettangian			Rotliegende Gp.			

Figure 10: Sequence stratigraphic framework figure created by Mannie, Jackson, and Hampson (2014) based on the J-sequences proposed by Partington, Mitchener, Milton, and Fraser (1993).

4 Data and Methodology

4.1 Data

4.1.1 Cores and Wells

The dataset included 18 wells, where the majority of the wells are located in the Ula Field area (Figure 11). Cores were examined from five of these wells, where three cores (from wells 7/12-6, 8/10-5S, and 8/10-6S) were selected to be the focus cores, representing the Ula Formation. The focus cores were selected based on their coverage and was determined to be representative of the Ula Formation through examination of the other cores. Additionally, three cores from production wells which were not included in the Petrel dataset was examined.

All the wells contain check-shot velocity data, and an extensive set of logs including gamma-ray, resistivity logs, neutron and density logs as well as calliper and sonic logs. Two sets of well tops were provided by Norske Shell, for chronostratigraphy and formation tops from Open Works as well as the official well tops from the Norwegian Petroleum Directorate.

4.1.2 Seismic

Two 3D seismic datasets were provided by Norske Shell, MC3D-JHUN99R09 (MEGA) and PGS16008 (PGS; Table 1). The PGS survey has been acquired recently, however it does not cover the entire study area and therefore the MEGA survey was provided to get a full coverage (Figure 11). The MEGA survey was created based on several different existing datasets in this area, the main survey used in the study area is called MC3D-JHUN99R09. Whereas, PGS is a recently acquired broadband seismic survey. Both seismic cubes have a European polarity, meaning that an increase in acoustic impedance will result in a trough, and a decrease in acoustic impedance will result in a peak. In this study the colour-table used show troughs as blue, and peaks as red. Regional interpretations of top salt and the BCU (Base Cretaceous Unconformity) were provided by Norske Shell to be used as a guide so that the focus could be on the reservoir interval as opposed to first having to understand the regional trends.

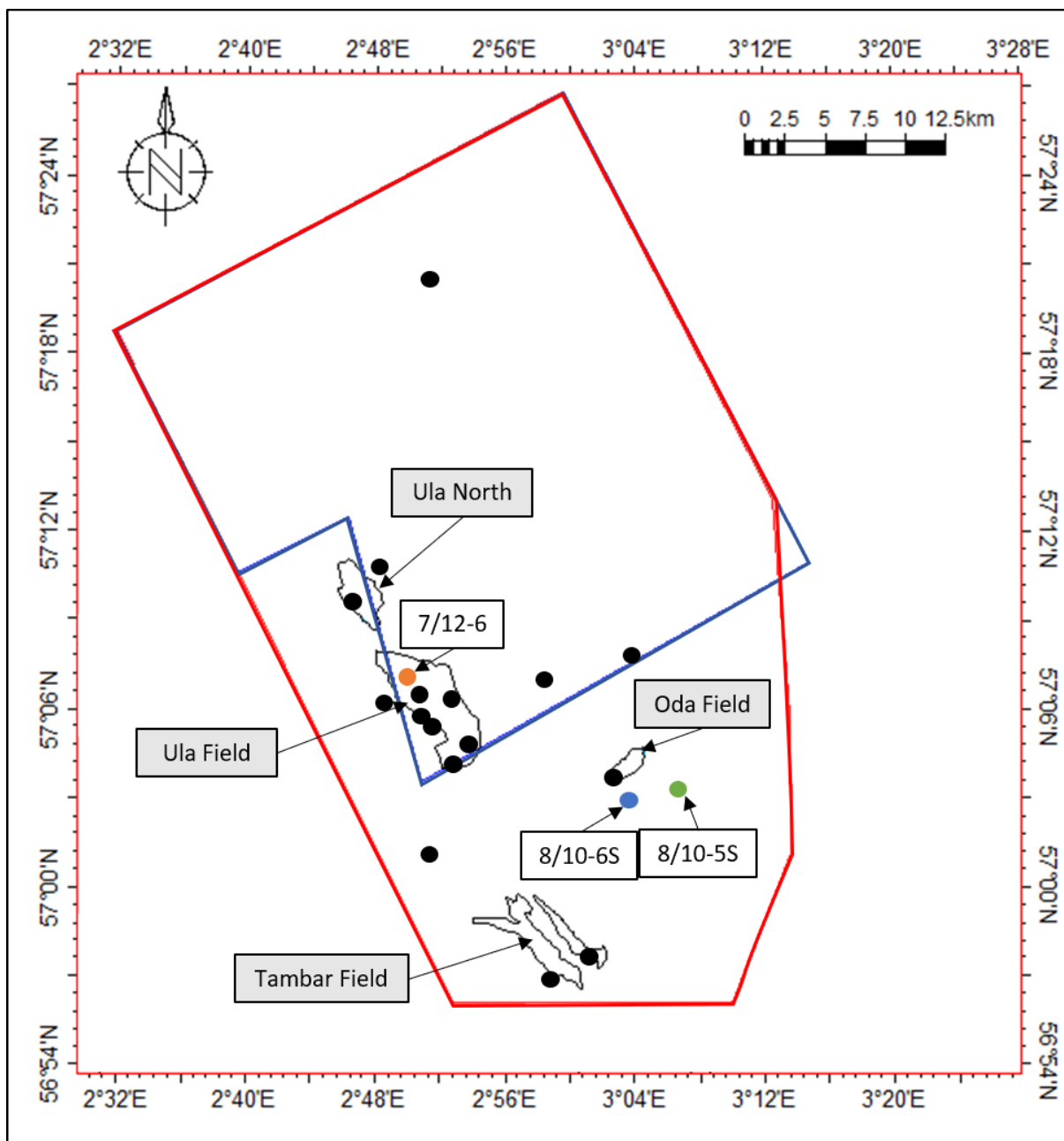


Figure 11: The blue polygon represents the area covered by PGS seismic, and the red polygon shows the outline of available MEGA seismic. Positions of available wells have been marked with black dots, and wells which were used for correlation have been highlighted. Outlines of fields have been provided by Norske Shell.

Table 1: Information about seismic cubes

	MC3D- JHUN99R09 (MEGA)	PGS16008 (PGS)
Year	1999	2016
Acquisition	Conventional	3S Geostreamer (2 different boats used, Ramford Vanguard, and Sanco Swift)
Source size	3090 cu.in.	G II Gun (Ramford) or Bolt 1900/1500 (Sanco)
Streamers	8	10 (Ramford) or 12 (Sanco)
Streamer length	3600 m	8100 m
Streamer spacing	100 m	75-94 m (fan-mode)

4.2 Methodology

4.2.1 Cores and Wells

Cores have been interpreted based on grain size, trace fossils, fossil content, sedimentary structures, and bed stacking pattern(s), with emphasis on identifying architectural elements and depositional sub environments. To get a full representative motif of the Ula Formation in the Sørvestlandet High, cores from two wells were used, one of them which was faulted (core from well 8/10-5S), and the other one which had not been cored in the youngest part of the formation (core from well 8/10-6S). There was another available core, 8/10-4S, the main reason that this was not used is that the oil stain made it more difficult to see the sedimentary structures and it seemed to show the same characteristics as the two selected wells. They were combined to generate a motif representing the entire evolution of the formation. Well 7/12-6 was used to represent an ideal log from the Cod Terrace, this is the thickest available core from the Ula Formation on the Cod Terrace (Table 2).

Additionally, three cores from a production well was examined, as they contained more sedimentary structures. The cores from wells 7/12-4, and 1/3-9S were logged as initial candidates to represent the Ula Formation in the Cod Terrace. However, they did not contain as much sedimentary structures compared to the core from well 7/12-6 which was finally selected.

Several published interpretations of the core from 7/12-6 exists most recently by Baniak et al. (2014) and Mannie et al. (2014) focusing on different parts of the sedimentology and ichnology. In this study the core from well 7/12-6 was interpreted and compared to the cores from the Sørvestlandet High. In addition to the three cores which were used to make

Table 2: Information about cores.

Well	Total metres of core	Location	Field	Comment
1/3-9S2	104.8	Cod Terrace	Tambar	Logged
7/12-4	108.2	Cod Terrace	Ula	Logged
7/12-A-12	25.5	Cod Terrace	Ula	Examined
7/12-A-15	143.7	Cod Terrace	Ula	Examined
7/12-A-18	137.3	Cod Terrace	Ula	Examined
8/10-5S	97.6	Sørvestlandet High	Oda	Logged, used to represent Ula in Sørvestlandet High
8/10-4S	69.4	Sørvestlandet High	Oda	Logged
8/10-6S	53.5	Sørvestlandet High	Oda	Logged, used to represent Ula in Sørvestlandet High

a general motif for the Ula Formation, several other cores were examined to determine if the selected ones were representative. The additional cores, were also used to strengthen the interpretation of certain facies. Intensity of bioturbation has been described using the bioturbation index (Figure 12) which was created by Reineck (1963) and later realized by Taylor and Gawthorpe (1993).

The three focus cores were used to divide the formation into facies, which were thereafter grouped into facies associations. Since the cores are heavily bioturbated, the facies which contain visible sedimentary structures have been weighted more during the interpretation. The bioturbation has led to the obliteration of any primary sedimentary structures, which makes interpretation of depositional process and setting highly uncertain in the strongly bioturbated sections. Therefore, the less bioturbated facies have been interpreted first to get a general idea of the depositional environment. The overly bioturbated facies have thereafter been interpreted with this environment in mind as well as based on how they occur among the less-bioturbated facies.

Well interpretation and correlation has been done along with the interpretation of the cores to further investigate the lateral changes of the sandstone successions. Depth matching of the cores and wells was achieved using the calcite nodules, as they give a very characteristic manifestation on the sonic and neutron-density logs and are easily identifiable in the cores.



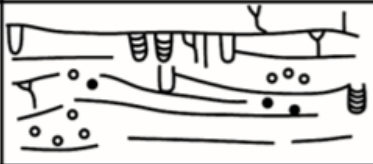




Grade	Percent bioturbated	Classification	Visual representation
0	0 %	Bioturbation absent	
1	1 to 4 %	Sparse bioturbation, bedding distinct, few discrete trace fossils	
2	5 to 30 %	Uncommon bioturbation, bedding distinct, low trace fossil density	
3	31 to 60 %	Moderate bioturbation, bedding boundaries sharp, trace fossils discrete	
4	61 to 90 %	Common bioturbation, bedding boundaries indistinct, high trace fossil density with common overlap	
5	91 to 99 %	Abundant bioturbation, bedding completely disturbed (just visible)	
6	100 %	Complete bioturbation (total biogenic homogenization of sediment)	

Figure 12: A visual description of the bioturbation index which has been used to describe the cores in this study, the classification is based on work done by Reineck (1963) which was later realized by Taylor and Gawthorpe (1993), Bann and Fielding (2004) (Baniak, Gingras, Burns, & Pemberton, 2014).

4.2.2 Seismic

4.2.2.1 Accounting for Evaporite Effect on Seismic Imaging

Since the zone of interest is situated directly above salt walls and diapirs, the difficulty of imaging around salt bodies (Jones & Davison, 2014) has been acknowledged as this affects the confidence of the interpretation. Salt/evaporites typically have an extremely high acoustic impedance compared to typical rock formations (Jones & Davison, 2014). They additionally often result in very steeply dipping flanks which also causes increased difficulty in seismic imaging (Jones & Davison, 2014). Knowing this and observing the effect of salt on the seismic data used in this study, the confidence has been adjusted accordingly in areas with high proximity to salt.

4.2.2.2 Seismic Vertical Resolution

The seismic vertical resolution defines how thick any layer has to be imageable. Since this study uses both seismic, wells, and cores it is important to consider the variability in scale for the different datasets. In the cored intervals millimetre scale sedimentary structures can be identified, while in seismic only larger trends can be picked. To get a better understanding of which interfaces the different seismic reflections represent it is therefore important to make an estimate of the vertical resolution. An estimate of the vertical resolution of seismic in the reservoir area was calculated by dividing the wavelength of the seismic by 4. Measurements were made in the seismic surrounding each well (Table 8), the resolution defines how thick a package of sediment has to be to be distinguishable in the seismic and it has been defined to be quarter of the wavelength (Widess, 1973).

4.2.2.3 Seismic Well-Tie

Both seismic surveys were tied to the wells to enable well log to seismic correlation. The well-ties were done using a standard Ricker wavelet, and they were calibrated focused on the reservoir area. The density and sonic logs have been used to calculate acoustic impedance. After this the reflection coefficient was calculated based on the relative change in acoustic impedance. Since the reflection coefficient is in depth domain the checkshots, measurements of one-way-travel time in the well resulting in a time-depth relationship, were used to convert to the time domain. The reflection coefficient is convolved with the Ricker wavelet to create a synthetic seismogram.

Initially the synthetic seismogram was positioned according to the time depth relationship extrapolated from the measured checkshots. Since the checkshots are based on one-way-traveltime measurements and seismic is measured in two-way-traveltime, the synthetic

seismogram does not always correlate nicely with the seismic initially. This was corrected by shifting the synthetic seismogram up or down to get the best possible fit between the synthetic and the seismic. The time shift results in a new time depth relationship which is then used as the final time depth relationship. As a result the synthetic seismogram being based on well log data, its resolution is much higher than the seismic data. Therefore, in some wells there were minor mismatches after correlation. Bulk shifting was used to avoid stretching or squeezing the time-depth relationship.

Synthetic seismograms were created for all wells which were present in the two seismic cubes, and for the ones where it was considered necessary time shifts were applied (see Table 7 under results). Figure 13 shows well 7/12-6 with the time depth relationship before and after well-tie, this well in particular was shifted -20 milliseconds to achieve the best possible correlation. Thereafter the new time depth relationship was applied to the well for it to be used to guide the seismic interpretation. The coverage of density and sonic varied but was always present in the reservoir interval (Table 3), a few other well-tie results can be seen in Figure 14 and Figure 15.

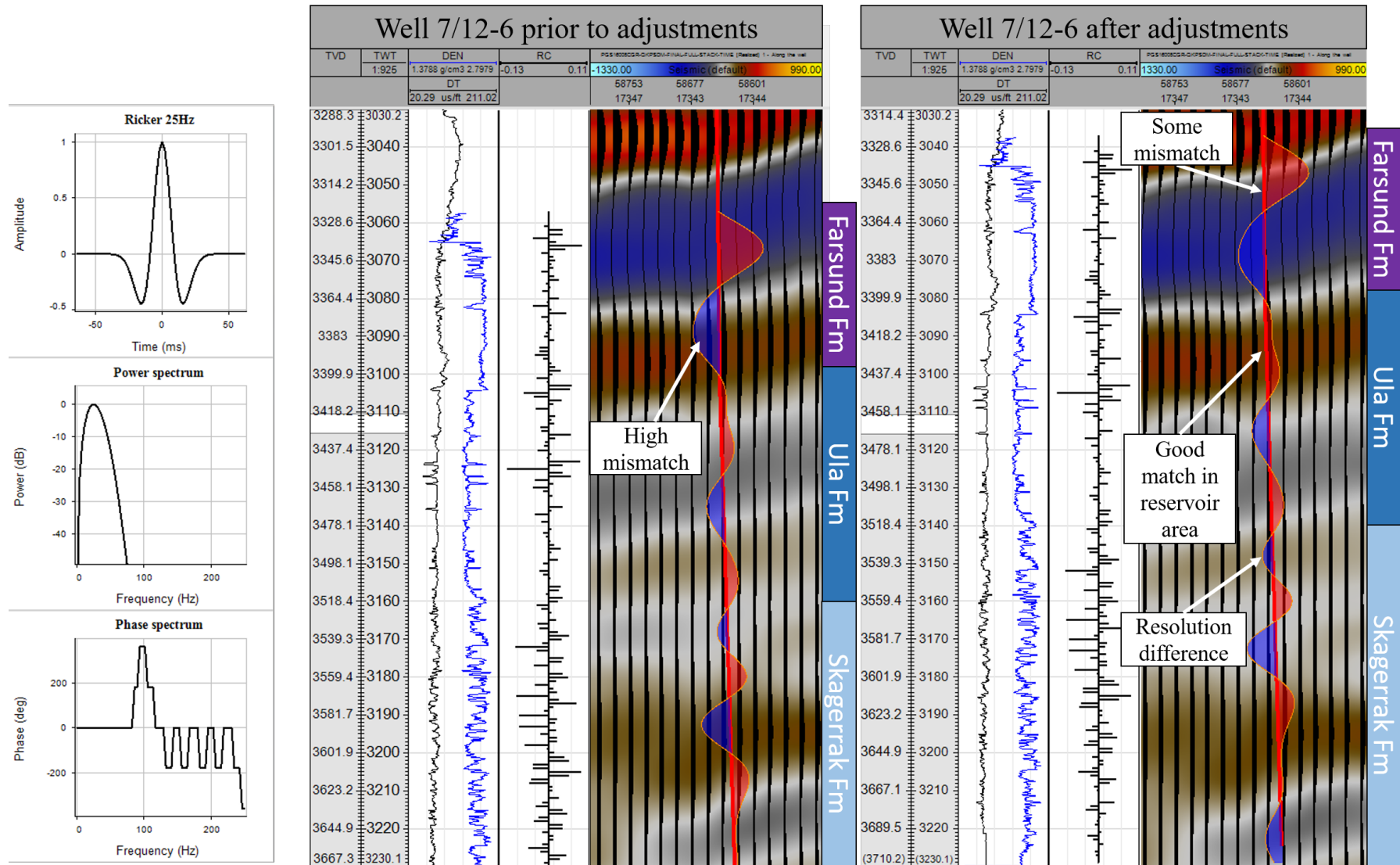


Figure 13: Synthetic seismogram and well-tie for well 7/12-6. The Ricker wavelet is displayed along with the power spectrum and frequency. Prior to adjustments there is a high mismatch, which is minimized after bulk shifting the well.

Table 3: Wells containing sonic and density.

Well	Sonic			Density		
	Present in reservoir	Overall presence [metres]		Present in reservoir	Overall presence [metres]	
		From	To [TVD]		From	To [TVD]
7/12-10	YES	954	3653	YES	2828	3156
					3598	3669
7/9-1	YES	1072	2937	YES	2144	2938
7/12-11	YES	934	3852	YES	2704	3864
7/12-13S	YES	172	4498	YES	3883	4520
7/12-2	YES	480	3659	YES	1510	3665
7/12-3A	YES	463	3960	YES	3467	3960
7/12-4	YES	491	3605	YES	3363	3616
7/12-5	YES	182	4437	YES	3691	4437
7/12-6	YES	169	3691	YES	3325	3699
7/12-7	YES	168	338	YES	3742	3844
		1004	3825			
7/12-8	YES	960	3895	YES	3710	3898
		172	354			
7/12-9	YES	945	3802	YES	3660	3816
1/3-3	YES	155	4867	YES	142	4872
8/10-5	YES	181	410	YES	751	2774
		701	2718			
8/10-4S	YES	235	3047	YES	2881	3043

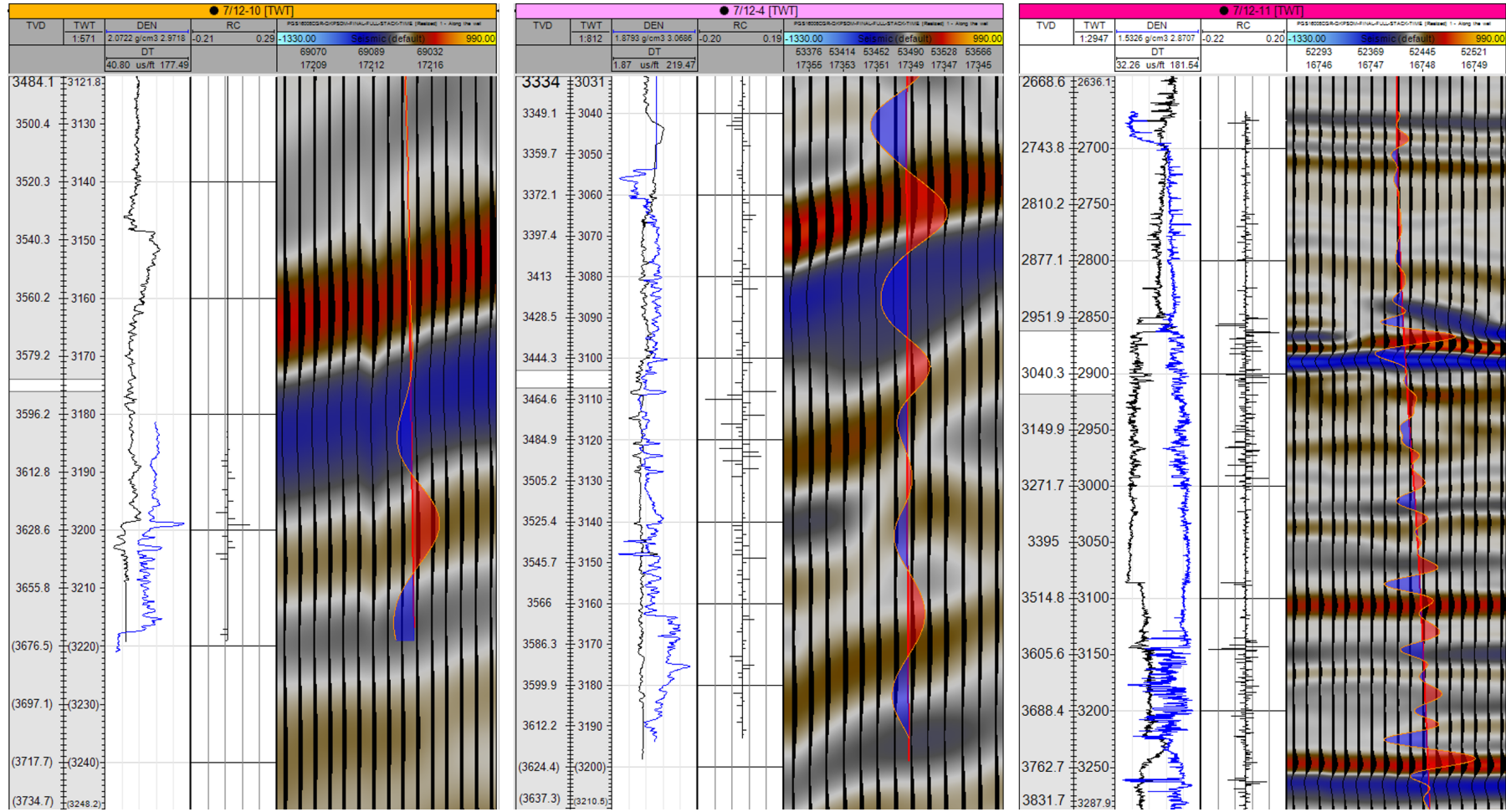


Figure 14: Synthetic seismogram and well-tie for well 7/12-10, 7/12-4, and 7/12-11.

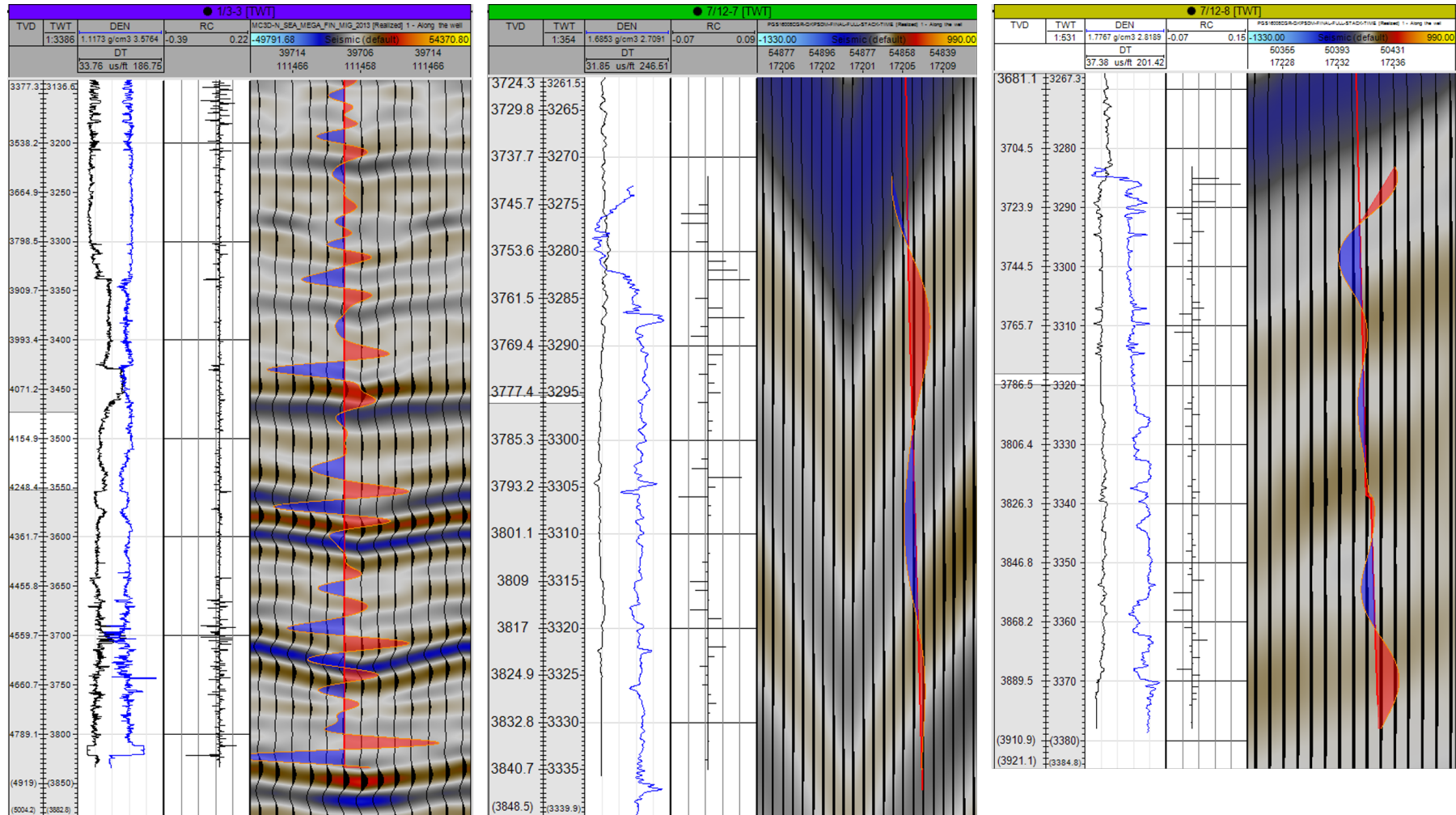


Figure 15: Synthetic seismogram and well-tie for well 1/3-3, 7/12-7, and 7/12-8.

4.2.2.4 Seismic Interpretation

Seismic interpretation was focused on defining regional bounding surfaces (base and top Upper Jurassic) and internal package-bounding reflectors where possible. Each seismic-stratigraphic unit was characterized, via seismic facies (e.g Reading and Levell (1996), Sangree and Widmier (1979)) and amplitude/frequency analysis was applied to infer the stratigraphic architecture, architectural elements, and thereby seismically defined depositional architectural elements. Seismic facies and attributes were tied to and calibrated by wells, and seismically defined architectural elements were calibrated to core data where available.

The interpretation was done in Petrel 2017 using guided autotracking, and different 3D and 2D autotracking methods dependent on the quality of the reflection. To retain the accuracy of the interpretations and inhibit the autotracking from ‘overinterpreting’, the parameters for autotracking were adjusted according to the quality of the reflector. For strong continuous reflectors the seed confidence was set at values from 50-30 percent starting at a high value, the correlation quality was kept at 0.60 and the quality was set to ‘Validated 5X5’. Weaker reflectors with higher discontinuities were typically first interpreted in a grid using the 2D autotracker along with guided autotracking. Thereafter, using a higher seed confidence (around 60-80 percent), a correlation quality of 0.85 or higher and a quality of ‘Validated 5X5’, the surfaces were 3D autotracked using seeded points as well as tracked within polygons excluding areas with high uncertainty. The settings were continuously adapted throughout the interpretation process, starting out with a ‘stricter’ set of parameters (high seed confidence, high correlation quality and a quality of Validated 5X5) thereafter the settings would be gradually lowered until a level where they were still regarded to provide an acceptable result. An acceptable result meaning that the auto-tracking tools do not jump between different reflectors or disregard abrupt changes creating an erroneous interpretation. For the reservoir top, the overlying strong reflector corresponding to the Farsund Formation was inserted as trend data to guide the 3D autotracking tools. This was done due to the top reservoir closely follows the overlying Farsund Formation reflector with hardly any change in thickness. All horizons were interpreted in both cubes as minor differences were noted.

The purpose of using 3D tracking tools where possible was to keep the interpolation to a minimum when the horizons were used to make surfaces. When the horizon is interpreted manually in a grid pattern the software will interpolate between datapoints in turn ‘smoothing’ the surface, when autotracking tools are used the interpretation will not be limited to a grid and the density of datapoints dramatically increase. Resulting in a more detailed surface making it possible to define faults and other features more clearly which might be present by simply using the lighting tools in Petrel.

In addition to the Upper Jurassic bounding horizons three other horizons were interpreted, the top Ekofisk Formation, internal Farsund Formation reflection, and an internal Ula Formation reflector. The Ekofisk Formation was interpreted to be used as a guide across the salt walls and diapirs as the interpretation has a very high confidence and the data quality in this area is good. Thereafter, the Farsund Formation internal reflector was interpreted. This reflector was chosen as opposed to the top reflector of the Farsund Formation because it had a higher amplitude and was more continuous. As well as having higher confidence it was also more proximal to the top reservoir. The top reservoir, or the top of the Ula Formation was thereafter interpreted. This reflector has higher uncertainty, as it is not as continuous and locally has a very low amplitude, in the areas of lower amplitude the amplitude of the Farsund Formation internal reflector was used to guide the interpretation. The internal reflector of the Ula Formation was only interpreted in the Ula Field where the confidence is higher due to the well density. Lastly the base Ula Formation was interpreted, this interpretation was done over the entire study area, but the reflector is highly discontinuous. Consequently, this interpretation is considered to be the one with the least confidence.

An isochore map was generated between the top and base of the Ula Formation in the Ula Field area. The map was made by subtracting the z values of the base surface from the top surface of the Ula Formation, therefore the map is in time. It was only created above the Ula Field as this is the area with the most confidence in the interpretation due to data quality. The thicknesses of the remaining areas were additionally estimated based on the seismic interpretation where the map was divided into three “zones”. The thickest zone being the thick interpod deposits, the intermediate being thin interpod deposits and the thinnest being the supra Triassic pods deposits.

4.2.2.5 Attributes

In order to visualize minor variations in amplitude and frequency continuity and intensity which could reflect the architectural element geometries, both amplitude and frequency attributes were applied. All attributes have been extracted along the top reservoir surface or on determined intervals above and below to represent sections of the reservoir. To compare the results attribute extraction was applied to both seismic surveys, on their corresponding surfaces with their corresponding windows.

After applying several different attributes (Root-Mean-Square (RMS), Average Amplitude, Frequency Decomposition, Sweetness, Sculpting, and also simply extracting the amplitudes) the best results were achieved for Sculpting provided by Norske Shell, which was used as the frequency attribute and RMS which was used as the amplitude attribute. Sculpting was provided by Norske Shell based on the interpretation of the top Ula Formation surface and calculated windows and shifts. RMS has been applied to the surface in

an attempt to enhance variability in the amplitude. It is based on calculating the average value of the amplitude, using the square root of the average to the power of two, of the amplitude over an interval. RMS is affected by changes in seismic impedance (Chopra & Marfurt, 2008).

Windows of attribute extraction were determined by measuring average thicknesses (in time) of reservoir units based on areas with good well control. They were determined to represent either the uppermost unit in the formation, the internal reflector, the basal unit or the Ula Formation as a whole. Two sets of windows were applied to account for both thicker and thinner reservoir areas.

In the thicker areas two units can be distinguished in seismic, the upper and lower unit, reflected in the wells as a flooding surface. The windows of attribute extraction were adapted to this, when measuring. There were also some differences between the two seismic cubes this was also accounted for. All the windows and shifts (from the top reservoir) are listed in Table 4, a-windows are measured in the interpod areas and b-windows are in the Triassic pod areas. Window 1 encompasses the top Ula Formation reflector, Window 2 represents the lower unit, Window 4 represents the upper unit, and Window 3 represents the entire Ula Formation.

The uppermost unit have stronger amplitudes and when interpreting the maps, which encompass both zones, the response from the uppermost zone overpowers the results of the lowermost zone making this map is nearly identical to the map for the uppermost zone (Figure 16; Figure 17). The map representing the lowermost zone is only valid in the interpod areas. However even when applying the map only to these areas it is very dim and do not contain a lot of information. Therefore, the upper unit maps were used for interpretation.

The amplitude extract maps from the PGS cube are dominated by artificial trends (Figure 17). These streaks/ripples are caused by the reflections disappearing and reappearing (Figure 18), likely as a result of multiples which occur frequently below the BCU (Base Cretaceous Unconformity). Because of this effect, results from the MEGA cube has been weighted as they show this to a lesser degree (Figure 16), most probably because this data is older and has had more time to be processed.

Table 4: Windows of investigation for attribute generation, measured in milliseconds.

PGS			
Window 1a	56	Window 1b	17
Start 1a	9	Start 1b	5
Window 2a	29	Window 2b	8
Start 2a	-18	Start 2b	-4
Window 3a	85	Window 3b	25
Start 3a	9	Start 3b	5
Window 4a	18	Window 4b	4
Start 4a	0	Start 4b	0
MEGA			
Window 1a	57	Window 1b	24
Start 1a	15	Start 1b	8
Window 2a	25	Window 2b	6
Start 2a	-17	Start 2b	-10
Window 3a	82	Window 3b	30
Start 3a	15	Start 3b	8
Window 4a	17	Window 4b	10
Start 4a	0	Start 4b	0

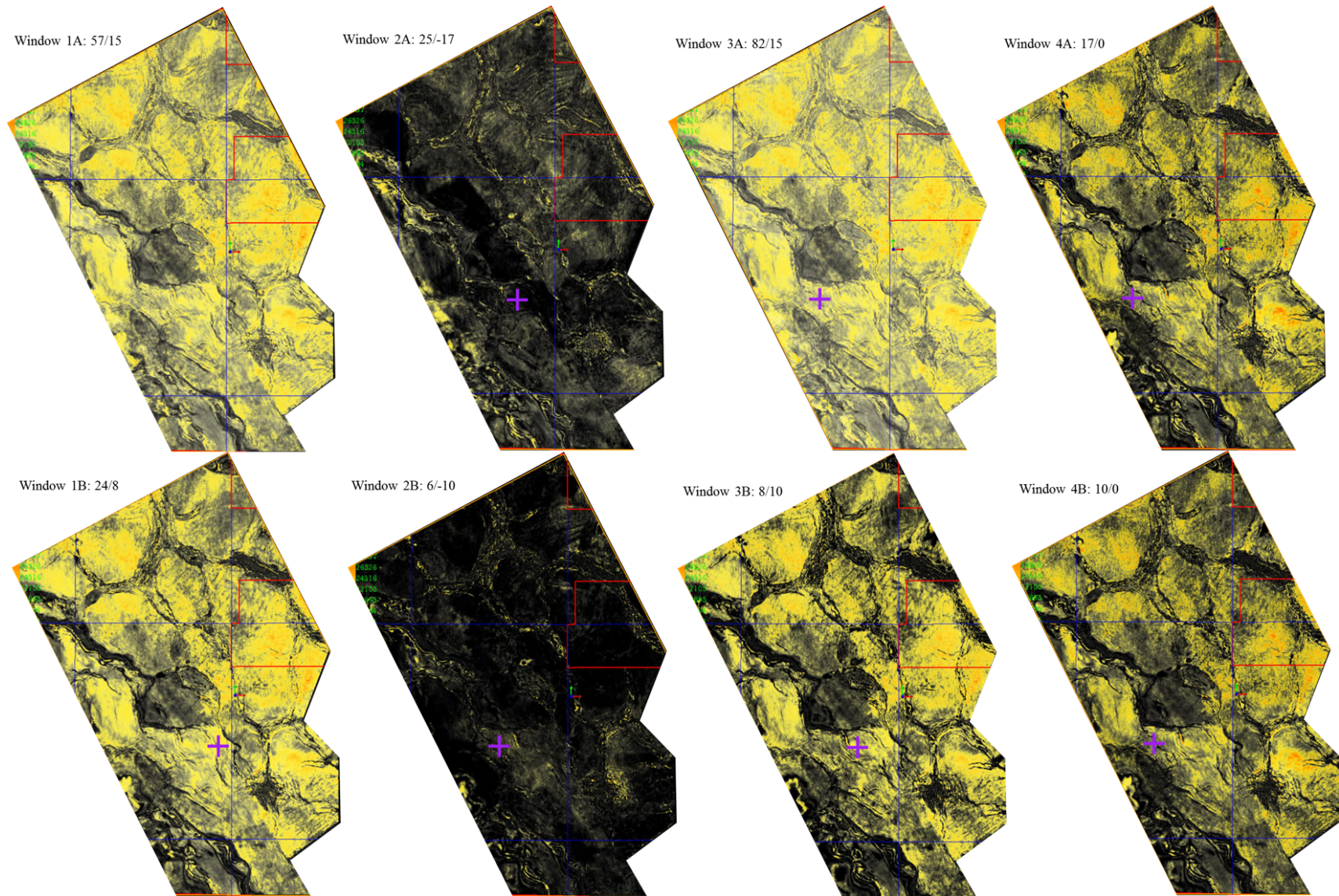


Figure 16: Attribute maps using sculpting for MEGA cube. For windows see Table 4.

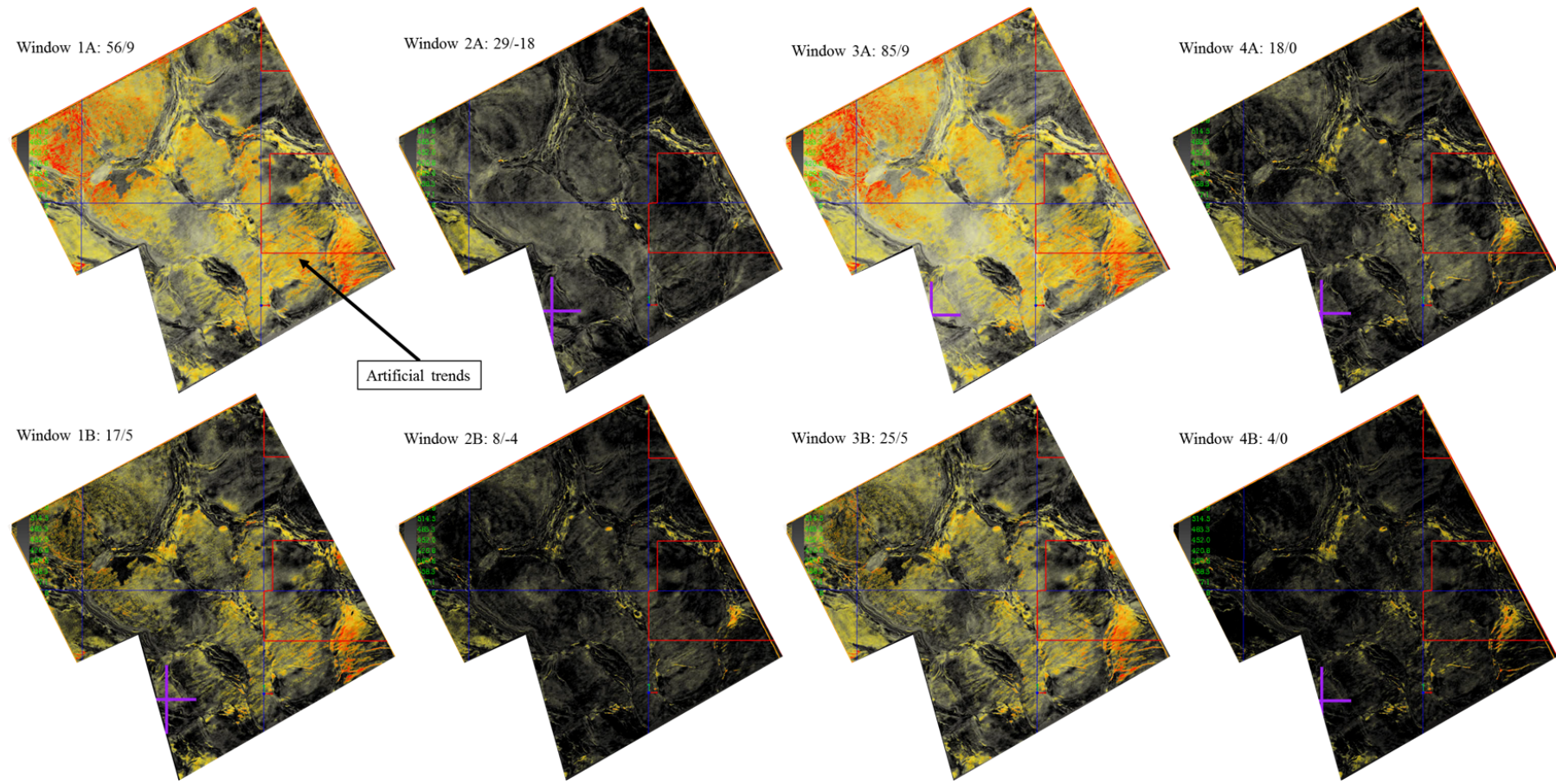


Figure 17: Attribute maps using sculpting for PGS cube. For windows see Table 4.

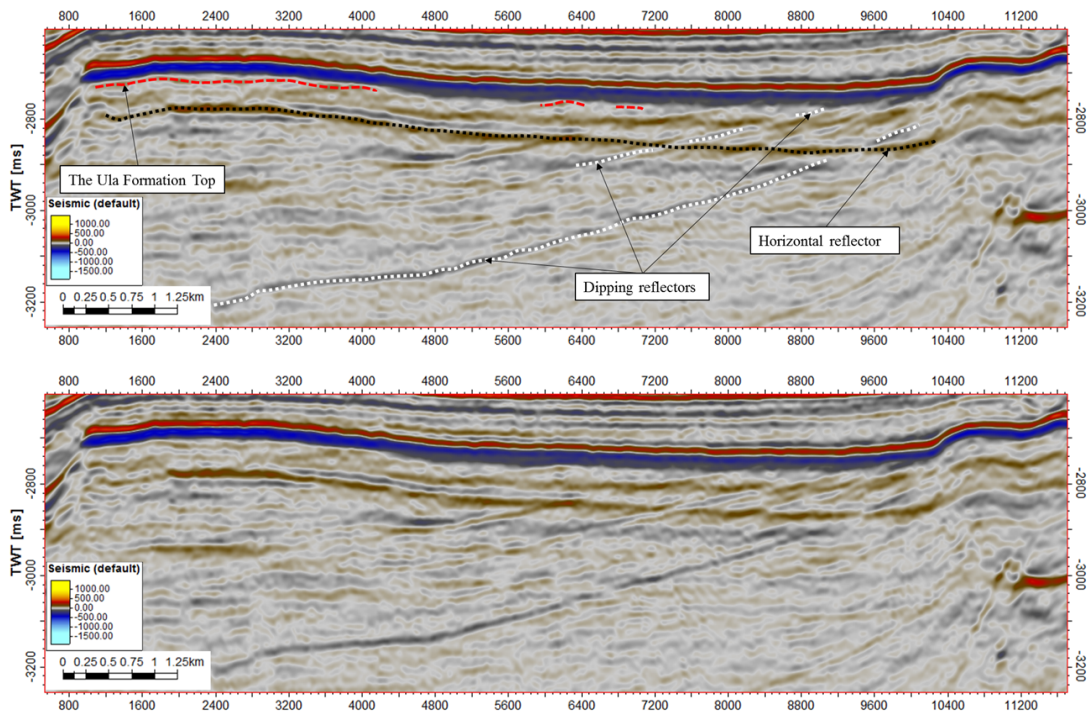


Figure 18: Seismic cross-section showing issues with artifacts influencing the attributes, the seismic lines show how there are intersecting reflections which cannot geologically be explained.

5 Results

5.1 Lithofacies Descriptions

5.1.1 Facies with Sedimentary Structures

Facies 1:

Description: Facies 1 (Table 6; Figure 19) consists of a fine- to medium-grained, cross-stratified sandstone. The facies commonly has a gradual base which transitions into Facies 5 or Facies 6. Cross-stratification occurs as sigmoidal sets with thicknesses below a decimetre, occurring as cosets with up to a few metres in thickness of vertically stacked sets. Double mud drapes and coal fragments occur locally. Bivalves and shell fragments are common. In areas with a high concentration of shell fragments calcite cemented patches occur, typically with rounded to irregular outer boundaries. The calcite cemented patches rarely reach thicknesses of more than a meter. Bioturbation diversity is intermediate to low, and the bioturbation index is 2 to 3, with local variations. There is typically an increase in shell concentration towards the end of each bed along with an increase in bioturbation.

Interpretation: The cross-stratified sandstone sets suggest formation by migrating dunes. Mud drapes suggest deposition as suspension fall-outs during repeated intervals of no current activity, i.e. slack water intervals. Sigmoidal cross-stratification in combination with presence of double mud-drapes indicating deposition of bi directional currents with a strong primary current and a weaker subordinate current is indicative of a tidal deposition. The occurrence of cross-stratified sandstone in cosets suggest that the facies normally combined to form vertically stacked dunes, likely in the form of compound dunes.

Intervening periods with lower energy or sedimentation likely resulted in lower dune migration rates or stillstand and allowed for colonization by marine faunas as evidenced by the increase in the shaly lamina zones and the presence of bivalve fragments in the more bioturbated sandstones. Bioturbation reflects a fairly open marine depositional environment. This facies is accordingly interpreted to have formed in a near to fully marine area with strong tidal current activity, such as distal reaches of tidal deltas, outer estuaries or in a tide-dominated shelfal setting. The relative shortage of mud in combination with a fairly open marine environment would rather favour an estuarine or shelfal setting above a deltaic origin. The thickness and curved bases of the calcite cemented patches is interpreted as calcite nodules as opposed to elongated calcite cemented layers. Nodules are likely not correlatable between wells.

Facies 2:

Description: Facies 2 (Table 6; Figure 19) is a well sorted, medium to fine grained cross-stratified sandstone, the cleanest sandstone encountered in the Ula Formation. The facies commonly has a gradual base overlying Facies 1 or Facies 3. Cross-stratification occurs as sets with decimetre thicknesses, stacked to form beds with thicknesses up to a few metres. Bivalves occur in specific intervals as in Facies 1, and calcite cemented intervals occur occasionally where the concentration of shells are highest. Bioturbation is minimal with a bioturbation index of 1, and the diversity of the tracks is low and they are typically medium sized. Bioturbation and shell fragments occur in higher frequency at the top of each bed.

Interpretation: The most notable characteristic of Facies 2 is the cross-stratification, which indicates deposition by mega ripples or dunes as in Facies 1. The sandstone is very clean and remarkably less bioturbated than the rest of the Ula Formation. This might indicate a higher energy or otherwise inhospitable environment. The partitioning into beds suggest that there were times of transport and deposition (the clean cross stratified sandstones) and periods of non-deposition or in the least less deposition (periods where organisms flourished, the top of each bed) when there might have been less sedimentation. The complete lack of mud deposition indicates a very high energy environment which did not allow for deposition of suspended material. Based on this, Facies 2 is interpreted to have been deposited in migrating dunes similarly to Facies 1, but in a higher energy environment.

Facies 3:

Description: Facies 3 (Table 6; Figure 19) is a conglomeratic to very coarse-grained sandstone. The base is always erosive and overlies Facies 2. Beds are normally graded, from conglomerates in the base to a coarse sandstone towards the top. Some of the large pebbles are very angular and the sorting is poor, in particular at the base. The bioturbation index ranges from 0 to 2. Higher bioturbation typically occur towards the top of a bed; the diversity is very low, and tracks are often of medium size. Beds are typically decimetres to metres thick. The facies is often cemented, with quartz or calcite and typically co-occurs with Facies 2, 7 and 8.

Interpretation: The erosive base indicates a period of erosion and non-deposition before sudden deposition of something very coarse and at times angular. The continuous deposition of coarse sand, and lack of bioturbation is indicative of a high energy environment. Due to the erosive conglomeratic base with angular grains, Facies 3 is interpreted as a channel lag.

Facies 4:

Description: Facies 4 (Table 6; Figure 19) is a very fine-grained sandstone with rare occurrences of asymmetric ripples. It is well sorted, normally graded with bed thicknesses varying from decimetres to metres. The facies is dominated by long vertical burrows and the diversity of the bioturbation is low with a bioturbation index is 4-5. The base and top of this facies is typically a gradual transition from Facies 10 or Facies 9.

Interpretation: The fine-grained nature of Facies 4 together with the faint ripple cross lamination indicate a low energy depositional setting dominated by unidirectional currents.

5.1.2 Facies Lacking Sedimentary Structures

Facies 5:

Description: Facies 5 (Table 6; Figure 19) is a silty fine-grained sandstone. It is heavily bioturbated, with a bioturbation index of 4. Burrows are often small to intermediate in size and the diversity is intermediate. Sedimentary structures cannot be recognized due to the intense bioturbation, and each bed can be anything from decimetres to a couple of metres in thickness. Coal fragments and clay clasts are present. Facies 5 typically co-occurs with Facies 1 and Facies 6.

Interpretation: The smaller size of the trace fossils combined with an intermediate diversity and high density of bioturbation could indicate a somewhat stressed environment (Gingras, MacEachern, & Dashtgard, 2012), while the fine grainsizes and silty content is indicative of a low energy regime. The coal fragments suggest terrestrial influence. Since Facies 5 lack any sedimentary structures the specific process of deposition cannot be definitively interpreted. Facies 5 is therefore interpreted to represent low energy possibly brackish environment with terrigenous influence.

Facies 6:

Description: Facies 6 (Table 6; Figure 19) is a siltstone, typically overlying Facies 5 with a gradual base and somewhat lower intensity of bioturbation with a bioturbation index of 3. As in Facies 5, bioturbation has obliterated any primary sedimentary structures. The bioturbation style is similar to that of Facies 5, and the diversity is low to very low. The Facies is very homogeneous and well sorted, some bivalve fragments are present along with rare occurrences of coal.

Interpretation: Facies 6 has characteristics similar to Facies 5, but with an environment which seems even more stressed and with lower energy than Facies 5. As in Facies 5 coal fragments can be identified which indicates a terrigenous influence. Therefore, Facies 6 is interpreted to have been deposited in a relatively lower energy environment compared to

Facies 5 also possibly with a brackish environment.

Facies 7:

Description: Facies 7 (Table 6; Figure 20) is a medium grained sandstone, it is very well sorted and homogeneous. The bioturbation can be categorized as cryptic and no primary sedimentary structures can be recognized. Recognisable burrows occur very rarely, when they do the diversity is low and the size is large. Facies 7 has a gradual base typically transitioning to the underlying Facies 2, Facies 3, or Facies 8. Shell fragments and patchy quartz cementation is common in this facies and occur periodically. The grading can be both normal and reverse, but in general the change in grain size is minimal. Beds have thicknesses of decimetres to metres. Facies 7 co-occurs with several different facies, Facies 6, 8, 8B, 2, 3, and 10.

Interpretation: The lack of sedimentary structures and the cryptic bioturbation gives room for several different interpretations of Facies 7. However, the grain size suggest a higher energy environment, and the cryptic bioturbation indicate that it was very hospitable. Since the facies is completely bioturbated the sedimentation rate cannot have been higher than bioturbation rate, unless sedimentation was only periodic. Although if the sedimentation was periodic one might expect to see mud deposited during the time it was inactive. The lack of finer grained sediments indicate that the energy might have been constantly high enough to keep suspended material from settling. Therefore Facies 7 has been interpreted as a high energy but hospitable depositional environment. Due to the intense bioturbation this facies has likely been deposited in a relatively open marine setting.

Facies 8:

Description: Facies 8 (Table 6; Figure 20) is a silty to fine-grained sandstone, it is heavily bioturbated and no primary sedimentary structures can be recognized. Both normal and reverse grading has been identified, and beds are thick with thicknesses of meters. The base of the facies is gradual transitioning into Facies 7 or Facies 3. The facies has a bioturbation index of 5 to 6 and the bioturbation consist of small to medium sized tracks with typically low to intermediate diversity. Calcite cementation has a curved top and base and occurs where there is a higher concentration of shell fragments.

Interpretation: The intense bioturbation has destroyed all sedimentary structures, but the fine grain size indicate a lower energy environment. High and consistent bioturbation activity indicates an environment with a relatively low sedimentation rate (as compared to the bioturbation intensity), which would allow the biota to thoroughly rework the sediment. Due to the low sediment input and extensive bioturbation, it is interpreted to have been deposited in an intermediate relatively constant energy setting and in a relatively open marine environment.

Facies 8B:

Description: Facies 8B (Table 6; Figure 20) is very similar to Facies 8, but Facies 8B contains more silt and is generally finer grained. It has been defined as a very silty fine-grained sandstone. Due to thorough bioturbation, no primary sedimentary structures can be identified. This facies typically has normal grading, and the thickness of beds are a few metres. The bioturbation is exactly the same as in Facies 8, low to intermediate diversity and small to medium size with a bioturbation index of 5 to 6. Shell fragments occur less in Facies 8B and this might be the reason for the lack of calcite nodules in this facies, however it should be considered that the nodules could have been present but were not cored.

Interpretation: The increase of finer grained material which might have been deposited from suspension is what separates this facies from Facies 8. Similarly, the intense bioturbation indicates an environment where the sedimentation rate is lower than the bioturbation rate. Due to the increase in mud, it is interpreted as a lower energy environment (relative to Facies 8). Additionally, the intense bioturbation is indicative of a relatively open marine environment without stressing factors for the biota.

5.1.3 Mudstone Facies

Facies 9:

Description: Facies 9 (Table 6; Figure 20) is a mud stone co-occurring with Facies 4. Like Facies 4 it is dominated by long vertical burrows and some smaller burrows (Chondrites) and has a low diversity of bioturbation. The burrows are sand filled, and it seems like they are burrowing down from the coarser Facies 4 into Facies 9. Beds generally have a thickness of decimetres and some parallel layering can be identified.

Interpretation: The parallel lamination indicates a very low energy environment. The large vertical burrows seem to be periodic, while the smaller Chondrite burrows are more persistent throughout the facies. Chondrite burrows are common in more distal settings as in a lower offshore setting after the classification of PEMBERTON ET AL 2012. Facies 9 is interpreted to have been deposited in a very low energy environment, where the deposition occurred by suspended fine grained material.

Facies 10:

Description: Facies 10 (Table 6; Figure 20) is a siltstone, varying from very poorly to moderately well sorted. It frequently contains large belemnite fossils with varying concentration. It is layered and has very little bioturbation with a bioturbation index of 0 to 1, the burrows present are small and diversity of them is low. Facies 10 co-occur with

Facies 7, 8, 8B, and 9.

Interpretation: The occurrence of large belemnite fossils and fine grained clastics indicate an open marine setting, where sediments are generally deposited from suspension and the belemnites falling down from higher up in the water column. The bioturbation also suggests a distal marine setting, small burrows with low diversity and little bioturbation in general. Facies 10 has been interpreted as representative of a very low energy environment where deposition mainly comes from material in suspension.

5.2 Facies Associations

Facies Association 1

Description: Facies Association 1 consists of the overall fining upwards to ungraded facies 1, 2, 3, normally overlaying the finer grained sandstones and siltstones of facies 5 and/or 6. Shell beds occur as calcite nodules typically on top of cross-stratified sets in the sandstones. The association typically has a sharp base marked by a *Glossifungites* surface. This facies association starts with finer grained facies 5 and 6 which are overlain by increasingly higher energy facies. There is an overall coarsening upwards, sometimes followed by a fining upwards where Facies 3 occurs followed by facies 1 or 2. Facies 5 and 6 both have indications of somewhat stressed environments and terrigenous influence, while the sandier facies (1, 2, and 3) are dominated more by high energy deposition. The bulk of the association is represented by cosets of either the cross-stratified sandstones of Facies 1 or the sigmoidal cross-stratified sandstones of Facies 2, interbedded with shell beds. The association is typically found in the lower half of the formation and is more dominant in the Sørvestlandet High compared to the Cod Terrace.

Interpretation: This association is interpreted as representing compound dunes formed in a high energy marine tide-influenced or dominated environment. The coarser sandstone facies (facies 1 and 2) are interpreted to represent migrating dunes formed during variable, stronger and weaker, respectively, current regimes. With the coarsest sandstones and conglomerates of Facies 3 likely representing winnowed lags or en-masse deposition from intermittent periods of higher energy. The likely open-marine environment for the compound dunes suggest formation in a central to outer estuary or alternatively in a high energy current dominated shelf, where shelfal currents were subject to tidal modulation and reversal. This would most likely suggest a shelfal strait setting with water exchange set up by a large tide-influenced system. Such systems are today observed e.g. between the Danish Islands with water exchange between the North Sea and the Baltic Sea, and in the Messina Strait in southern Italy.

The presence of conglomerates suggests an origin from a nearby coarse shoreline or fluvial

delivery system. Co-occurrence with the compound dune facies suggests that the finer material might have been winnowed and removed by the prevailing background current regimes. The conglomerates to coarse and pebbly sandstones are accordingly interpreted to have formed within channel thalwegs as candidate channel lags, possibly related to major river-derived floods.

The finer grained facies might represent periods of dune abandonment and transition into moribund dune stages. However, considering they typically occur stratigraphically below the dune facies and they have clear signs of terrigenous input and likely brackish conditions a more probable interpretation is that they represent a more proximal deposit relative to the coarser facies. This further strengthens the interpretation that this association is tidally dominated or modulated, a proximal deposit with a stressed environment and finer grained deposits relative to the more distal migrating dunes possibly in tidal sand flats.

The association, in general, represents a proximal tidal setting with fresh water influx, basal channel lags and compound dunes, which migrated laterally or down-current, with shell interbeds representing periods of dune migration stillstand.

Facies Association 2

Description: Facies Association 2 consist of thoroughly bioturbated silty to clean sandstones, facies 7,8, and 8B. Facies 7 representing the coarsest and cleanest sandstone and Facies 8B the siltiest. The association is ungraded and consisting of beds with thicknesses from a couple of decimetres to a few metres, with shells occuring in higher concentrations in some areas. Overall the association is fining upwards to ungraded, typically with Facies 7 at the base of the association. Facies 7, 8, and 8B are characterized by intense bioturbation and therefore a lack of primary sedimentary structures. This association generally occurs after Facies Association 1.

Interpretation: Facies Association 2 is clearly representative of a depositional environment which favoured bioturbation. However, Facies 7 has many similarities to Facies 2 when disregarding the lack of cross-stratification, which could have been present prior to extensive bioturbation. As in Facies 2, Facies 7 consist of repeating shell concentrations and medium grained sand, it lacks grading, and beds are decimetres to a few metres thick. Based on this, Facies 7 might be interpreted as a migrating dune deposit which has undergone extreme bioturbation following deposition. Facies 8, and 8B have different characteristics, finer grained material and a different style of bioturbation. The intense bioturbation overall in the association indicate a relatively open marine environment. Therefore, this association is interpreted to represent some dune migration but also sand sheet deposits. Deposition has likely occurred through currents, where Facies 7 represents the highest energy currents and Facies 8B the lowest.

Facies Association 3

Description: Facies Association 3 consist of laminated mudstones from facies 9 and 10, as well as the rippled very fine-grained sandstone of Facies 4. The association has a gradual base. It generally occurs as the fine-grained sandstone facies (Facies 4) interbedded with the mudstone facies (facies 9 and 10). The bioturbation consists of long vertical burrows which are frequently sand filled and burrowing into the muddier facies. Transitions between facies are very gradual. The association occurs typically in the younger half of the Ula Formation, and it is more represented in the Sørvestlandet High.

Interpretation: The association consist of facies which have all been interpreted to have been deposited in low energy and open marine environments. Facies 4 contain asymmetric ripples which indicate unidirectional currents, while the sedimentary structures in the mudstone facies are parallel laminations indicative of deposition from suspension. The gradual transitions between finer and coarser grains indicate that the sandier facies are not mass flow deposits or a result of storm deposition. It has, therefore, been interpreted as deposition caused by marine currents which has slowly weaned and increased in strength over time. Stronger currents leading to sandier deposition and weaker currents only carrying suspended sediments. Since the vertical burrows are sand filled and seem to burrow from the sandy layers into the mudstone these burrows have been interpreted as opportunistic populations.

The association represents a distal marine environment which is periodically influenced by currents causing deposition of very fine-grained sands, background deposition is dominated by settling of suspended material.

Table 6: Lithofacies description

Facies	Lithology	Sorting	Grading	Lithological accessories	Cement	Bed thickness	Lower contact	Sedimentary structures	Bioturbation index	Trace fossil size/diversity	Interpretation	Occurring with
Facies with sedimentary structures												
F1	Medium to fine grained sandstone	Moderately well sorted	No grading	Bivalves, rare coal fragments	Some calcite nodules	Few metres, can be divided into decimetre sized inter-beds	Gradual	Sigmoidal cross stratification. Double mud-drapes	2-3	Small to medium/intermediate to low	High energy migrating dunes with variable flow strength and direction, relatively hospitable	F6, F3, F2, F6
F2	Medium to fine grained sandstone	Well sorted	No grading	Bivalves at the top of dunes	Some calcite nodules	Few metres, can be divided into decimetre sized inter-beds	Gradual, but internal beds are amalgamated and planar	Cross stratification	1	Medium/ low	Migrating dunes in a high energy environment, inhospitable	F1, F7, F6, F3
F3	Conglomerate to coarse grained sandstone	Very poorly sorted	Normal grading	Bivalves	Tight either calcite cement or quartz cement	Decimetres to metres sized	Erosive	Not recognisable	0-2	Medium/low	Channel lag	F2, F7
F4	Very fine grained sandstone	Well sorted	Normal grading	N/A	N/A	Decimetres to metres sized	Gradual	Rare indications of ripples	4-5	Large/low	Unidirectional flow deposition, low energy environment	F9
Intensely bioturbated sandstone dominated facies												
F5	Silty fine-grained sandstone	Moderately well to poorly sorted	No grading	Clay clasts, coal	N/A	Decimetres to few metres	Bioturbated erosive Glossifungites surface	Not recognisable	4	Small/intermediate	Low energy environment, possibly brackish environment with terrigenous influence	F6, F1
F6	Siltstone	Well sorted	No grading	Bivalves, coal	N/A	Couple metres	Gradual	Not recognisable	3	Small/intermediate to low	Low energy environment, possibly brackish environment with terrigenous influence	F1, F5
F7	Medium grained sandstone	Very well sorted	Reverse and normal grading	Bivalves	Patchy quartz cementation	Decimetres to metres sized	Gradual	Not recognisable	1 to cryptic bioturbation	Large/low	High energy environment	F10, F8, F8B, F3
F8	Silty fine-grained sandstone	Well sorted	Reverse and normal grading	Bivalves rare occurrences of clay clasts	Calcite nodules	Few metres	Gradual	Not recognisable	5-6	Small to medium/intermediate to low	Proximal to distal estuarine deposits	F9, F10, F7
F8B	Very silty fine grained sandstone	Well sorted	Normal grading	Bivalves rare occurrences of clay clasts	N/A	Few metres	Gradual	Not recognisable	5-6	Small to medium/intermediate to low	Intermediate relatively constant energy setting and a relatively open marine environment	F10, F7
Mudstone facies												
F9	Shale	Very well sorted	Reverse grading	N/A	N/A	Decimetres sized	Gradual	Some faint layering	4-5	Large/low	Deposited from suspension	F4, F10
F10	Siltstone	Very poor to moderately well sorted	No grading	Belemnites	N/A	Few metres	Gradual	Layered	0-1	Small/low	Deposited from suspension	F9, F7, F8B, F8

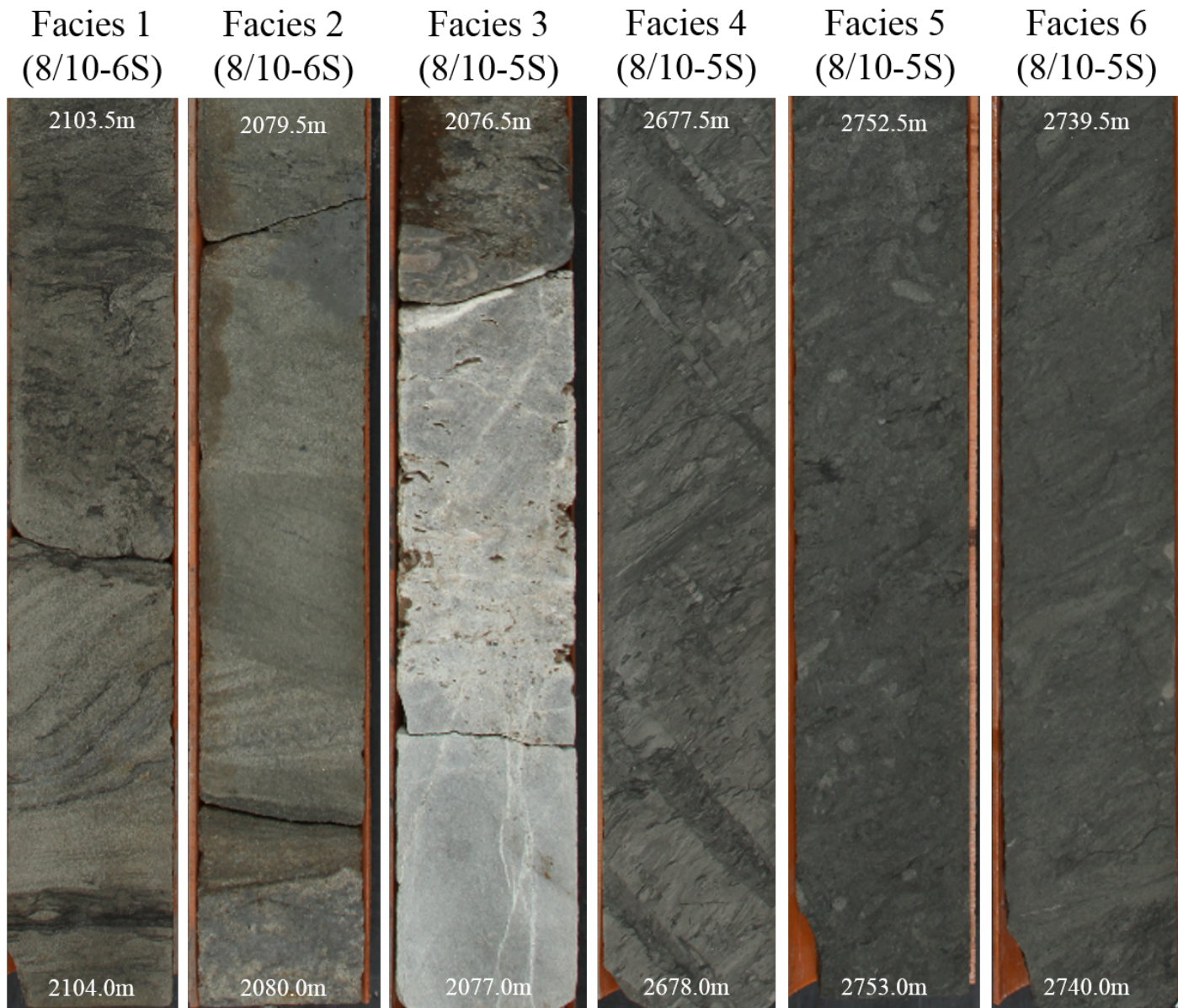


Figure 19: For location of wells see Figure 11.

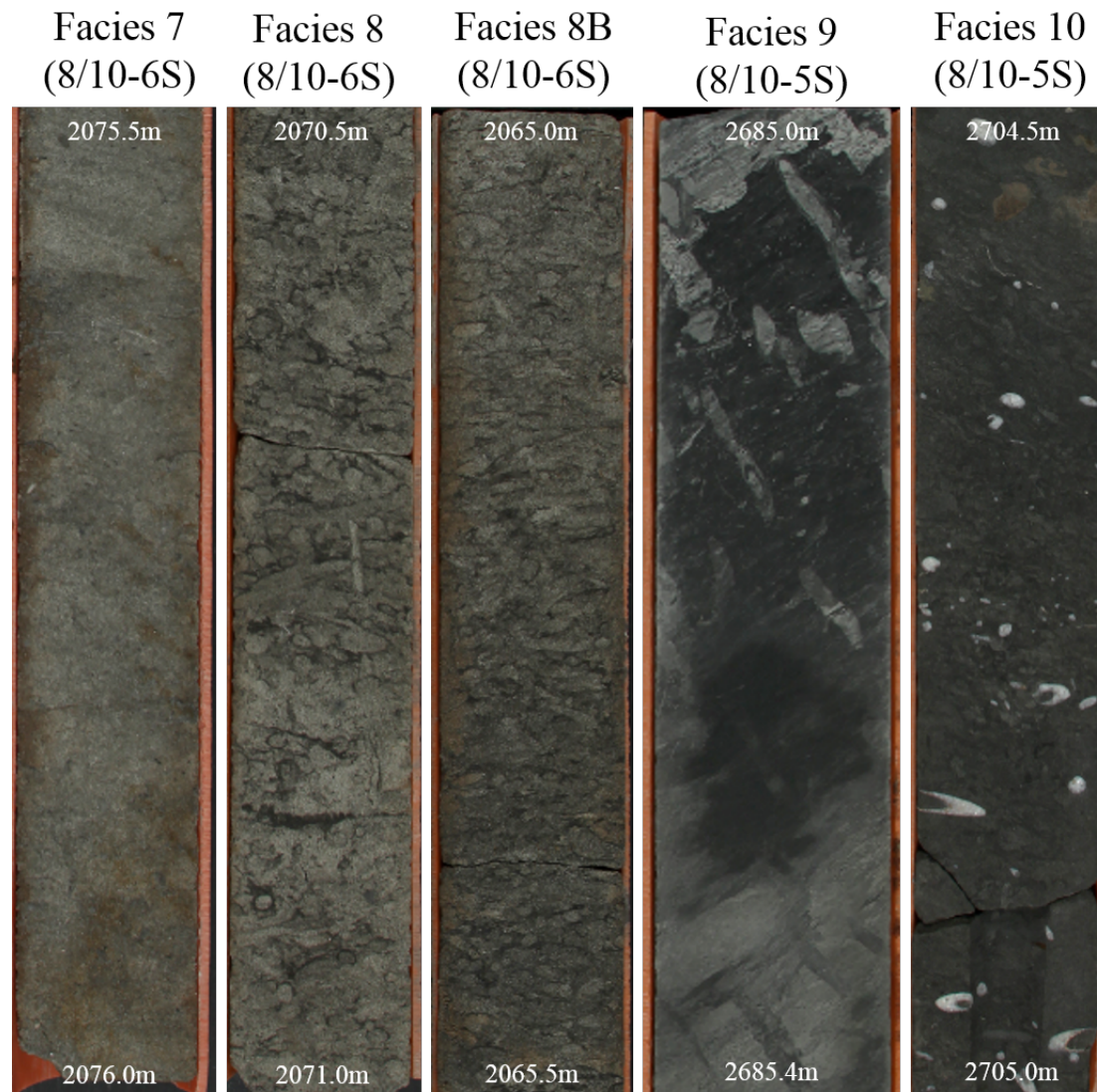


Figure 20: For location of wells see Figure 11.

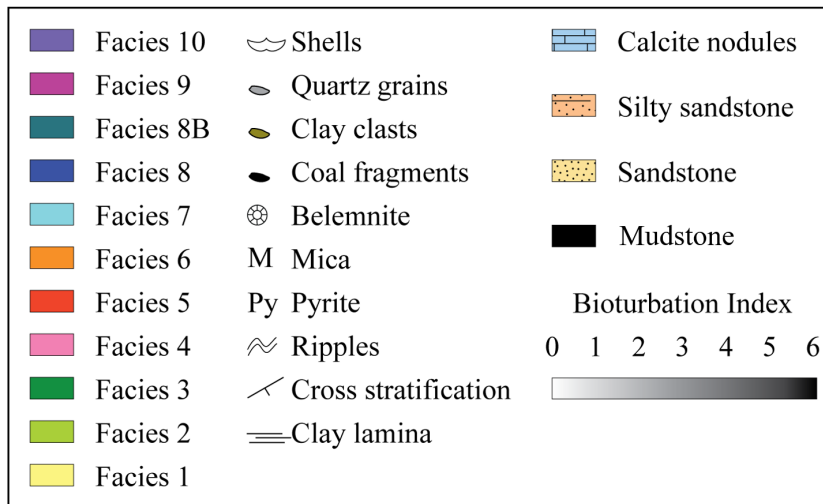


Figure 21: Legend for core descriptions in Figure 23, 22, and 24.

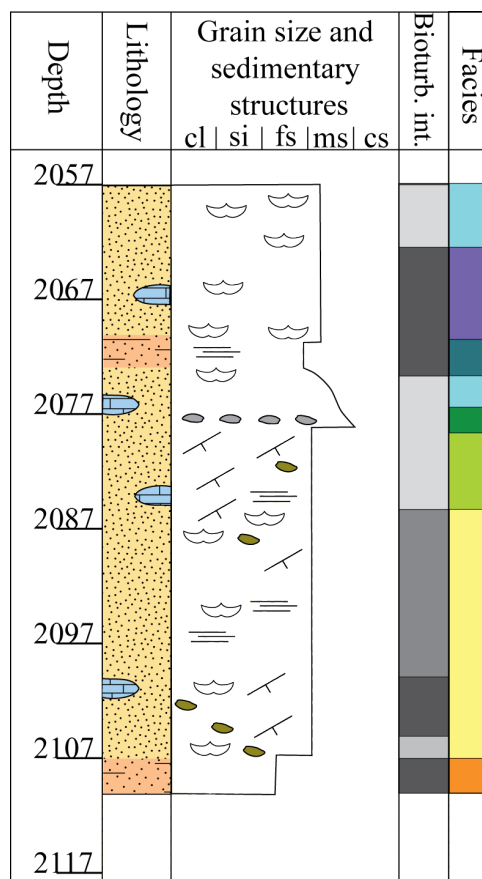


Figure 22: Core description of well 8/10-6S, for legend see Figure 21.

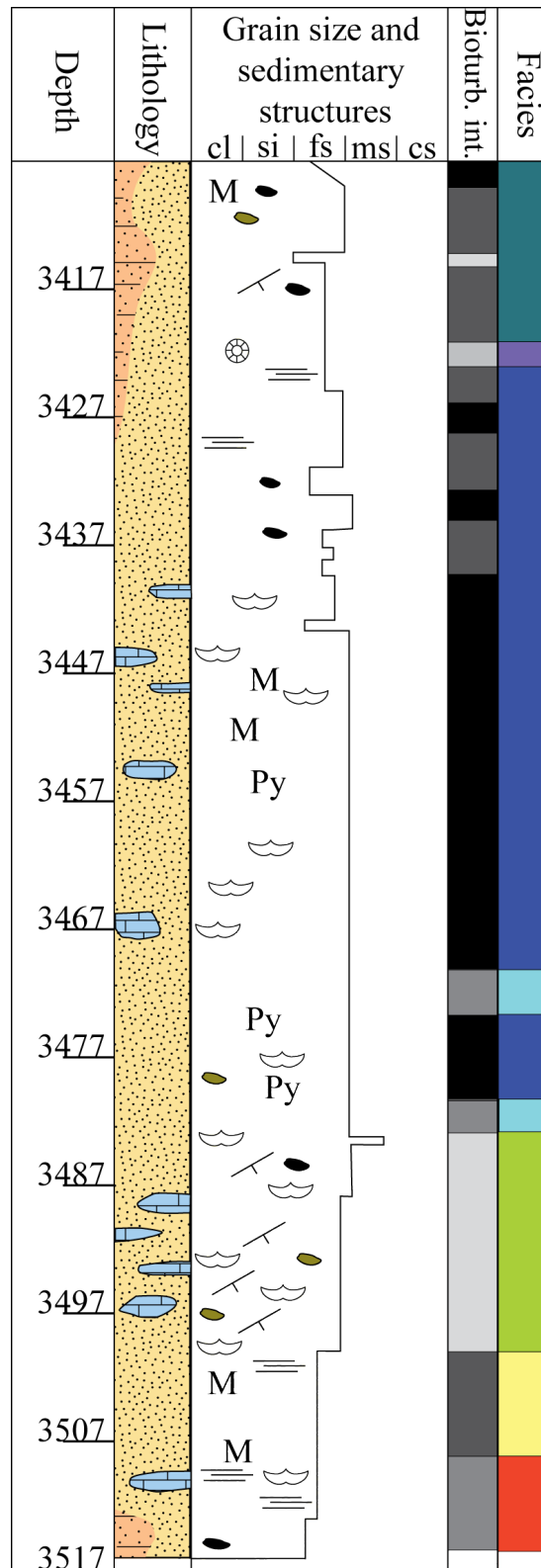


Figure 23: Core description of well 7/12-6, for legend see Figure 21.

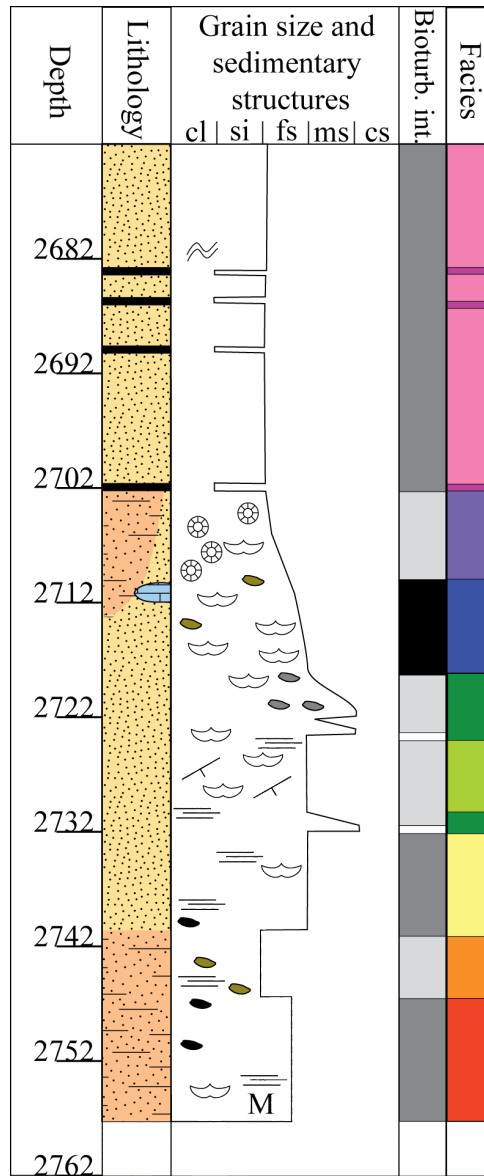


Figure 24: Core description of well 8/10-5S, for legend see Figure 21.

5.3 Seismic

5.3.1 Well-Tie

The well tie results can be seen in Table 7. In general, bulk shifts varied from 7 to -30 milliseconds.

Table 7: Wells tied to seismic with amount of bulk shift which was applied during the well-tie process.

Well	Density and sonic well logs	Checkshots	Seismic cube	Applied bulk shift [ms]
7/12-10	YES	YES	PGS	0
7/9-1	YES	YES	PGS	7
7/12-11	YES	YES	PGS	0
7/12-13S	YES	YES	MEGA	0
7/12-2	YES	YES	MEGA	-8
7/12-3A	YES	YES	MEGA	-30
7/12-4	YES	YES	PGS	0
7/12-5	YES	YES	MEGA	-15
7/12-6	YES	YES	PGS	-20
7/12-7	YES	YES	PGS	0
7/12-8	YES	YES	PGS	0
7/12-9	YES	YES	PGS	-2
1/3-3	YES	YES	MEGA	-15
8/10-5	YES	YES	MEGA	-14
8/10-4S	YES	YES	MEGA	0
8/10-6S	YES	YES	MEGA	0
8/10-1	YES	YES	PGS	0

5.3.2 Vertical Resolution

There is a high variability in the resolution from the various locations. Therefore an average resolution has been calculated, based on wells present in both seismic surveys. The average of all measurements in the MEGA seismic survey is 19.7 metres, whereas the average vertical resolution for the PGS survey is 19.4 metres. Packages above 20 metres can be expected to be distinguishable in both seismic surveys.

Table 8: Measurements of seismic vertical resolution from both seismic cubes.

Well	PGS			MGA		
	From [m]	To [m]	Resolution [m]	From [m]	To [m]	Resolution [m]
7/12-6	3415.6	3512.8	24.3	3374.93	3488.15	28.305
7/12-4	3478.58	3534.75	14.0425	3448.82	3523.84	18.755
8/10-6S	-	-	-	1829.72	1893.69	15.9925
7/12-13	-	-	-	3495.19	3572.74	19.3875
7/12-5	-	-	-	3800.76	3877	19.06
7/12-11	3759.21	3857.89	24.67	3747.8	3819.43	17.9075
7/12-8	3767.62	3814.72	11.775	3724.29	3777.04	13.1875
8/10-1	2792.84	2881.73	22.2225	2781.99	2864.09	20.525
8/10-4S	-	-	-	2883.82	2940.36	14.135
8/10-5S	-	-	-	2493.73	2553.44	14.9275
Average			19.402			19.736

5.3.3 Seismic Interpretation

5.3.3.1 Confidence Map

The confidence map (Figure 25) illustrates in which areas the seismic interpretations have a very high, high, intermediate, or highly uncertain confidence. In general, the highest confidence is in the Ula Field area as the well coverage is high and the seismic quality ok to good.

5.3.3.2 Surfaces

Ekofisk Formation Top: This top is marked by a strong negative amplitude continuous and relatively parallel reflector (Figure 26; Table 9). The area consists of elevated zones which are directly above the salt walls, the northernmost wall is clearly faulted along the middle (Figure 27). Although no major faults can be observed several smaller faults can be identified in areas of salt doming. There is a distinct change in elevation from the Sørvestlandet High in the north-east to the Cod Terrace in the south-west, this is reflected in the surface as generally lower elevation values in the Cod Terrace. However no abrupt change can be identified. The post-rift salt doming seems to dampen the effect in particular around the Ula Field. In general, this surface reflects well the broad trends in the area, deepening towards the south-west, as well as elongated salt walls which cause topography and suprasalt faulting.

Farsund Formation Internal Reflector: The top of the Farsund Formation is marked by a positive reflector of variable energy (Figure 26; Table 9). Therefore the underlying internal Farsund Formation reflector was interpreted as this is a more continuous higher

amplitude reflector. The reflections of this formation are parallel, but heavily faulted. Two types of faults can be seen in the surface, faults related to halokinetsm and the bounding faults between the Sørvestlandet High and Cod Terrace. The salt related faults are typically situated directly above salt walls and diapirs. In this surface (Figure 28) a clearer distinction can be made between the Sørvestlandet High region to the north-west and the Cod Terrace to the south-east due to the faults separating the regions compared to the (Figure 27). The interpod basins can be somewhat extrapolated from this map as being the areas above salt walls, the elongated and circular high elevation areas. Importantly, the interpod areas are also the areas above saltwalls which have deflated causing small “grabens” to appear above them.

Ula Formation Top: The reflector is nearly parallel to the overlying reflector of the Farsund Formation. This is also reflected in the resulting surface (Figure 29; Table 9), which is nearly indistinguishable from the Farsund Formation surface. The positive amplitude implies a decrease in acoustic impedance. The Ula Formation reflector is continuous across the basin, and the Ula Formation locally onlaps the Triassic minibasin pods. As in the Farsund Formation surface it can be used to somewhat define the interpod basins, which are located on the elevated salt wall structures and the deflated saltwall structures which, together on the Sørvestlandet High forms a polygonal connected network (Figure 29).

Internal Ula Formation: The Internal Ula Formation reflector is marked by an increase in acoustic impedance and has a positive low amplitude character (Figure 26; Table 9). This reflector was not present everywhere and generally not correlatable across minibasins. It is only present in the thickest area of the Ula Field (Figure 31).

Base Ula Formation: The Base of the Ula Formation is marked by a negative reflector with a high to very low amplitude. The surface show many of the same structures as the Top Ula Formation, and as mentioned, it is not present everywhere frequently onlapping the underlying reflectors (Figure 30; Table 9).

Table 9: Horizon characteristics.

Horizon	Amplitude	Acoustic Impedance	Reflector characteristics
Above Ekofisk Formation	Positive	Increase	Continuous, strong.
Farsund Formation Top	Negative	Decrease	Continuous, strong.
Ula Formation Top	Positive	Increase	Discontinuous, strong to very weak.
Internal Ula reflector	Positive	Increase	Highly discontinuous, weak.
Skagerrak Top	Negative	Decrease	Highly discontinuous, strong to weak.

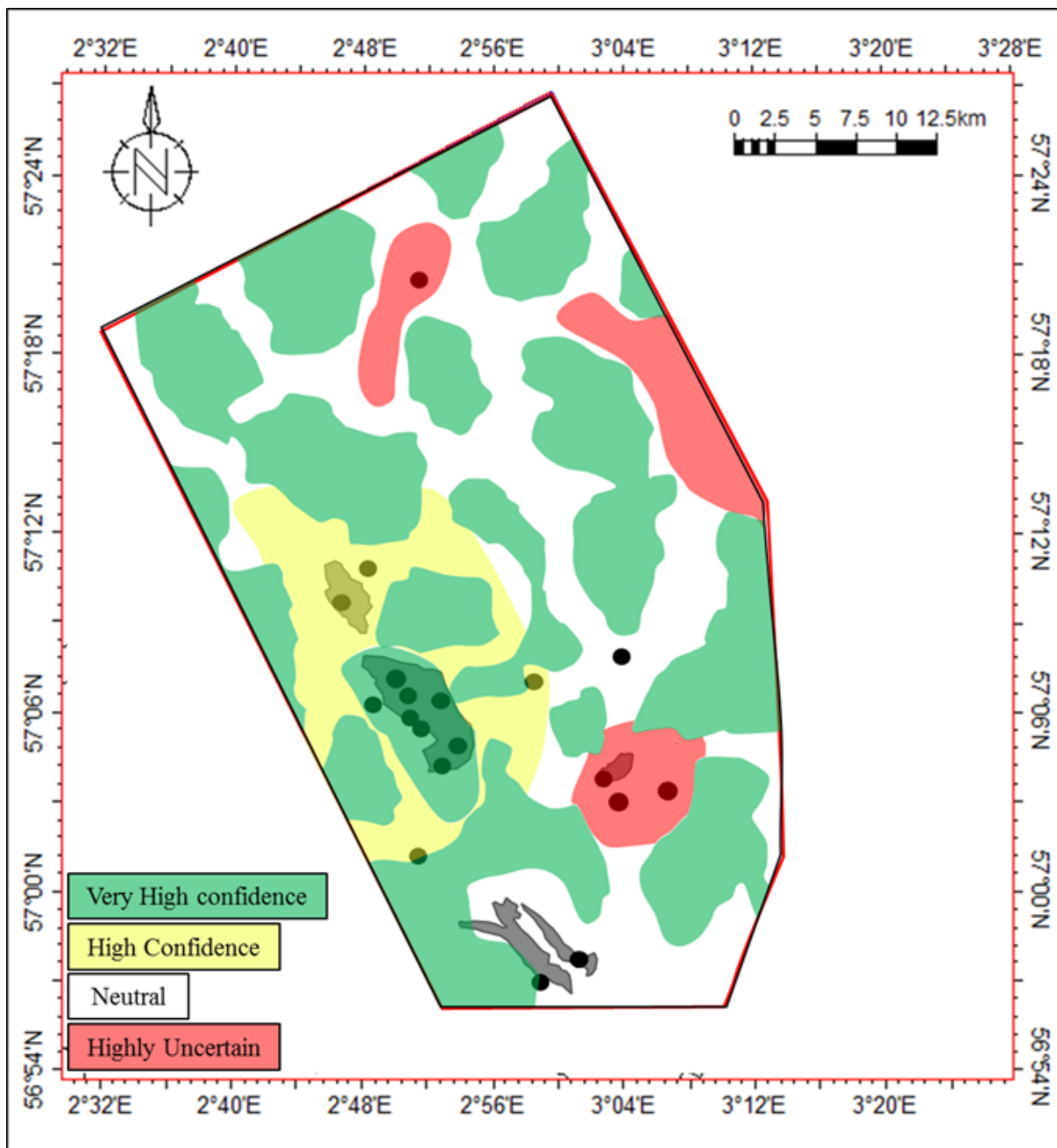


Figure 25: Confidence map for seismic interpretation based on well coverage, seismic quality and continuity of reflectors.

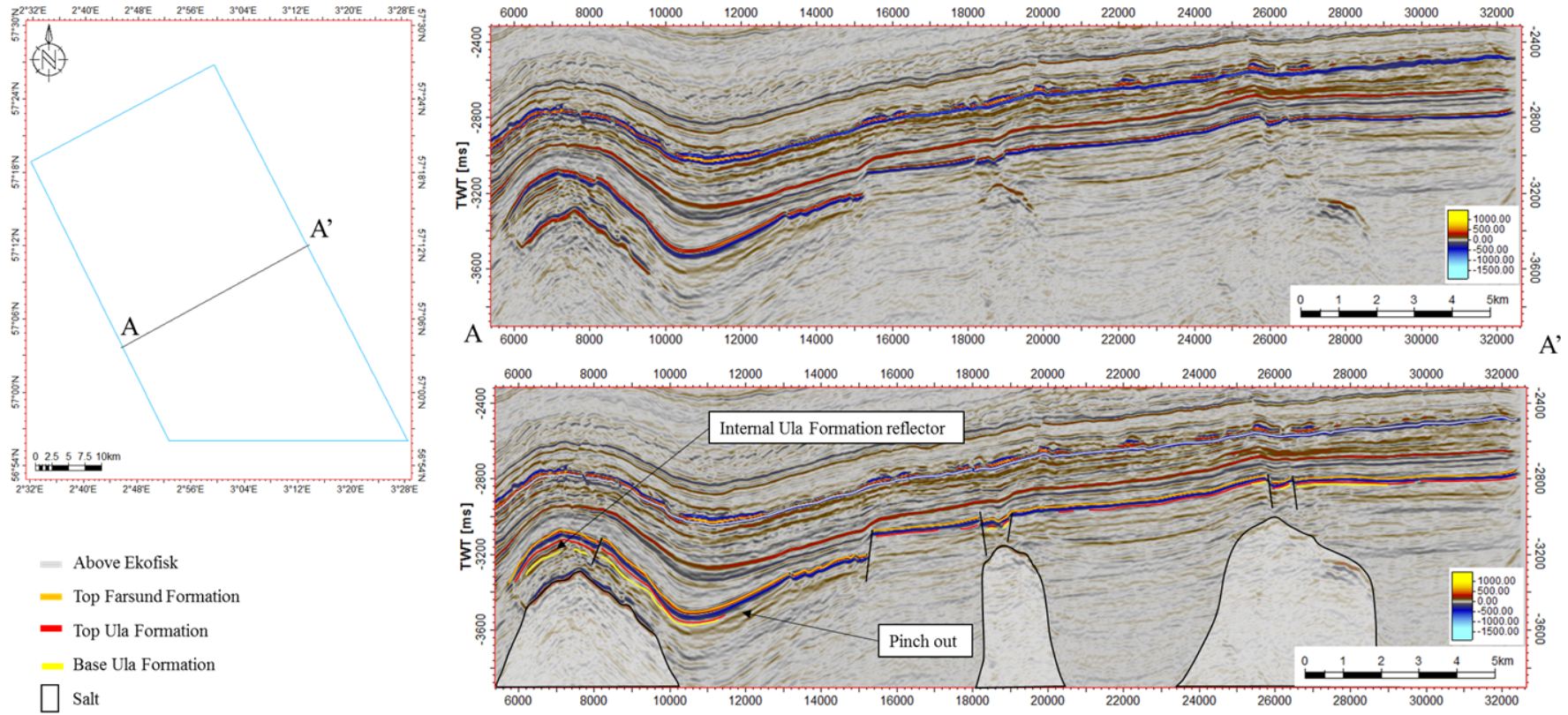


Figure 26: Seismic cross-section of the area

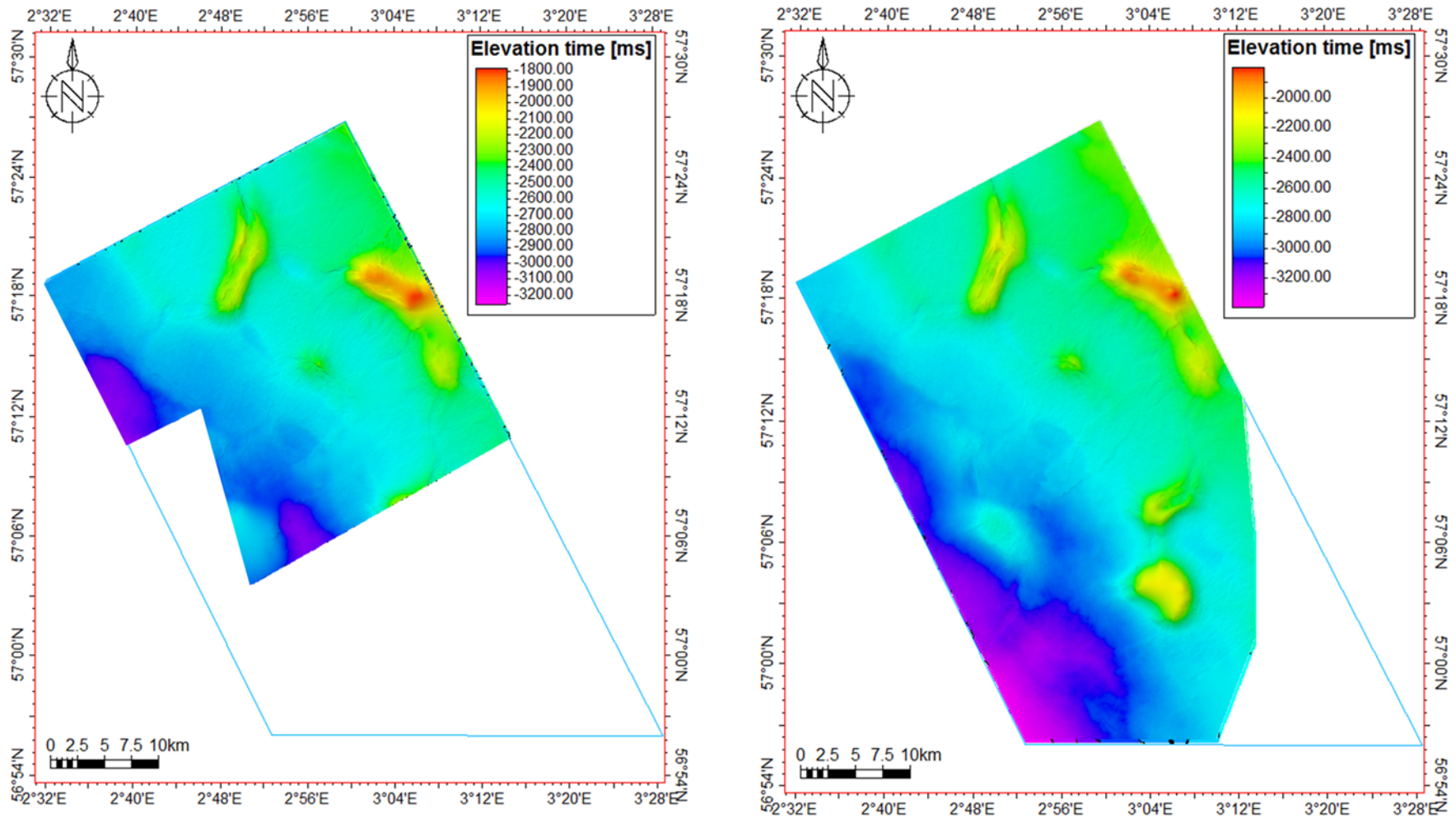


Figure 27: Top Ekofisk Formation surface. Interpreted on the PGS cube to the left and the MEGA cube to the right.

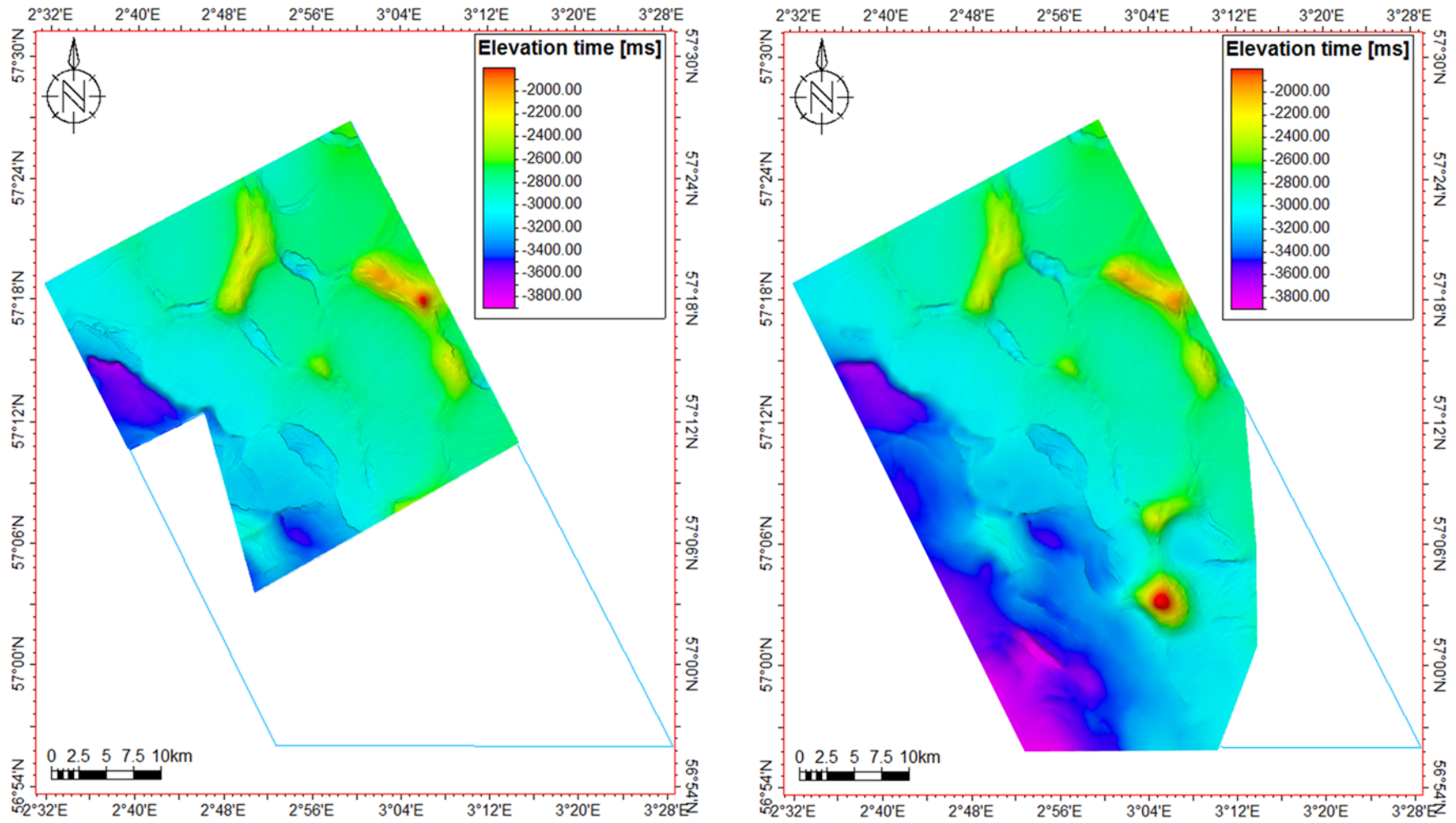


Figure 28: Farsund Formation internal reflector surface. Interpreted on the PGS cube to the left and the MEGA cube to the right.

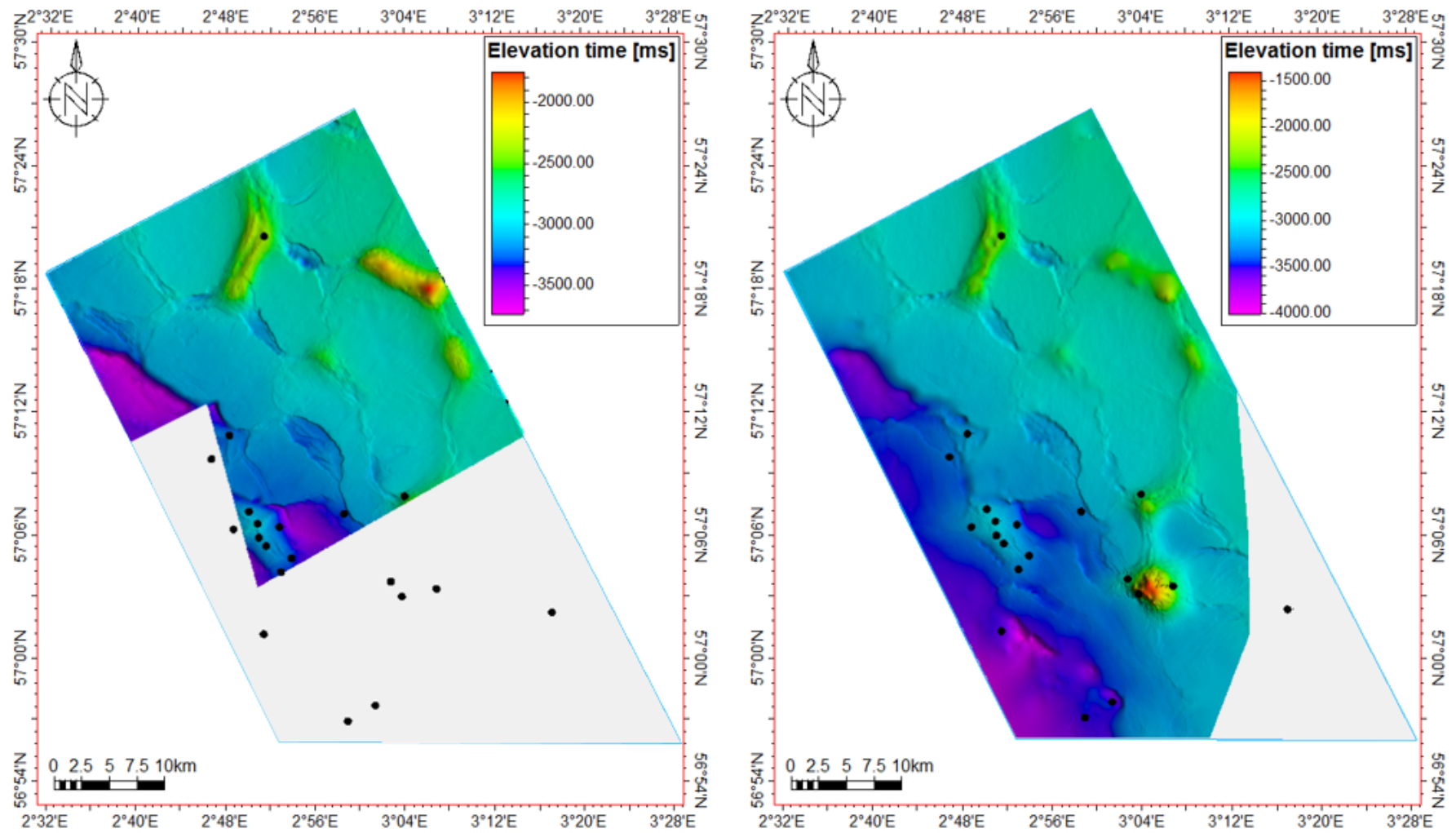


Figure 29: Top Ula Formation surface. Interpreted on the PGS cube to the left and the MEGA cube to the right.

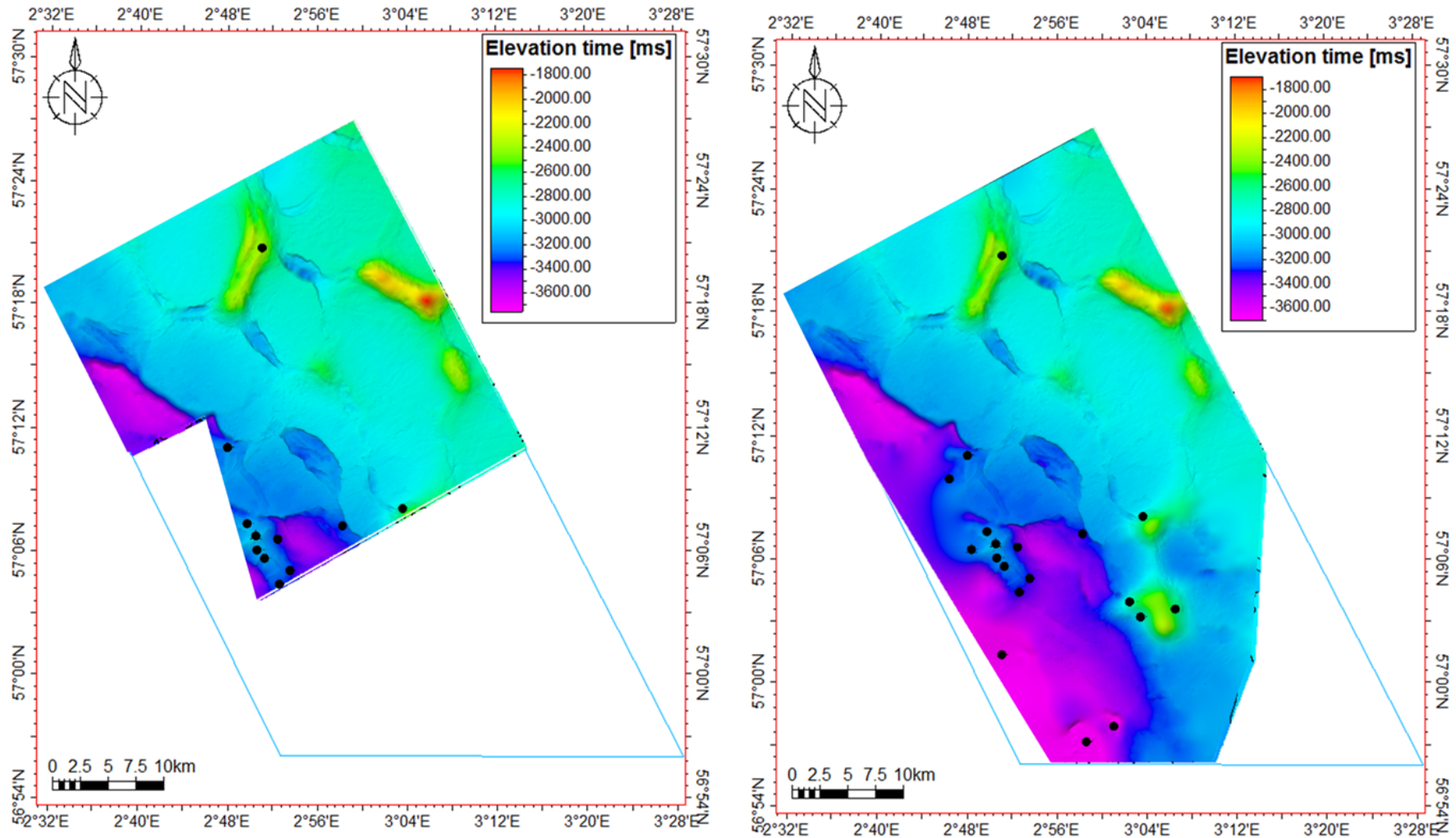


Figure 30: Base Ula Formation surface. Interpreted on the PGS cube to the left and the MEGA cube to the right.

5.3.4 Ula Formation Isochore Map

The Ula Formation isochore map shows the thickness variations of the Ula Formation (Figure 32). In the northern part of the Ula Field the thickness is between 100 and 50 milliseconds, decreasing to less than 50 milliseconds in the southern part. The thickness variations are abrupt and can in some cases be linked to the faults. This corresponds well to the area where the internal reflector is present in the Ula Formation (Figure 31), the thickest areas are where the internal reflector is present.

The Figure 32 shows thickest areas to be in the middle of the interpod basins thinning towards the edges of the interpod basins. This indicates that the highest accommodation was along the central axis of the interpod basins, this might have been the deepest areas during deposition. A “shoreface” might be found along the edge of the pods, the margin of the interpod deposits as this is the shallowest area.

5.3.5 Ula Formation Thickness Estimation Map

Additionally, an estimate of the thicker and thinner areas in the entire study area was made (Figure 33). Three types of thickness was grouped; the thick interpod deposits (i.e. Ula Field); the thin supra-minibasin deposits (in these areas there is also a possibility that there is no Ula Formation deposited); and the thin interpod deposits (Figure 33). This map shows the different regions of the study area and where to expect thicker deposits of the Ula Formation. It has been based on the interpretations of the salt walls and on the interpretations of the Ula Formation horizons. As seen in the thickness estimation map (Figure 33) the Ula Formation is at its thickest above the salt walls and thinning towards the Triassic pods.

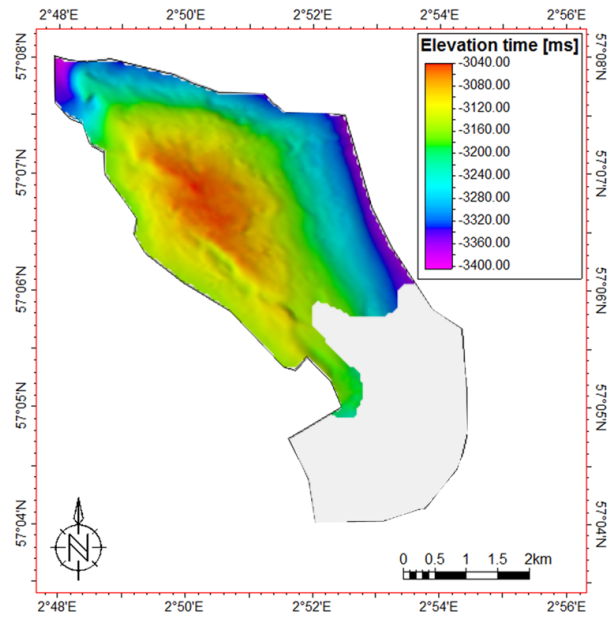


Figure 31: Oxfordian surface, a surface of an internal Ula Formation reflector. The surface corresponds to a flooding event.

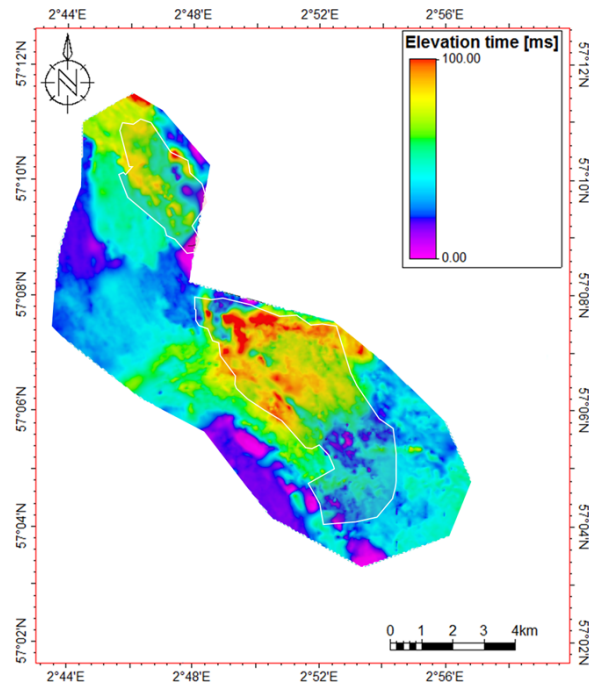


Figure 32: Ula Formation isochore measured in milliseconds

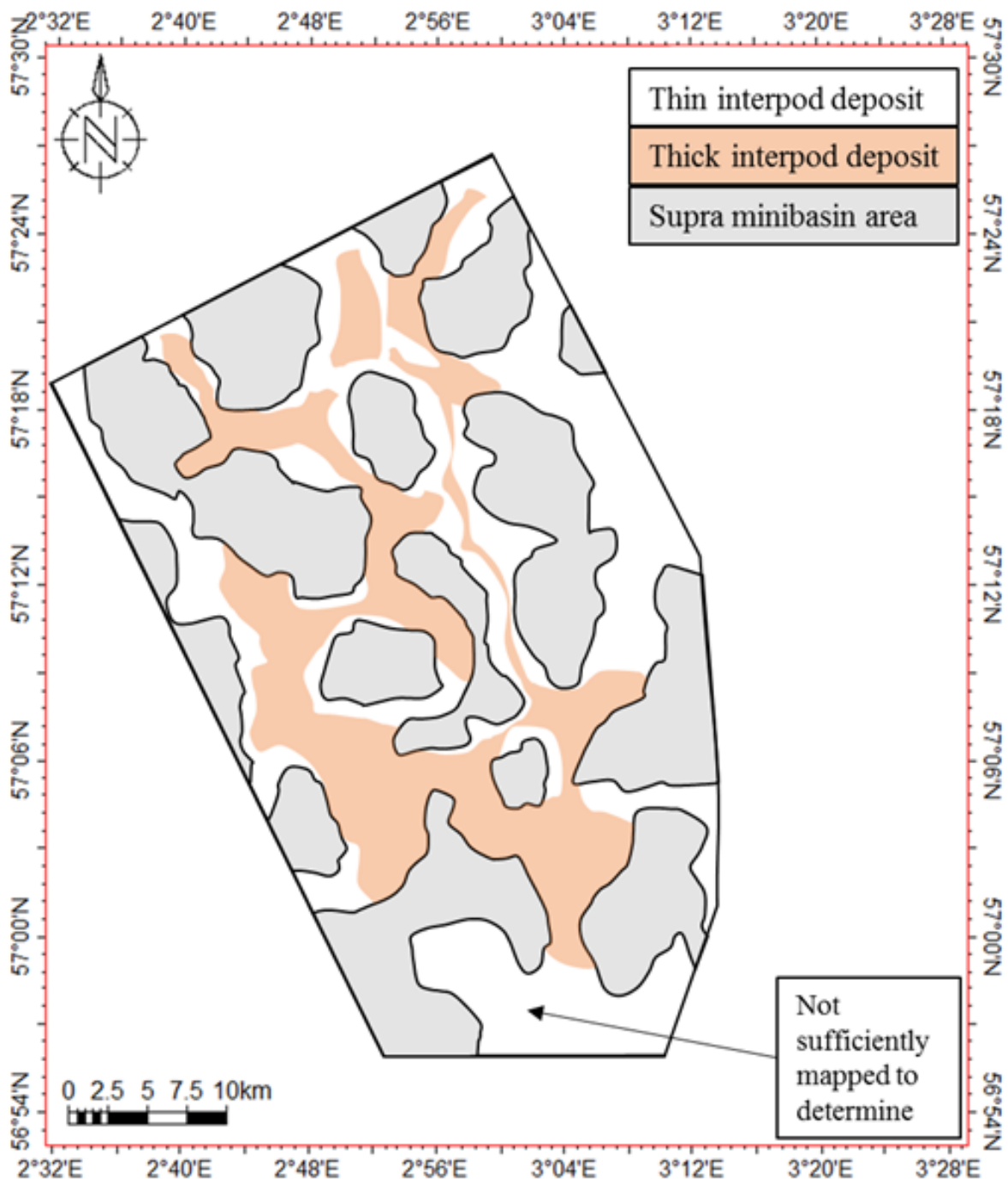


Figure 33: A map showing the variations in thicknesses, thick interpod deposits are between 30-50 meters and up in thickness. While thin are not present or below 30 meters.

5.3.6 Seismic Attributes

The attribute maps for window 1B (corresponding to the upper interval of the Ula Formation in thin areas) (Table 4) from the MEGA cube shows some anomalies, both with positive values and negative values. The thickness estimation map has been superimposed onto the attribute maps, this has been done so that it can be determined which areas are affected by underlying Triassic reflections and not just the Ula Formation. The area which is whited out corresponds to the Triassic pods. Therefore, the high value anomalies which have been indicated in this area should be disregarded when interpreting the amplitude variations in the Ula Formation as they are most likely reflecting the underlying formations or tuning. Additionally, the areas which are marked in orange/black corresponds to areas estimated to contain a thicker Ula Formation.

The effects tuning has been noted, well control in the indicated area (well 7/12-11) shows that the reservoir is thinner than vertical resolution, and the base of the reservoir is onlapping the Triassic, which leads to a high value anomaly. However, it is caused by tuning and not indicating anything about the lithology and should therefore be disregarded. There are also some anomalies which can be confirmed to be caused by steepening beds, in particular on the slopes of the tallest diapirs. These have therefore been disregarded in the interpretation. On the diapir, as a result of disruptions from the salt and steeply dipping reflectors on the seismic, no interpretations or indications can be made. In general, the diapir and crests of the steeper salt-walls lead to a chaotic response.

5.3.6.1 Sculpting

Description: In the focus area there are two clear negative anomaly areas, and a third one which is less obvious (Figure 37). They are areas with distinct borders (caused by faults) and, in general, there is a lack of positive values. These negative anomalies have no particular orientation and there is a dim blurry character. The positive anomalies can be found between these low value anomalies, they gather in clusters of elongated shapes. Some of the shapes have more irregular outlines and others are more rounded. There is also a range of sphericity, in general they have low sphericity. However there are some in particular in the Ula Field area which have even lower sphericity. There is a general trend, with local variations, they are 'striking' in a north-west-south-east direction. The sizes of the positive anomaly shapes vary a lot, one shape in the north, measuring 1400 metres in length and 440 metres in width, smaller shapes measure 220 metres in length and 88 metres in width.

There are two wells situated relatively close to each other, one of them is on the background response (well 7/12-9), and the other one directly on one of the high value anoma-

lies (well 7/12-8). Since the window of extraction encompasses the uppermost part of the Ula Formation, the wells were examined to provide any additional information about the possible lithological variabilities between the high value anomalies and the background. In well 7/12-9 the gamma-ray log indicates sand, and the character of the log in the upper part show a relatively ungraded motif with somewhat high values for sand indicating mud-dier content (Figure 39). However, in well 7/12-8 the gamma-ray log shows a coarsening to fining upwards character and the values are lower indicating a cleaner sand compared to well 7/12-9 (Figure 39).

Interpretation: The negative anomalies represent areas with a very weak Ula reflector, they also coincide with areas of thin reservoir and Triassic pods. Therefore, they are interpreted to be areas of low deposition during the Upper Jurassic. There is no well control to check this and in general the wells have been drilled on the structural highs and not the Triassic pods. However, since the two wells 7/12-8 and 7/12-9 show a cleaner sand with a higher value it can be assumed that an anomalously low value could indicate a muddier composition. The lack of deposition of Upper Jurassic sediments in the minibasin/pod areas indicate that these areas were topographical highs. It cannot be determined exactly how much higher they were than the surrounding areas and if they were subaerially exposed or acted as shallow banks just by using the attribute map. The onlapping reflector close to well 7/12-11 also supports that they were topographical highs, and during the lower part of the Ula Formation there was minimal to no deposition close to the pods. Either way the position of the negative anomaly geometries relative to each other are forming a strait striking north-west. The width of the interpreted strait is at its widest (around 5000 m) and at its narrowest (around 3500 m). The positive anomalies have been interpreted, based on well control, to be areas of cleaner and thicker sand packages in the uppermost section of the Ula Formation.

The positive anomalies typically occur between the three low anomaly fields, indicating that they have been deposited in the strait. In a strait the direction of transportation is parallel to the shoreline (Longhitano & Steel, 2017), which in this case is in the same strike as the elongated high value anomalies. Based on this the elongated shapes might be interpreted as tidal sandbars or sand patches as seen in the Fehmarn strait (Feldens et al., 2015). The cleaner sand in this area supports this interpretation, as the bars would be more prone to reworking and therefore cleaner than the surrounding area.

5.3.6.2 RMS

Description: As in the sculpting attribute the Triassic pods have different values compared to the interpod areas (Figure 38). In the Triassic pods values are typically low, in blue colours, while the interpod areas there is a range with mainly greens yellows and

reds, which are all high values. The low value anomalies, blues, correspond well to the circular areas which was defined by negative values in the sculpting attribute. In the RMS amplitude map there are more internal variations in these areas. This might be due to increased detail being brought forward by having a more detailed colour table.

The high amplitude anomalies, corresponding to positive anomalies in the RMS map, have similar shapes to the ones interpreted in the sculpted map. As in the low value anomalies more distinct detail can be seen in the RMS amplitude map, compared to the sculpting map. The highest value anomalies, coloured red, typically have the same orientation as the larger interpreted shape but their positioning in it varies. Shapes identified as high value anomalies are typically lobate and have low sphericities. Some can be grouped together as individual parts of a larger group. Their sizes vary with a large shape in the north, measuring 1400 metres in length and 440 metres in width, smaller shapes measure 220 metres in length and 88 metres in width. There are also several sizes in-between these two extremes. Well control was used to see what the difference in RMS value meant lithologically. Well 7/12-19, which is in a lower value area, has a muddier composition relative to well 7/12-8 which is in a higher value area (Figure 39).

Interpretation: The RMS attribute map corresponds very closely with the sculpting attribute map, both maps show anomalies in the same areas. Positive anomalies in the sculpting map correspond to high RMS values in the RMS map, and the negative anomalies correspond to low RMS values. The interpretation of the RMS attribute map shows the same “lobate” features which can be observed in the sculpted attribute map (Figure 38). Since both the RMS and sculpting attribute maps show the same anomalies this strengthens the confidence in the attributes illustrating the real condition of the subsurface, and that they indeed are representing lithological variations and architectures.

The low value anomalies are generally restricted to the Triassic pods, and based on the observations from the wells, lower values are interpreted to contain relatively muddier compositions. While the high value anomalies generally have lobate shapes and based on well evidence are expected to have a sandier lithology. High value anomalies are mainly present in the interpod areas, with the exception of anomalies which have been defined as caused by tuning or steepening reflectors and been disregarded in the interpretation.

Interpretations from the RMS map support the interpretations from the sculpted attribute map and conclusions by previous authors of a linked valley network during deposition (Wonham et al., 2014). The Triassic pods seem to have experienced minimal deposition, whereas the majority of the sands have been deposited in the interpod basins. The lobate shapes are found in the more central parts of the basins with some exceptions.

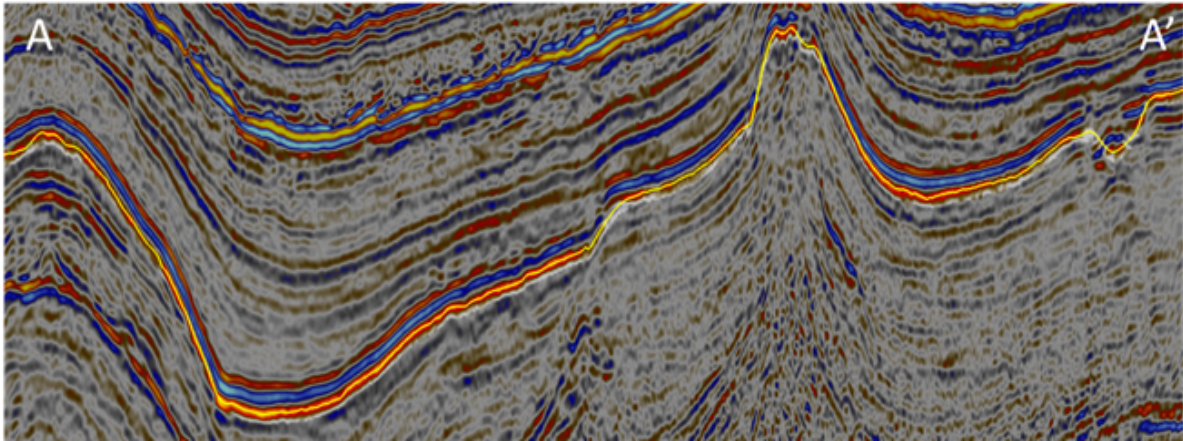


Figure 34: Seismic line illustrating window of examination for RMS and Sculpting, for location of cross-section see Figure 35 or Figure 36. The yellow line is the interpreted top reservoir (Top Ula Formation), and the area which has been highlighted on and slightly below show which interval has been extracted.

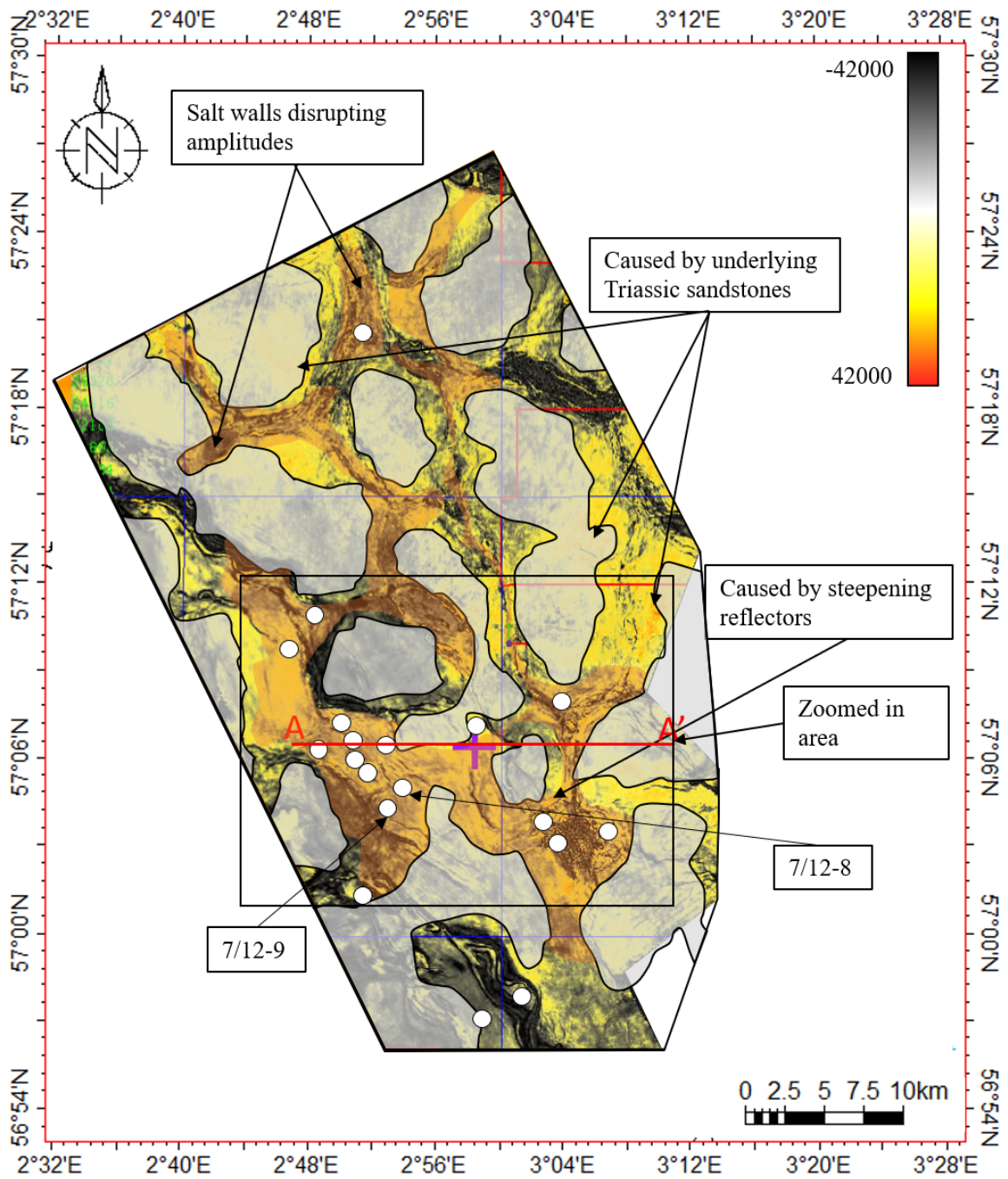


Figure 35: Sculpt frequency attribute map. White areas are the Triassic pods, while the orange areas are areas expected to have a thicker Ula Formation.

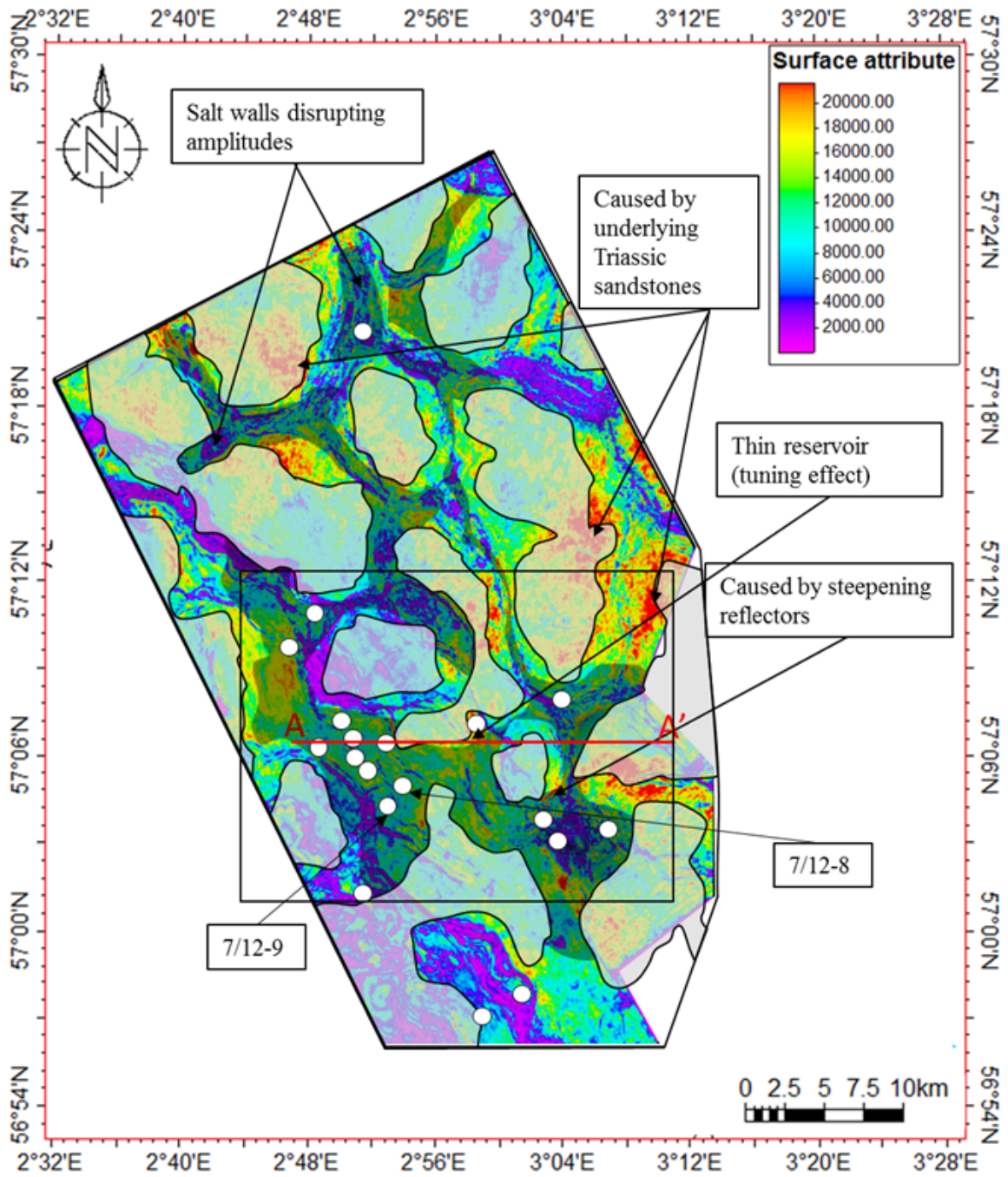


Figure 36: RMS amplitude attribute map. White areas are the Triassic pods, while the black areas are areas expected to have a thicker Ula Formation.

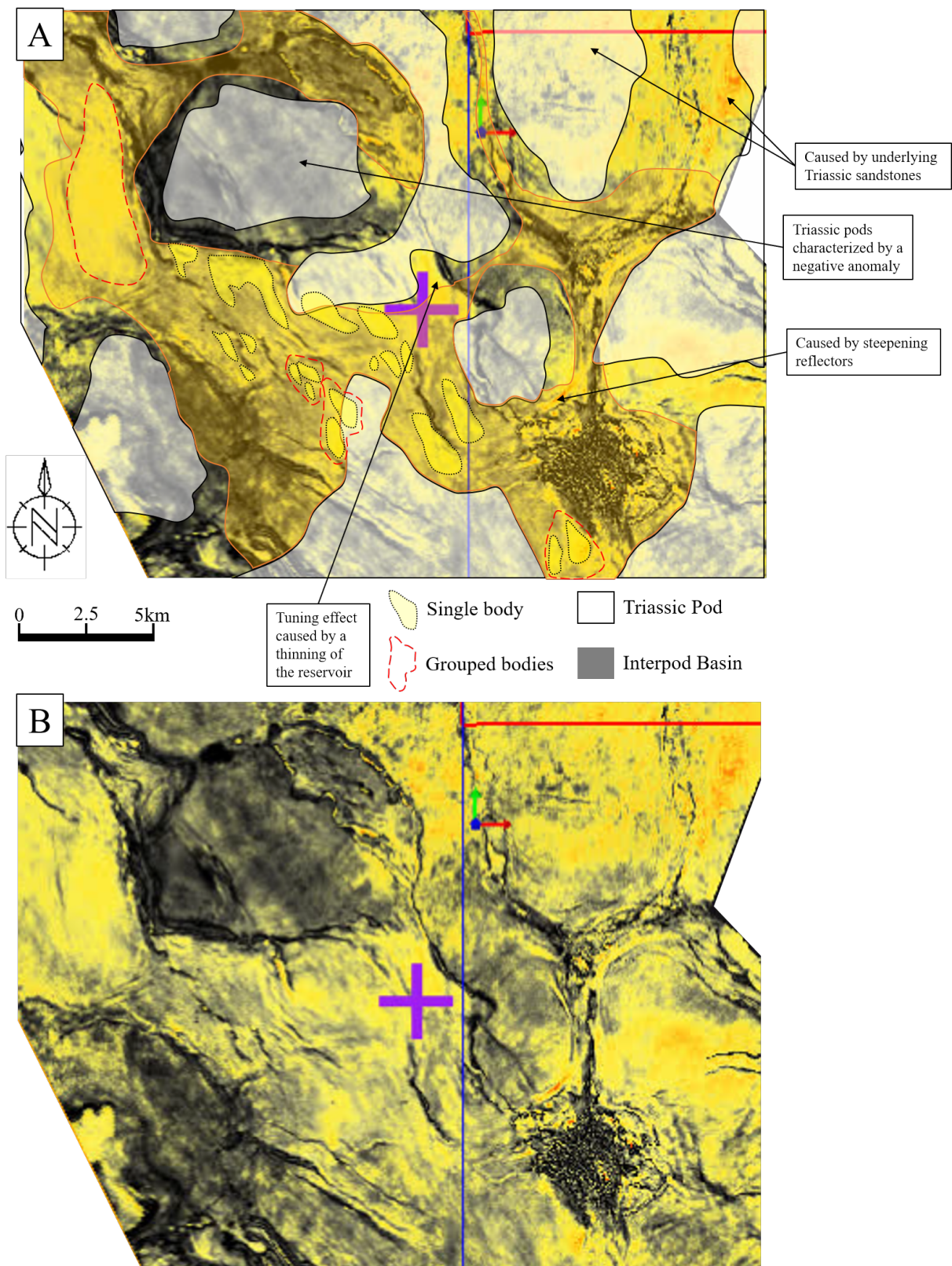


Figure 37: Interpretation of geometries in Sculpt's attribute, for location see Figure 35.

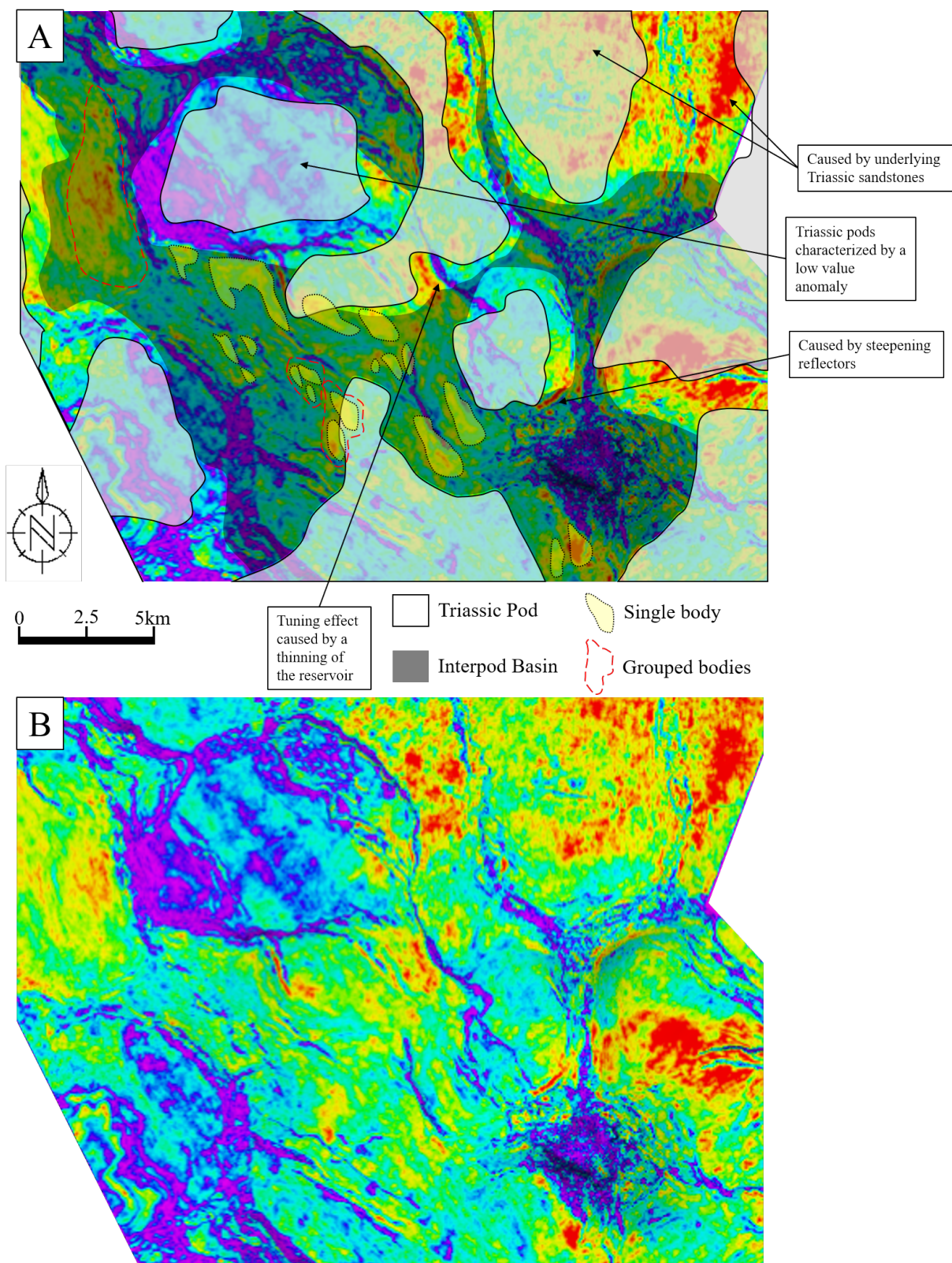


Figure 38: Interpretation of geometries in RMS attribute, for location see Figure 35.

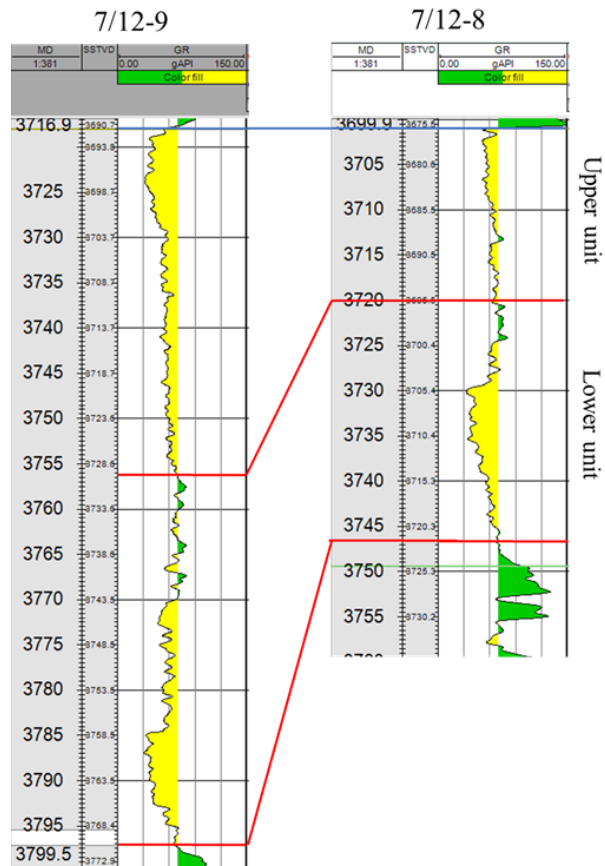


Figure 39: Well 7/12-9 and 7/12-8 show how the upper unit is thicker and cleaner in the well which is situated in one of the positive anomalies in the Sculpted map. For location of wells see Figure 35 or Figure 36, the distance between them is 1427 metres.

5.4 Correlation

Description: The initial observation is that the Ula Formation is significantly thicker in the Cod Terrace core, with a thickness of more than 100 metres, while it is only half the thickness in the Sørvestlandet High cores and wells. Additionally, the cores of the Sørvestlandet High consist mainly of the shallow facies and consequently Facies Association 1, while the main component of the Cod Terrace core is Facies Association 2 and a slightly overall smaller grainsize. The two Sørvestlandet High cores also, although the distance between them is less than 3 kilometres, vary both in thickness and in facies. As previously mentioned well 8/10-5S is faulted, and contains more of Facies Association 3 compared to the other wells in core, but a very short Facies Association 2.

The gamma-ray log of well 8/10-6S is overall more boxy and ungraded than the two other wells (Figure 40). The gamma-ray log of well 7/12-6 contains several coarsening upwards sequences, where the upper part is mainly ungraded. Well 8/10-5S has a coarsening upwards sequence in the base and the top is relatively ungraded until the more shaly facies which is marked by an abrupt change.

Interpretation: The change in thickness indicates either that the Ula Formation on the Sørvestlandet High has been eroded, or that part of it was never deposited due to lack of accommodation space. Based on the flooding surface (flooding 2; Figure 40) which seems to be correlatable between well 7/12-6 and well 8/10-6S the latter seem to be the case (Figure 40). Therefore, only the youngest part of the Ula Formation has been deposited on the Sørvestlandet High. In the seismic the upper unit corresponds to everything above the high gamma-ray interval in well 7/12-6, which is everything above approximately 3465 metres depth in true vertical depth measured in that well. This high gamma-ray unit cannot be distinguished in the cores but might be caused by an increase in mud which makes it visible in the logs. This high gamma-ray interval from 3460 metres to 3467 metres has been correlated with a flooding surface below the core in well 8/10-6S which marks the base of the Ula Formation. In core from well 8/10-5S, this flooding cannot be identified. Below this flooding surface there is a thick sandstone package in the Cod Terrace (well 7/12-4), while in the Sørvestlandet High there is only a small sand package. In this unit below the flooding surface is the most proximal facies of the Cod Terrace, with deposition of migrating dunes. This is where the cross-stratified sandstones occur in core. In well 8/10-6S the sandstone package below this flooding event has been interpreted to represent fluvial deposition.

This suggests a backstepping system and a system which is more proximal in the Sørvestlandet High. During the initial deposition of the Ula Formation the most proximal part of the formation can be found in the Cod Terrace. At this time the Sørvestlandet High was likely dominated by erosion or fluvial deposits bringing the sediments out into the

Cod Terrace.

Above this partly correlatable flooding surface the Cod Terrace core is dominated by more distal deposits, which has been defined in core as Facies 8. In well 8/10-6S the sediments have a more proximal character, belonging to Facies Association 1, and even further onto the Sørvestlandet High in well 8/10-5S this proximality is increased. Both Sørvestlandet High cores also contain channelized deposits in this interval.

Following this is a minor flooding event (Flooding 3) marked by the occurrence of Facies 10 in well 7/12-6, which indicates a more open marine setting. This flooding cannot be identified on the Sørvestlandet High. Therefore, this seems to only represent a minor flooding, before the system continues to build out.

The following flooding surface (Flooding 4) can also be identified in the most proximal well, 8/10-5S, as the more open marine facies, Facies 10. This causes a large step back for the system, following this there are only very fine distal sands deposited in the Sørvestlandet High, with some migrating dune deposits, while in the Cod Terrace the deposition is of the Farsund Formation shales. Additionally, the wells provide further evidence for the interpretation that the calcite patches are nodules and not regional layers as they cannot be correlated between wells.

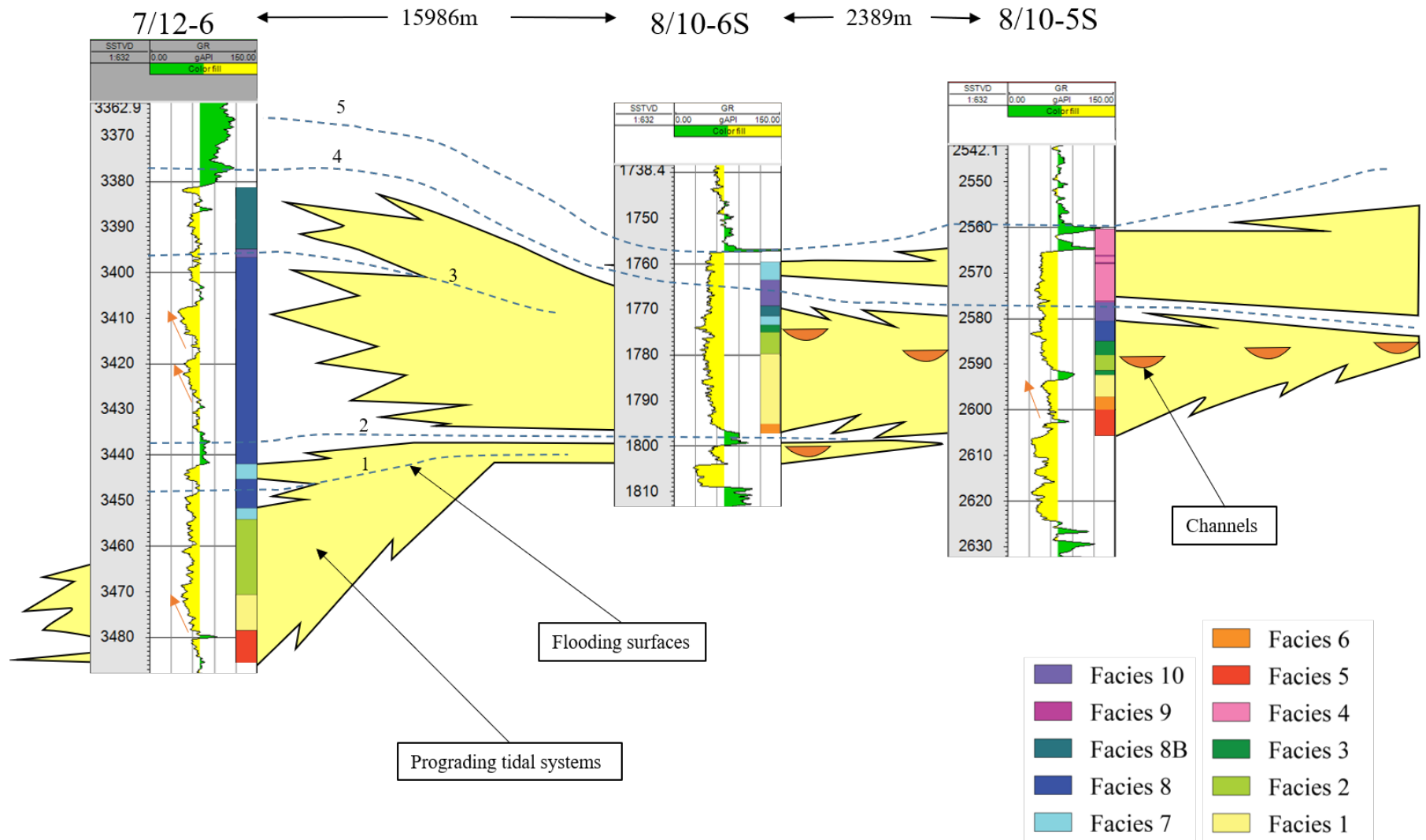


Figure 40: Well log correlation, for location of wells see Figure 11

6 Discussion

6.1 Data

Originally the new PGS seismic cube was expected to provide higher resolution which in turn could open for more interpretation and importantly also provide better results for geophysical attributes, however the results show otherwise. There are artefacts in the PGS cube, which affect the reservoir reflector disrupting the results acquired from this cube. Additionally, the cube appears to have a similar resolution to the MEGA cube. These differences can be explained by the processing step, since the MEGA seismic cube has been around for a long time this consequently leads to a longer time period to perfect the processing. While the PGS cube is more recent and still has some room left for improvement.

6.2 Salt Effect on Depositional Environment

The isochore map shows a thinning towards the Triassic pods and both attribute maps indicate a muddier composition in these areas, additionally the seismic shows onlaps onto the Triassic pods. This is all indicative of the Triassic pods being non-depositional areas, or areas with minimal deposition during the Upper Jurassic. This corresponds well with what is the current understanding of the system. Importantly this indicates that the Ula Formation was deposited in a valley network. As described by Hodgson et al. (1992)), the topography of the land which was being transgressed during the Late Jurassic might have been very complex. Although previous authors have described these areas as lacking deposition, possibly being topographic highs, the currently accepted depositional model does not account for this. The storm influenced shoreface model which was initially introduced by Gowland (1996) and has since been supported by Wonham et al. (2014), Mannie et al. (2014) and Baniak et al. (2014), is based on a linear coastline. Based on the observations made by Ainsworth, Vakarelov, and Nanson (2011) regarding the relationship between shoreface morphology and dominant processes, linear coastlines tend to be more exposed for wave reworking. However, in a valley network, highly complex topographic shoreface one might expect the waves to be abated and not be acting as the dominant process.

6.3 Depositional Environment in the Interpod Setting

Although they are sparse core interpretations show sedimentary structures which are indicative of tidal processes, like mud drapes and sigmoidal cross-stratification. The bioturbation diversity and intensity are in some facies indicative of a brackish environment, mainly in the older parts of the formation. While the youngest part of the formation contains bioturbation indicative of an open marine setting. Previous interpretations by Baniak et al. (2014) also showed how the cores of the Ula Formation contain tubular tidalites and tidal bundles. Additionally, there are asymmetric ripples indicating a unidirectional current in the youngest part of the cores.

The architectures which can be extracted from the attribute maps are elongated sand rich sand patches or dune fields, these geometries are typically found in straits or tidally dominated settings. A tidal dominance is also expected based on the interpretation of the paleomorphology of the coastline. Based on all the observations from seismic to cores a new model is proposed as an estuarine tidal dominated setting, which due to transgression becomes a more current dominated shelfal strait setting in the younger part of the Ula Formation. Although in typical tidal depositional systems one might expect more heterogeneity the lack of this might be caused by currents which persistently washed suspended mud out of the system. In general, the observations made in this thesis can not be explained by a storm influenced shoreface depositional environment.

6.4 Ula Formation Distribution and Architectural Elements

The main restraint on distribution of the reservoir is the interpod basins, the Ula Formation appears to be restricted to the interpods and thickening towards the centre of the basins. Based on the core interpretations it becomes clear that the Ula Formation contain very thick units of sandstone which is why finding an analogue has been challenging (Bowman, 1981). However, the thick sandstone units are frequently divided into smaller beds separated by shell concentrations, this is seen in facies 1, 2, and partly in Facies 7.

The facies model after Mutti, Rosell, Allen, Fannesu, and Sgavetti (1985) describes a tidal bar with a thickness of typically 5 metres). This definition of a tidal bar has later been redefined by Dalrymple and Choi (2007) to be a representation of a compound dune. The tidal bar (compound dune), according to Mutti et al. (1985), should contain a bar crest which fits both Facies 1 and 2 with the top of each bed showing an increase in bioturbation and shell fragments. In Facies 7 this is reflected as a shell deposit concentration. It should also contain a cross-stratified bar slope, which fits facies 1 and 2, and bottomsets. The bottomsets cannot be identified. This could be caused by amalgamation and consistent high energy which caused the finer sediments to be moved further out into the system.

Alternatively, they are found in one of the intensely bioturbated facies described and due to the bioturbation they cannot be identified.

These compound dunes are reflected in seismic attribute maps as elongate shapes which are sandier than the surrounding background facies and can be compared to the geometries seen in the Fehmarn strait (Feldens et al., 2015). The sizes vary and they can be as long as 1400 metres with a width of 440 metres, and smaller ones are only 220 metres in length and 88 metres in width. Based on measurements from vertical resolution in the seismic what can be seen is likely not individual compound dunes, but areas where there was a higher concentration of dune deposition through time.

The extreme thickness of amalgamated dunes can be explained by the model used by Longhitano and Steel (2017) for tectonically active straits. In their model there are tidal deltas which continuously feed sediment into subsiding straits, this results in very thick clean sand packages. A setting like this might be comparable with the Ula Formation deposition in interpods, and it is dependent on continuous subsidence and sediment supply.

6.5 Correlation From the Cod Terrace to the Sørvestlandet High

Bioturbation in the cores indicate at times a brackish environment, conglomerates with coarse sand and angular pebbles require a source area with coarse material, and the amount of sediment which has been deposited in the interpod basins is likely too much to only be a result of eroding Triassic pods. Previous authors have also suggested that there might have been fluvial systems transporting the sediments (Weibel et al., 2010; Mannie et al., 2014). The well log correlation shows a backstepping system with fluvial transport into a tidal environment. Any fluvial systems which might have transported the sediments out likely flowed through the valley network. Therefore, time equivalent to the Ula Formation deposition in the Cod Terrace fluvial deposits are expected in the interpod basins further onto the Sørvestlandet High. As previously mentioned the Ula Formation is highly diachronous and to test this theory biostratigraphy must be utilized. The Ula Formation thickens towards the centre of the interpod basins, this is likely because this is where the displacement of salt was higher which created more accommodation space.

Assuming this theory is correct, there might be connectivity through sandpackages which can allow for migration through fluvial deposits onto the Sørvestlandet High. Vertically through the Ula Formation there are no clear seals and few possible baffles, but these are not laterally extensive, the main concern is lateral migration.

7 Conclusions

1. Both previous literature and seismic interpretation indicate that the Ula Formation was deposited in a salt valley network which influenced the depositional environment through abating of wave processes and locally creating strait morphologies.
2. Initially the deposition was tidally dominated with some fluvial input, this is reflected in cores as a brackish environment and tidal sedimentary structures are present.
3. Towards the end of deposition the environment becomes increasingly more affected by unidirectional currents and an open marine environment. This is reflected in cores by asymmetric ripples and in seismic attributes as large sand sheets or compound dunes. There is also a deepening and backstepping which eventually leads to the end of the Ula Formation sands as they transition into the open marine shales of the Farsund Formation.
4. The Ula Formation deposits consist of compound dunes and sand sheets which have geometries identifiable in the attribute maps of variable sizes, and the thicknesses of beds are typically a couple of metres based on core interpretations.
5. Tidal systems in the Cod Terrace might have been sourced by fluvial systems on the Sørvestlandet High. As the Ula Formation was affected by the salt valley network morphology, the fluvial systems are likely also restricted to these valleys.

References

- Ainsworth, R. B., Vakarelov, B. K., & Nanson, R. A. (2011). Dynamic spatial and temporal prediction of changes in depositional processes on clastic shorelines: Toward improved subsurface uncertainty reduction and management. *AAPG Bulletin*, *95*(2), 267–297. doi:10.1306/06301010036
- Andsbjerg, J., Nielsen, L. H., Johannessen, P. N., & Dybkjær, K. (2001). Divergent development of two neighbouring basins following the Jurassic North Sea doming event: the Danish Central Graben and the Norwegian-Danish Basin. In *Norwegian Petroleum Society Special Publications* (Vol. 10, pp. 175–197). Elsevier.
- Bailey, C., Price, I., & Spencer, A. (1981). The Ula oil field, block 7/12, Norway. In *Norwegian Symposium on Exploration* (pp. 1–26).
- Baniak, G. M., Gingras, M. K., Burns, B. A., & Pemberton, S. G. (2014). An example of a highly bioturbated, storm-influenced shoreface deposit: Upper Jurassic Ula Formation, Norwegian North Sea. *Sedimentology*, *61*(5), 1261–1285. doi:10.1111/sed.12100
- Baniak, G. M., Gingras, M. K., Burns, B. A., & Pemberton, S. G. (2015). Petrophysical Characterization of Bioturbated Sandstone Reservoir Facies In the Upper Jurassic Ula Formation, Norwegian North Sea, Europe. *Journal of Sedimentary Research*, *85*(1), 62–81.
- Bann, K. L. & Fielding, C. R. (2004). An integrated ichnological and sedimentological comparison of non-deltaic shoreface and subaqueous delta deposits in Permian reservoir units of Australia. *Geological Society, London, Special Publications*, *228*(1), 273–310. doi:10.1144/gsl.Sp.2004.228.01.13
- Bjørnseth, H. & Gluyas, J. (1995). Petroleum exploration in the Ula Trend. *Norwegian Petroleum Society Special Publications*, *4*, 85–96.
- Bowman, M. B. J. (1981). *The sedimentology and reservoir geology of the Upper Jurassic Ula Formation in well 7/12-6 NOCS and its relationship with other block 7/12 wells*. Report Number: (OC18236). Retrieved from http://www.npd.no/engelsk/cwi/pbl/wellbore_documents/281_7_12_6_The_sedimentology_and_reservoir_geology.pdf
- Chopra, S. & Marfurt, K. J. (2008). Emerging and future trends in seismic attributes. *The Leading Edge*, *27*(3), 298–318.
- Clark, J., Cartwright, J., & Stewart, S. (1999). Mesozoic dissolution tectonics on the west central shelf, UK Central North Sea. *Marine and Petroleum Geology*, *16*(3), 283–300.

- Coward, M., Dewey, J., Hempton, M., & Holroyd, J. (2003). Chapter 2 Tectonic evolution. In D. Evans, C. Graham, A. Armour, & P. Bathurst (Eds.), *The Millennium Atlas: Petroleum Geology of the Central and Northern North Sea* (Chap. 2, pp. 26–65). London: The Geological Society of London.
- Dalrymple, R. W. (2006). Tidal depositional systems. In R. G. Walker & N. P. James (Eds.), *Facies models response to sea-level change* (Chap. 11, pp. 195–218). Canada: Geological Association of Canada.
- Dalrymple, R. W. & Choi, K. (2007). Morphologic and facies trends through the fluvial–marine transition in tide-dominated depositional systems: A schematic framework for environmental and sequence-stratigraphic interpretation. *Earth-Science Reviews*, 81(3-4), 135–174. doi:10.1016/j.earscirev.2006.10.002
- Dalrymple, R. W., Zaitlin, B. A., & Boyd, R. (1992). Estuarine facies models: conceptual basis and stratigraphic implications: perspective. *Journal of Sedimentary Research*, 62(6).
- Feldens, P., Diesing, M., Schwarzer, K., Heinrich, C., & Schlenz, B. (2015). Occurrence of flow parallel and flow transverse bedforms in Fehmarn Belt (SW Baltic Sea) related to the local palaeomorphology. *Geomorphology*, 231, 53–62. doi:10.1016/j.geomorph.2014.11.021
- Fraser, S., Robinson, A., Underhill, H. J., Kadolsky, D., Connell, R., Johannessen, P., & Ravnås, R. (2003). Chapter 11 Upper Jurassic. In D. Evans, C. Graham, A. Armour, & P. Bathurst (Eds.), *The Millennium Atlas: Petroleum Geology of the Central and Northern North Sea* (Chap. 11, pp. 373–440). London: The Geological Society of London.
- Gingras, M. K., MacEachern, J. A., & Dashtgard, S. E. (2012). The potential of trace fossils as tidal indicators in bays and estuaries. *Sedimentary Geology*, 279, 97–106. doi:10.1016/j.sedgeo.2011.05.007
- Glennie, K., Higham, J., & Stemmerik, L. (2003). Chapter 8 Permian. In *Millennium Atlas: Petroleum Geology of the Central and Northern North Sea* (pp. 91–103). Geological Society of London.
- Gowland, S. (1996). Facies characteristics and depositional models of highly bioturbated shallow marine siliciclastic strata: an example from the Fulmar Formation (Late Jurassic), UK Central Graben. *Geological Society, London, Special Publications*, 114(1), 185–214. doi:10.1144/gsl.Sp.1996.114.01.09
- Hodgson, N., Farnsworth, J., & Fraser, A. (1992). Salt-related tectonics, sedimentation and hydrocarbon plays in the Central Graben, North Sea, UKCS. *Geological Society, London, Special Publications*, 67(1), 31–63.

- Home, P. (1987). Ula. In A. M. Spencer (Ed.), *Geology of the Norwegian oil and gas fields : an atlas of hydrocarbon discoveries, containing full descriptions of 37 of Norway's major oil and gas fields and finds* (pp. 143–152). London; Boston: Published by Graham & Trotman for the Norwegian Petroleum Society.
- Hudec, M. R. & Jackson, M. P. (2007). Terra infirma: Understanding salt tectonics. *Earth-Science Reviews*, 82(1-2), 1–28.
- Jones, I. F. & Davison, I. (2014). Seismic imaging in and around salt bodies. *Interpretation*, 2(4), SL1–SL20.
- Kubala, M., Bastow, M., Thompson, S., Scotchman, I., & Oygard, K. (2003). Chapter 17 Geothermal regime, petroleum generation and migration. In D. Evans, C. Graham, A. Armour, & P. Bathurst (Eds.), *The Millennium Atlas: Petroleum Geology of the Central and Northern North Sea* (Chap. 17, pp. 289–315). London: The Geological Society of London.
- Longhitano, S. G. (2013). A facies-based depositional model for ancient and modern, tectonically-confined tidal straits. *Terra Nova*, 25(6), 446–452.
- Longhitano, S. G. & Steel, R. J. (2017). Deflection of the progradational axis and asymmetry in tidal seaway and strait deltas: insights from two outcrop case studies. *Geological Society, London, Special Publications*, 444(1), 141–172. doi:10.1144/sp444.8
- Mannie, A. S., Jackson, C. A. L., & Hampson, G. J. (2014). Shallow-marine reservoir development in extensional diapir-collapse minibasins: An integrated subsurface case study from the Upper Jurassic of the Cod terrace, Norwegian North Sea. *Aapg Bulletin*, 98(10), 2019–2055. doi:10.1306/03201413161
- Mannie, A. S., Jackson, C. A. L., Hampson, G. J., & Fraser, A. J. (2016). Tectonic controls on the spatial distribution and stratigraphic architecture of a net-transgressive shallow-marine synrift succession in a salt-influenced rift basin: Middle to Upper Jurassic, Norwegian Central North Sea. *Journal of the Geological Society*, 173(6), 901–915. doi:10.1144/jgs2016-033
- McCave, I. (1971). Sand waves in the North Sea off the coast of Holland. *Marine geology*, 10(3), 199–225.
- Mutti, E., Rosell, J., Allen, G., Fønnesu, F., & Sgavetti, M. (1985). The Eocene Baronia tide dominated delta-shelf system in the Ager Basin. In *Excursion guidebook: 6th International Association of Sedimentologists European Regional Meeting* (pp. 577–600).
- Norwegian Petroleum Directorate. (2017). NPD Factpages. Retrieved October 19, 2017, from <http://factpages.npd.no/factpages/>

- Partington, M., Mitchener, B., Milton, N., & Fraser, A. (1993). Genetic sequence stratigraphy for the North Sea Late Jurassic and Early Cretaceous: distribution and prediction of Kimmeridgian–Late Ryazanian reservoirs in the North Sea and adjacent areas. *Geological Society, London, Petroleum Geology Conference series*, 4(1), 347–370.
- Penge, J., Munns, J., Taylor, B., & Windle, T. (1999). Rift–raft tectonics: examples of gravitational tectonics from the Zechstein basins of northwest Europe. In A. J. Fleet & S. A. R. Boldy (Eds.), *Petroleum Geology of Northwest Europe: Proceedings of the 5th conference* (pp. 201–213). Geological Society of London.
- Penge, J., Taylor, B., Huckerby, J., & Munns, J. (1993). Extension and salt tectonics in the East Central Graben. In *Geological Society, London, Petroleum Geology Conference series* (Vol. 4, pp. 1197–1209). Geological Society of London.
- Reading, H. & Levell, B. (1996). Controls on the sedimentary rock record. In H. G. Reading (Ed.), *Sedimentary environments: processes, facies and stratigraphy* (Chap. 2, pp. 5–36). Blackwell Publishing.
- Reineck, H.-E. (1963). Sedimentgefüge im Bereich der südlichen Nordsee. *Abhandlungen der Senckenberg Gesellschaft für Naturforschung*, 505, 138.
- Reynaud, J.-Y. & Dalrymple, R. W. (2012). Shallow-Marine Tidal Deposits. In R. A. Davis Jr & R. W. Dalrymple (Eds.), *Principles of Tidal Sedimentology* (pp. 335–369). Dordrecht: Springer Netherlands. doi:10.1007/978-94-007-0123-6_13
- Sangree, J. & Widmier, J. (1979). Interpretation of depositional facies from seismic data. *Geophysics*, 44(2), 131–160.
- Snedden, J. W. & Dalrymple, R. W. (1999). Modern shelf sand ridges: from historical perspective to a unified hydrodynamic and evolutionary model.
- Snedden, J., Dalrymple, R., & Bergman, K. (1998). Modern shelf sand bodies: an integrated hydrodynamic and evolutionary model. *Isolated Shallow Marine Sandbodies: Sequence Stratigraphic Analysis and Sedimentologic Interpretation: SEPM, Special Publication*, 64, 13–28.
- Steel, R. & Ravnås, R. J. (1998). Architecture of marine rift-basin successions. *AAPG bulletin*, 82(1), 110–146.
- Taylor, A. & Gawthorpe, R. (1993). Application of sequence stratigraphy and trace fossil analysis to reservoir description: examples from the Jurassic of the North Sea. *Petroleum Geology Conference series*, 4(1), 317–335.

- Walker, R. G. & Plint, A. G. (2006). Wave-and storm-dominated shallow marine systems. In R. G. Walker & N. P. James (Eds.), *Facies Models-response to sea level change* (Chap. 12, pp. 219–238). Canada: Geological Association of Canada.
- Weibel, R., Johannessen, P. N., Dybkjaer, K., Rosenberg, P., & Knudsen, C. (2010). Chemostratigraphy of upper Jurassic reservoir sandstones, Danish Central Graben, North Sea. *Marine and Petroleum Geology*, *27*(7), 1572–1594. doi:10.1016/j.marpetgeo.2010.06.001
- Widess, M. (1973). How thin is a thin bed? *Geophysics*, *38*(6), 1176–1180.
- Wonham, J. P., Rodwell, I., Lein-Mathisen, T., & Thomas, M. (2014). Tectonic control on sedimentation, erosion and redeposition of Upper Jurassic sandstones, Central Graben, North Sea. *From Depositional Systems to Sedimentary Successions on the Norwegian Continental Margin*, 473–512.